THESE

pour l'obtention du grade de

DOCTEUR DE L'UNIVERSITE DE REIMS CHAMPAGNE-ARDENNE

Spécialité : GENIE INFORMATIQUE, AUTOMATIQUE ET TRAITEMENT DU SIGNAL

présentée et soutenue par

Artem MELIKHOV

le 26 November 2008

Automatisation des opérations de contrôle de démarrage sans à-coups des machines asynchrones pour pompes d'un système d'alimentation en eau

JURY

Yury Kolokolov	Professeur	Directeur de thése
Abdelaziz Hamzaoui	Professeur	Co-directeur de thése
Najib Essounbouli	Maître de conférence	Co-directeur de thése
Janan Zaytoon	Professeur	Examinateur

Abstract

A soft-start of induction machines with an application of series silicon-controlled rectifiers (SCRs) is a along-term tendency in ac drive development because it allows increasing an induction machine reliability and power consumption efficiency. The positive indices of a soft-start are more characteristic for ac drives of centrifugal engine applications.

The modern design level of soft-starters with SCRs and pulse-phase control system is characterized by unification of their power stage that is why the efficiency increase of energy conversion via soft-starter application is more connected with an improvement of control algorithms of IM transient responses.

In most of publications devoted to the development of IM soft start algorithms the main attention is given to the problems of current transient components limitation in stator windings and IM electromagnetic torque in transient responses. However, the interconnected problems of an efficient control of an IM soft start and, as a result, constraints introduced are not considered. This circumstance complicates the development of new efficient algorithms for IM soft start control. In particular, the new algorithm of an adaptive formation for start-stop operation modes of the IM pump station is considered in the thesis. This algorithm secures an energy loss decrease in the IM soft-starter of the water supply system in a pump station.

The essence of the proposed algorithm consists in the determination of optimal (according to the criterion of energy loss minimization) program parameters of the soft start for each IM taking into account maximum current and temperature constraints of IM stator windings as well as maximum pressure increase in the pipeline during the transient response. An adaptation of the algorithm proposed is provided by means of the individual start program formation sequentially for each pump station IM taking into account current values of the state variables of electrical and hydraulic subsystems of the pump station.

The individual calculated reference increase of the maximum allowed transient current for each IM leads to the energy loss decrease in the windings up to 12-18% depending on IM power in comparison with the losses that appear during the use of the traditional control algorithm for a soft start with the fixed reference.

Author's Acknowledgments

It gives me great pleasure to take this opportunity and express my sincere gratitude to all people who directly or indirectly played a key role in the successful completion of this work. Their constant support and encouragement was a tremendous help for me in many ways.

First and foremost, I would like to thank sincerely and deeply my advisor, Prof. Yury V. Kolokolov. His support, encouragement, assistance, and friendship led me through all the steps of my doctoral program at the University. He has been a great example of a person who has achieved excellence in both scientific research and a life. His creativity and deep respect of each of his students have empowered many bright minds and helped them to realize their talents.

I am particularly grateful to my co-advisors Prof. Abdelaziz Hamzaoui and Associated Prof. Najib Essounbouli for a number of important discussions and encouragement. I thank Professors Janan Zaytoon, Kondo Adjallah, Krishna Busawon, Malek Ghanes for having found time to sit in committee meetings connected with the presentation of my thesis.

I express the gratitude to my colleagues Ms Anna Monovskaya, Mr. Dmitry Tey and Pavel Ustinov for their assistance in the presentation of my thesis.

I am grateful to the IUT de Troyes and Conseil Régional de Champagne-Ardenne for providing and fostering teaching and research excellence. I am also grateful to my previous University, the Orel State Technical University, for the given solid education which made it possible for me to pursue my Doctor's degree.

Finally, I would like to address my deepest gratitude, love, and respect to my family, my mother Tatyana and my wife Natalia, who made all this possible from the beginning.

Table of Contents

List Of Abbreviations And Symbols

ACS – Automation Control System

AD – Asynchronous Drive

ERKM – Embedded Runge-Kutta Method

IC – Initial Condition

IM – Induction Machine (Motor)

Mathematical CAD – Mathematical Computer-Aided Design

ODE – Ordinary Differential Equation

PPCC – Pulse-Phase Control Circuit

PS – Pump Station

PU – Pump Unit

RKM – Runge-Kutta Method

SCI – Structure Constancy Interval

SCRs – Silicon-Controlled Rectifiers

I_{TSC}	Transition surge current in windings of IM [A]
I_{SC}	Starting current of IM (from IM manufacturing data) [A]
I_{SCS}	Starting current setting (in current limitation algorithm) [A]
T_{TP}	Transient process settling time [s]
ΔP_{max}	Maximal pressure rise in pipeline [Pa]
$\Delta P_{max,perm}$	Maximum permissible pressure rise in pipeline [Pa]
$\omega_{r,s}$	Steady-state angular velocity of induction machine rotor [rad·s^{-1}]
ω_r	Angular velocity of induction machine rotor [rad·s^{-1}]
T_r	Rated electromagnetic torque of IM [N·m]
T_L	Friction torque load on shaft of IM [N·m]
P_r	Rated motor power [W]
k_I	Index indicating limit value of starting current
I_r	Rated current of IM [A]
$\Delta V_{max,perm}$	Maximal permissible voltage drop in electrical network (relative to rated network voltage) [V]
θ_s	Temperature of IM windings [ºC]
Θ_{max}	Maximal temperature of IM windings [ºC]
$\Theta_{max,perm}$	Maximal permissible temperature for used type of winding isolation [ºC]

List Of Tables

List Of Figures

CHAPTER 1

Introduction

1.1. Motivation

The automation of technological processes of electromechanical energy conversion continues to develop at present time in three main fields: increase of reliability, energy efficiency and economy [Altmann-05]. This tendency obtains a fundamental importance in such industry branches where IM as an operating mechanism is a base of technological processes. The evident example in this case is a centrifugal machine IM (fans, compressors, pumps etc.), which consumes up to 25% of all generated electrical energy according to the different evaluations [Sannino-03].

The most part of the energy consumed by centrifugal machines belongs to the centrifugal pumps that are used generally for liquid transportation in the water supply, sewerage and trunk pipelines. This circumstance along with the rapid increase of electrical energy prices adds the particular urgency to the automation and energy saving problem both in the public and industry water supply systems.

The problem solution of the pump station automation in a water supply system is connected, first, with a choice and application of such an IM type, which allows satisfaction of technological process requirements in reliability, energy efficiency and economy.

Thanks to high reliability, reasonable cost, mass-overall dimensions and adjustment properties, the IM without the speed feedback and with the pulse-phase control system of series silicon-controlled rectifiers is the most widespread for the pump station automation [Alger, et al. − 76], [Blaabjerg and Pederson − 97], [Bredthauer and Struck − 95], [Hamed and Chalmers − 90] and [Lipo−71].

The basis of the theory of asynchronous drive with the pulse-phase control circuit has been founded in the late 1960s. At present the development of this direction in researches is continued by the schools of thought: I. Ya. Braslavsky, Z. Sh. Ishmatov, A. M. Zuzev et al. (Ural State Technical University, Russia); V. Chrisanov (State University of Telecommunications, St. Petersburg, Russia), R. Brzesinski (Technical University of Zielona Gora, Poland); O. Andrushenko, A. Boyko et al. (Odessa National Polytechnic University, Ukraine); N.A. Demerdash, B. Mirafzal, M.G. Solveson (Marquette University, Milwaukee, USA); Gürkan Zenginobuz, Isik Cadirci et al.

(Hacettepe University (HU), Ankara, Turkey); Yu.V. Kolokolov (UGRA State University, Russia), S.L. Koschinsky (Orel State Technical University, Russia).

The main destination of a pump station control system is to form such a start (stop) trajectory (mode) of a pump drive beginning from the start (rated) to rated (start) speed, which on the one hand could ensure limitations of temperature, current inrushes in stator windings and alternating oscillations of a drive electromagnetic torque on the other hand could keep pressure increase within the limits allowed in the pipeline. The essence of the above-mentioned problem solution had led to the fact that the IM providing this problem solution is called a soft-starter.

The modern design level of soft-starters is characterized by unification of their power stage. That is why the efficiency increase of energy conversion via soft-starter application is more connected with an improvement of control algorithms of IM start-stop operation modes.

In most of publications devoted to the development of IM soft start algorithms the main attention is given to the problems of limitation of the current transient components in the stator windings and IM electromagnetic torque in the transient responses. However, the interconnection problems of the efficient control of the IM soft start and at the same time limitations introduced are not considered. This circumstance complicates the development of new power efficient algorithms for the IM soft start control. This fact stipulates an *urgency* and *practical importance* of the thesis.

The aim of the thesis: to obtain electric energy loss decrease in the IM windings of the water supply pump station during the controlled realization of the start-stop trajectories. It is necessary that the following problems should be solved to achieve the above-mentioned aim:

- Formulation of limitations and definition of an efficiency criterion for electromechanical energy conversion in the IM soft-starter of the pump station.
- Development of a mathematical model and modeling method of electromechanical energy conversion in the IM soft-starter of the water supply system in a pump station.
- Development of the control algorithm for the IM soft start that allows decrease of electric energy loss in IM windings with a simultaneous fulfillment of the requirements to the transient response performance of the IM of the water supply system in a pump station.
- Carrying out an experimental investigation of an adequacy of the mathematical model "power network-soft starter- IM-pump-pipeline".

1.2. Summary of Scientific Contributions

In this work, the problem of the IM soft start control in the water supply system a pump station is solved. In particular:

- The adaptive control algorithm of the IM soft start based on the start program formed sequentially for each IM taking into account the current values of the state variables of the pulse-phase control system and hydraulic subsystem of the pump station is developed.
- The optimal (according to the criterion of the computer time consumption) algorithm of the numerical integration of the pulse-phase control system mathematical model is developed. It is based on the adaptation of the difference integration method to the current model state.
- The modeling method of an IM soft start of the water supply pump station that includes an adaptive algorithm of the IM soft start and optimal integration algorithm of the pulse-phase control system model with the IM is developed. This method allows realization of researches of transient responses in the system "power network-soft starter-IM-pump-pipeline" for the time-dependent liquid movement in the pipeline of arbitrary configuration.

The program realization of the proposed mathematical model, modeling method and adaptive algorithm of IM soft start control allow decrease of energy losses in the motor windings during transient modes by means of an introduction and application of the developed software in a dispatcher's work station of a pump station.

The analytical transformations while deriving a symbolic representation of the pulse-phase control system with the IM have been realized with the help of Symbolic Math Toolbox ("*MATLAB 7.4*®, The MathWorks, Inc.). The software for the automatic control system of a pump station has been also developed in Symbolic Math Toolbox with the purpose of carrying out the numerical experimental investigations.

The physical experimental investigations took place with the application of the experimental plant designed by the laboratory of pulse systems of the Department of Design and Technology of Electronic and Computer Systems of the Orel State Technical University.

1.3. Organization of the Thesis

The thesis is organized in the following way. The first chapter is devoted to an

introduction. In the second chapter:

- The analysis of a composition and choice substantiation of the components in the automatic control system of IM soft start is carried out.
- The purposeful functioning efficiency of automatic control system of IM soft start is presented; the limitations imposed on the formation process of IM start-stop operation trajectories are enumerated.
- The analysis of IM soft start control algorithms is carried out.
- The interconnection between transient process indices and energy losses is revealed.
- The mathematical model structure of an automatic control system of IM is presented; the requirements to its components are formulated.
- The purpose and objectives for energy loss decrease in IM windings are formulated as a result for the controlled formation of start-stop trajectories of pump aggregates.

In the third chapter:

- The approach to description of the IM non-symmetrical connection to alternating current network is proposed.
- The numerical algorithm to reduce the computer time consumption during the integration of the pulse-phase control system model with the IM in transient modes is developed.
- The analysis of the performance indices in static and dynamic modes of the pulse-phase control system model with the IM of two synchronization types (by supply-line voltage and load current) is carried out.
- The transformer substation model is given with a load as IMs functioning in nominal conditions.
- The simplified IM thermal mathematical model is presented.
- The mathematical model of pump load is derived in transient and steady-state modes.
- The mathematical model of unbalanced liquid movement in the pipeline with an arbitrary configuration is obtained; the integration method of such a model is considered.

The fourth chapter is devoted to setting and carrying out of experimental investigation of the pump station mathematical model of automatic control system with IM with the purpose of adequacy verification in the developed mathematical models. In particular:

- The physical and numerical investigations of IM start with a soft-starter is realized on the basis of the experimental plant designed by the problem laboratory of pulse systems of the Department of Design and Technology of Electronic and Computer Systems of the Orel State Technical University.
- The numerical modeling of the non-stationary heating of IM windings as well as functioning energy and hydraulic subsystems in automatic control system of water supply pump station are realized.
- The substantiation of a simulation environment choice for realization of the mathematical model and soft start control algorithm is given.

In the fifth chapter:

- The adaptive algorithm of a pump station IM soft start is developed.
- The software for the control and monitoring IM soft start automatic control system is developed.
- The numerical experimental investigation of the transient processes of IM soft start for the typical water supply system pump station is carried out. The conclusions regarding efficiency of the adaptive algorithm for the IM soft start developed in the thesis are drawn.

CHAPTER 2

Analysis of Current Trends in Automation of Electromechanical Energy Conversion Process in Induction Machine Soft Starters for Pump Station Water Supply System

2.1. Standard Structure of Water Supply System

The automation control system (ACS) of water supply processes represents the complex of technical, informational, mathematical and software resources for realization of control actions in water supply systems in accordance with the following criterion: minimization of water delivery prime cost on condition of essential quality of water and volume required [Chapple–03], [Girdhar and Moniz – 05], [Guevara and Carmona – 90], [Sanks–98], [Kolokolov and Melikhov – 07] and [Menon–04].

ACS of water supply has a hierarchical structure and includes the following major subsystems:

– ACS of water lifting intended for control of both artesian wells and source pump stations).
– ACS of water purification systems.
– ACS of water supply and distribution.
– ACS of trunk pipelines intended for control of trunk pipeline pump stations.

The proposed structure scheme is considered from the viewpoint of the definition presented in [Larock, et al. – 00]: the system of hydraulic constructions and equipment, which provides water lifting from wells and water delivery to head-ponds by pump units is called a pump station. This definition and also the structure schemes of water lifting, supply and distribution systems [Chapple–03], [Guevara and Carmona – 90], [Sanks–98], [Larock, et al. – 00] and [Kolokolov and Melikhov – 07] allow suggesting the general structure of a standard pump station (see Figure 2.1). Such a structure includes the following necessary components:

– A water intake reservoir into which water discharges from artesian wells or a proper processing in a water purification unit (in case of a pump station of I water lifting), directly from an artesian well (in case of a pump station of II water lifting) or from a pipeline of the previous section of the water supply system (in case of a pipe station of III, IV water liftings);

– A pump unit assembled in a single drive-unit, reduction gear and centrifugal pump.
– A trunk pipeline of *L*-length consisting of *n* segments and intended for water delivery into a head-pond of trunk water pipe line;

A transformer substation providing power supply of the main and auxiliary electrical equipment of the pump station.

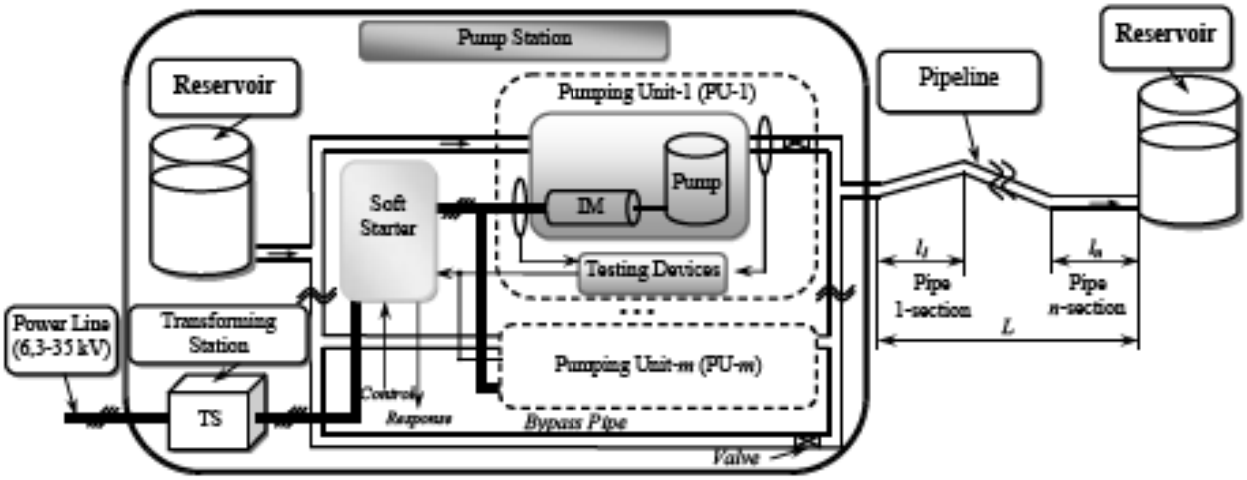

Figure 2.1: A structure chart of a standard pump station.

As the analysis of literature [Blaabjerg and Pederson – 97], [Kolokolov and Melikhov – 07], [Dewinter and Kedrosky – 89] and [Volk – 05] shows the problem of power losses reduction in windings of electrical motors throughout the transient processes is very important problem when there is a necessity in frequent starts of pump units (e.g., water supply systems where middle-size reservoirs (tanks) are used because of technological reasons). For example, let us refer to the sewerage system used on the territory of Konstantinovsky Palace and known as "State Residence - Palace of Congresses" (St. Petersburg, Russia). This system includes ten pump stations installed in 2002 at Strelna, an object of the national significance. After that, the number of pump unit starts reaches 60 starts per hour [Berezin and Chernota – 08].

ACS of electrical drives belongs to the lower level of the hierarchy of water supply ACS. A soft start of pump motors is one of the main functions of electrical drives. Initially, pump unit motors were connected directly to a power supply network. Numerous disadvantages of direct starts and stops lead to the necessity of application of semiconductor converters meant for the controlled formation of start- and stop trajectories (hereafter “transient” trajectories) of mechanical loads.

A transient control is a multi-aspect problem and its effective solution proposes the use of an information, mathematical and software support. As a result, a new ACS

subclass of electrical drives, named as ACS of electrical machine soft start, appeared in [Pozdeev and Erezeev – 06].

2.2. Automation Control System of Electrical Drive Soft Start for Water Supply Pump Stations

2.2.1. Structure and Functions

Definition

ACS of electrical machine soft start represents a system of technical means, information, mathematical support and software for conditioning control signals and their transmission without losses and distortion on to a soft starter of induction machine with the purpose of ensuring effective transients in dynamics of "power supply – soft starter – electrical machine – centrifugal pump – pipeline".

In this definition, "efficiency" means the minimization of energy losses at the satisfaction of corresponding limitations.

The standard structural scheme of ACS of electrical machine soft start is shown in Figure 2.2.

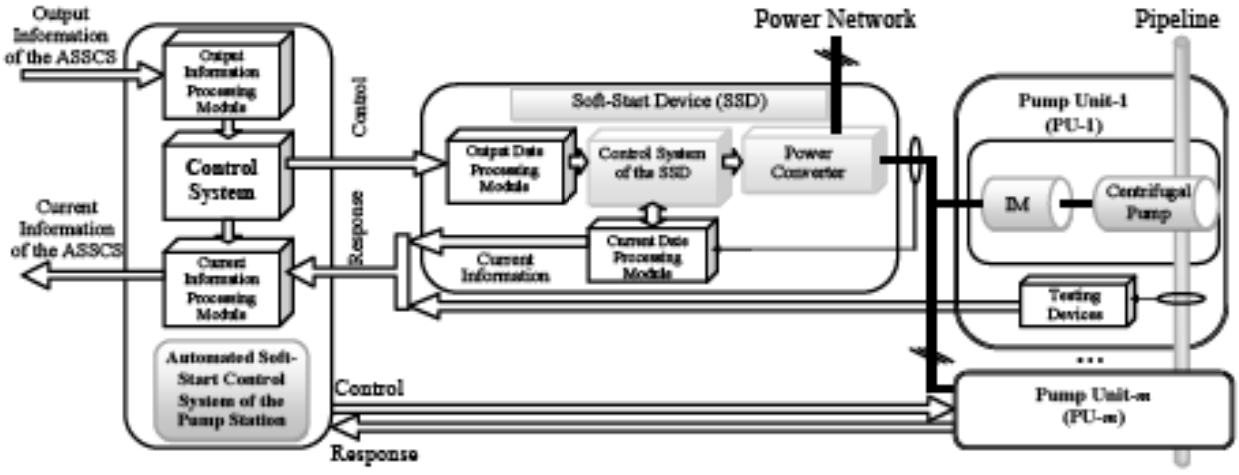

Figure 2.2: A structural scheme of ACS of electrical machine soft start.

There are a lot of pump units used in water supply and sewerage systems, in chemical industry, in underground mines and so on operating under the conditions of high humidity, high temperature, corrosive medium and explosive atmosphere. Asynchronous protected squirrel-cage motors are generally used in such units

[Zenginobuz and Çadirci − 04], [Zenginobuz and Çadirci − 01], [Girdhar and Moniz − 05] and [Deleroi, et al. − 89].

A direct online start of induction motors (IM) is characterized by some shortcomings [Bredthauer and Struck − 95], [Çadirci, et al. − 99], [Ginart, et al. − 99], [McElveen and Toney − 01]:

1. The amplitude of transient components in currents of IM windings at direct starts exceeds than 6-8 times the amplitude of steady-state currents. Meanwhile, conductors located in coil ends are affected by considerable mechanical efforts resulting in loosening a coil banded fastening, a gradual insulation failure and finally in coils short circuit and early IM breakage. Moreover, high-power starting current leaking can lead to voltage drop up to about 40% [Pozdeev and Erezeev − 06] because of voltage drop in internal resistance of a power source with the use of self-contained generators or other low-powered sources.
2. The amplitude of transient components of an IM electromagnetic torque during direct start exceeds 4-5 times the amplitude of rated torque. At the same time the bearings and an actuating mechanism are affected by enhanced loads resulting in a gradual increase of gaps between a motor and mechanism reducing overhaul life.
3. A rapid start or stop of IM pump units in water supply and sewerage systems can be the reason of water hammers in a pipeline that leads to additional loads on pipes, connecting sleeves, flanges, compressors and other assembling units causing their premature wear and breakage.

The mentioned disadvantages of a direct start-stop of IM resulted in the necessity of development and use of technical and organizational measures which allow the elimination and, if impossible, limitation of the enumerated undesirable phenomena.

The following restrictions are accepted hereafter taking into account the literature sources analysis [Bredthauer and Struck − 95], [Çadirci, et al. − 99], [Zenginobuz and Çadirci − 2004], [Chrisanov and Brzesinski − 02], [Sastry, et al. − 97]:

1. The value of IM surge start current I_{TSC} (the highest amplitude of start currents in an engine during a transient) should not cause rated voltage drop in the point of common connection to a power supply below the value $\Delta V_{max,perm}$, set by a standard [Pozdeev and Erezeev − 06]. The fulfillment of this condition provides stability of operating modes of electrical equipment in a pump station including computers and control instrumentations.
2. The value I_{TSC} should not exceed that of a start current I_{SC}, which is preset by a manufacturer of the particular electrical motor. Fulfillment of this condition provides

protection of IM windings from mechanical overloads exceeding a value set by manufacturing works.

3. A current change behavior in IM stator windings during transients should not cause increase of a steady-state temperature in IM stator windings more than the maximum permissible temperature $\Theta_{max,perm}$, that is set by the standard [Boys and Miles – 94], [Mellor, et al. – 91] in relation to the insulation system of the corresponding class of thermal-life characteristics for a winding insulation.
4. The transient duration T_{TP} (sec) should be chosen taking into account arising therewith a free component of IM stator currents, which, from the one hand, should not result in the violation of the mentioned conditions 1-3, and, from the other hand, should not lead to such a maximum pressure increase a pipeline ΔP_{max} (Pa) caused by such a transient should not exceed the maximum permissible value of the pressure $\Delta P_{max,perm}$, (Pa), preset for certain type of pipelines.

Searches of ways for a problem solution of the reduction of negative consequences connected with an IM direct start resulted in four approaches [Bredthauer and Struck – 95], [Sanks–98], [Solveson, et al. – 06]:

1) Use of auto-transformers; start, a tapped transformer is used to supply reduced voltage to the electrical motor.
2) During a start a motor winding change-over in star-delta connection.
3) Series connection of supplementary resistors or inductances in motor winding.
4) Semiconductor converter use.

The main disadvantage of the first three approaches is connected with absence of the possibility to control a transient duration that violates the 4th limitation condition accepted above.

The choice of an electric drive type for soft start problem solution in accordance with the forth approach is based on the following propositions.

As is well known the most universal type of induction motor drives is based on PWM rectifier-inverter [Girdhar and Moniz – 05], [Sanks–98], [Dewinter and Kedrosky – 89], [Novotny and Lipo – 03], that stipulates its wide use in automation systems of electromechanical energy conversion. The vector-controlled induction motor drives are characterized by a wide range of velocity variation and possibility of power-saving. However, vector-controlled induction motor drive is usually characterized by its high cost, multi-circuit structure and complex control algorithms. Therefore, such drive usage cannot be advisable for induction motor soft start only in the critical application such as nuclear power plants, thermal power plants, water supply and sewerage systems due to

strict requirements to its reliability [Bredthauer and Struck – 95], [Zenginobuz and Çadirci – 04], [Girdhar and Moniz – 05] and [Sanks–98]. As a result, the sensorless pulse-phase control circuit of series-connected silicon-controlled rectifiers (SCRs) are used widely for realization of soft starters [Alger, et al. – 76], [Blaabjerg and Pederson – 97], [Dewinter and Kedrosky – 89], et al. Meanwhile, implementation of basic and auxiliary functions in soft starters requires an application of a microcontroller with flash memory, user interface, control instrumentations and external interfaces (see Figure 2.3).

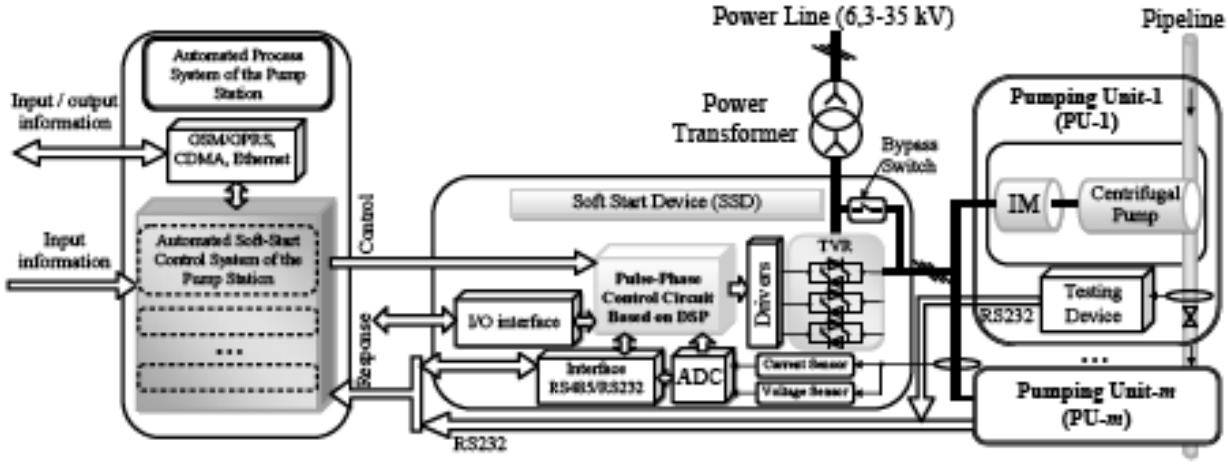

Figure 2.3: A specified structural scheme of the ACS of electrical motor soft start for a water supply pump station.

2.2.2. Formation of Control Trajectory for Start Modes

The analysis of literature [Çadirci, et al. – 99], [Hamed and Chalmers – 90], [Solveson, et al. – 06], [Tsukanov and Melikhov – 06] allows choosing two fundamental approaches to formation of firing angle control:

1. Control algorithm with voltage build-up.
2. Control algorithm with current limitation.

The first type of algorithms requires the assignment of functional dependence of the control angle on time. As a rule producers save several standard start-braking programs of control angle changes and suggest users choosing their parameters independently. An example of such a program is presented in Figure 2.4.

The caption of Figure 2.4 consists of the following designations: α_{min}, (α_{max}) – the minimum (maximum) value of the control angle; α_{SP} and t_{SP} – the value and duration of the start pulse, correspondingly.

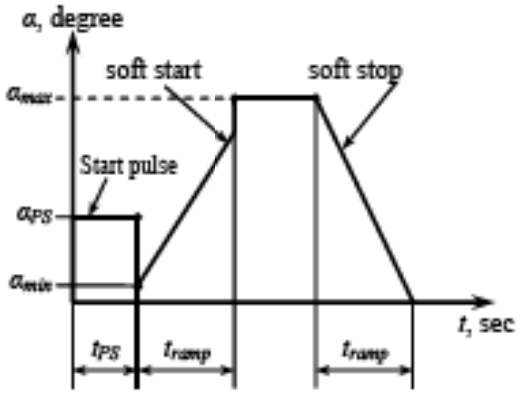

Figure 2.4: A standard form of a control angle curve.

An implementation of the current limiting control algorithm can eliminate such a defect. The current repetition factor at the controlled start is defined by the expression:

$$k_I = I_{SCS}/I_r, \tag{2.2.1}$$

where I_r is a rated current of IM; I_{SCS} is a current reference.

There are several ways for the realization of a control algorithm with current restriction. In particular, one of the ways consists in use of PI-regulator [Hamed and Chalmers − 90]. But difficulties of this way are connected with the optimization of this regulator since its tuning leads to limitations in oscillations of the current amplitude:

$$I_{SCS} = k_I \cdot I_r. \tag{2.2.2}$$

In this thesis, the current limitation algorithm described in [Çadirci, et al. − 99], [Zenginobuz and Çadirci − 04] and [Zenginobuz and Çadirci − 01], is used. This algorithm includes three steps:

1. Discrete time reckonings (t_i, where i=1,2,3…n) are introduced at which the condition $I_{TSC}=k \cdot I_{SCS}$ is fulfilled, where k is a safety factor ($k \in [0.1k_I; 0.4k_I]$).
2. The control angle α obtains the initial value $\alpha=\alpha_0$ at the point of time t_1=0.
3. At the moment t_i the control angle α is computed in accordance with the following rule:

$$\alpha_i = \begin{cases} \alpha_{i-1} \cdot \sin(t_i k_f + \pi/2), I_{TSC} < k \cdot I_{SCS}; \\ \alpha_{i-1}, I_{TSC} \geq k \cdot I_{SCS}, \end{cases} \tag{2.2.3}$$

where k_f is a frequency of a control sinusoidal curve.

For example, in Figure 2.5 the simulation results with two I_{SCS} values are presented: under $I_{SCS}=2.5 \cdot I_r$ (a,b) and $I_{SCS}=2.1 \cdot I_r$, (c,d). In both cases the angular velocity (ω_r) and electromagnetic torque (T_e) are calculated on the basis of the

described algorithm relative to IM "4AC250M4Y3" (described in Appendix A) under initial zero condition.

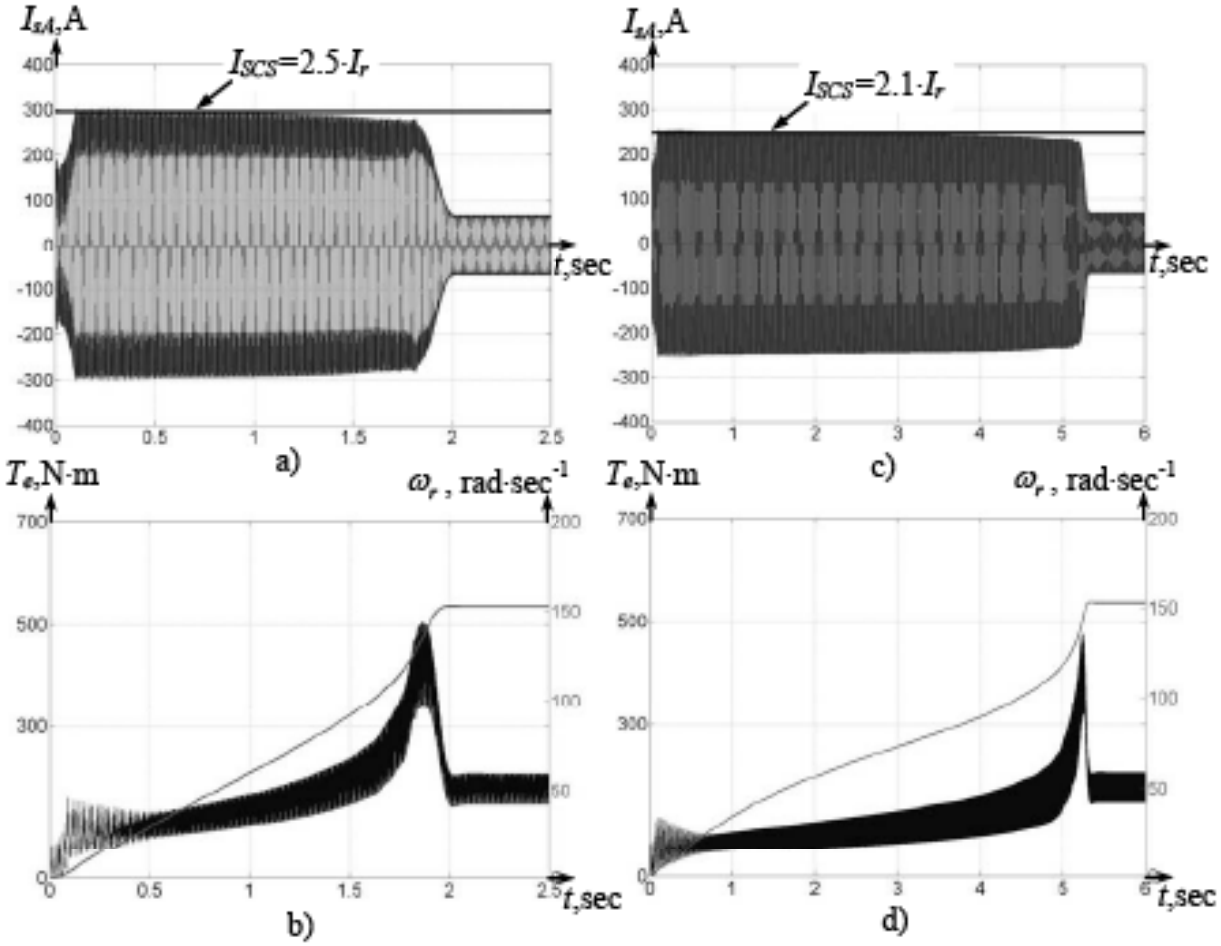

Figure 2.5: Curves of transient stator currents (a,c), angular velocity and electromagnetic torque (b,d) during the start of induction motor 4AC250M4Y3 controlled by current limitation algorithm.

The analysis of diagrams in Figure 2.5 allows concluding, that the current set I_{SCS} is formed correctly and the envelope curve of currents is smooth. Start durations T_{TP} are $T_{TP}\big|_{I_{SCS}=2.5I_r} = 1.85$ s and $T_{TP}\big|_{I_{SCS}=2.1I_r} = 5.23$ s.

2.2.3. Analysis of Primary Indices of Start Transients

The essential part of power losses in induction machines is concerned with the losses in stator and rotor windings [Kolokolov and Melikhov – 07], [Solveson, et al. – 06], [Mezani, et al. – 05] and [Lee and Habetler – 03].

One of the expressions which is used for determination of power losses in stator

and rotor windings of the three-phase IM becomes [Kolokolov and Melikhov−07] and [Solveson, et al. − 06]:

$$\Delta P(t) = \Delta P_s(t) + \Delta P_r(t) = R_s\left[i_{sa}^2(t) + i_{sb}^2(t) + i_{sc}^2(t)\right] + R_r\left[i_{ra}^2(t) + i_{rb}^2(t) + i_{rc}^2(t)\right], \quad (2.2.4)$$

where R_S (R_r) is the resistance of stator (rotor) windings;

$i_{sa}(t), i_{sb}(t), i_{sc}(t)$ $\left[i_{ra}(t), i_{rb}(t), i_{rc}(t)\right]$ are instantaneous currents of stator (rotor) windings in $a-b-c$ co-ordinates.

Meanwhile, energy losses (ΔW) during the transient T_{TP} can be defined as

$$\Delta W = \int_0^{T_{TP}} \Delta P(t)dt\,. \quad (2.2.5)$$

The ratio of IM energy losses ΔW_{DS} during a direct start and IM energy losses ΔW_{SS} during a soft start is the function which shows dependence of the duration of control angle using (t_{ramp}) within the range [α_{min}; α_{max}] (see Figure 2.6).

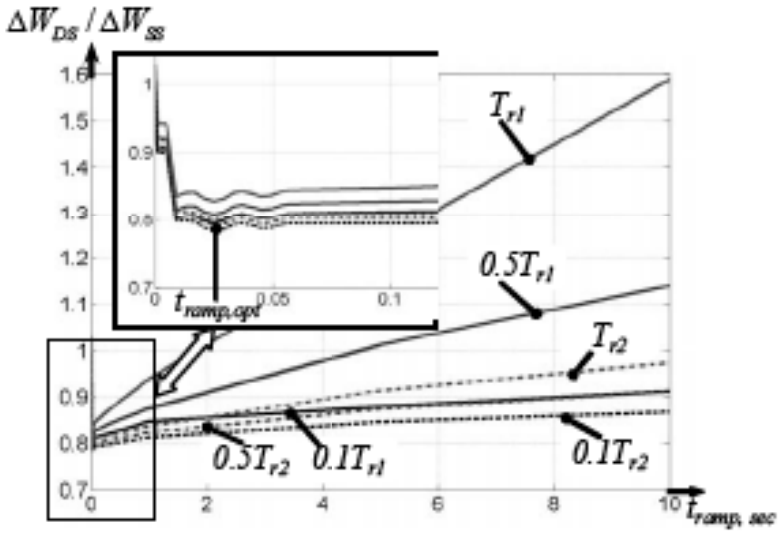

Figure 2.6: Evolution of relative losses during IM soft start.

The curves presented in Figure 2.6, were computer simulated for two IM mathematical models:

1. The induction machine 4AC132S4Y3 which is characterized by the moment of resistance on shaft T_{L1}={0.1·T_{r1},0.5·T_{r1},T_{r1}}, where T_{r1}=58 N·m is a rated electromagnetic torque.
2. The induction machine 4AC250M4Y3 which is characterized by the moment of resistance on a shaft T_{L2}={0.1·T_{r2},0.5·T_{r2},T_{r2}}, where T_{r2}=430 N·m is a rated electromagnetic torque.

The analysis of the dependences shown in Figure 2.6 allows to conclude that

there are several time instants (t_{ramp}) of duration of control angle rising t_{ramp}= $t_{ramp,opt}$ ≈0,02…0,03 sec, under which power losses decreased by 14-20% during soft start in comparison with an IM direct start. If t_{ramp}-value increases then power losses increase also due to the existence of additional time of IM operating in an underspeed mode. Consequently, unjustified increasing of the soft start duration leads to exceed of power losses as compared with the direct on-line start up of IMs.

One can analyze the logic diagram of IM automatic control system operation, which is presented in Figure 2.7, where the independent soft-starter is used for each IM start with the purpose to simplify Figure 2.7. In reality (as it will shown in Section 3.2), one soft-starter is connected in series with each IM with the help of the commutation equipment.

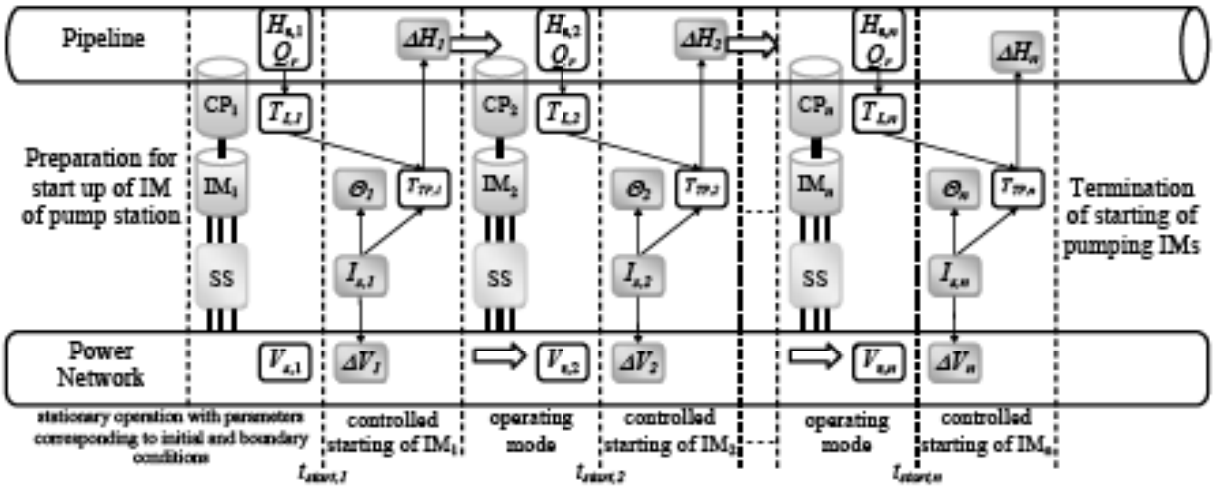

Figure 2.7: Operation diagram of IM automatic control system of pump station.

Let us consider a conventional start of IM pump aggregates with an application of soft-starters and current limitation algorithm, when the current reference I_{SCS} is the same for all pump station IMs, i.e. I_{SCS} = $I_{SCS,1}$ = $I_{SCS,2}$ =…= $I_{SCS,n}$. The root-mean-square linear voltage has the value V_1 in the secondary circuit of the transformer substation before the start of the first IM_1; there is a stable water head $H_{s,1}$ in the pipeline, this water head along with the initial water discharge Q_r stipulate the resistance torque value $T_{L,1}$ of the centrifugal pump CP_1. The controlled start of the first IM begins at the point of time $t_{start,1}$ after a corresponding instruction execution on the soft-starter. During the transient process: (1) the start currents lead to the voltage drop ΔV_1; (2) the stator winding temperature increases up to Θ_1; (3) the water head in the pipeline increases up to the maximum value ΔH_1. After a transient is over a water head sets in, which along with the water discharge Q_r will stipulate the resistance torque value $T_{L,2}$ of

the centrifugal pump CP_2. All n pump aggregate IMs are started in such a sequence and the values of state variables determined at the start of previous IMs are initial conditions for a start of each subsequent drive. In the course of use of a current-limited soft start, a user sets a maximum permissible value of factor k_I (2.2.1), which determines the total duration of transient T_{TP}. If the same quantity k_I is used while soft start for all of the induction machines of a pump station then changes occurred in the "power supply – soft-starter – induction machine – centrifugal pump – pipeline"-system are not taken into account. In particular, a choice of an understated value k_I can lead to the unfounded increase of transient and, correspondingly, decrease of the operating efficiency because of delay from the point of view of energy-saving. On the other hand, assign of an overstated value k_I cannot guarantee the safety mode for both induction machine windings and pipeline operation.

So, with the purpose of decrease of the electrical energy losses in induction machine windings, it is necessary to design the algorithm of k_I-value computation which allows ensuring $T_{TP} \to T_{TP,opt}\big|_{t_{ramp}=t_{ramp,опт}}$ and satisfaction of the above mentioned restrictions I_{SC}, $\Theta_{max,perm}$, $\Delta V_{max,perm}$, $\Delta P_{max,perm}$ applied on transients.

The achievement of this objective is possible if there is a mathematical model of "power network – soft-starter – induction machine – centrifugal pump – pipeline" system.

Both the presented definition of the induction machine soft start ACS and structural schemes in Figure 2.1, 2.3, allow concluding that the mathematical model of a pump station reflect adequately transients in the "power network – soft-starter – induction machine – centrifugal pump – pipeline" system.

The analysis of papers devoted to the problem of starting trajectories during transients in soft starter dynamics [Alger, et al. − 76], [Blaabjerg and Pederson − 97] and [Çadirci, et al. − 99] allows concluding that majority researches consider the peculiarity of electromechanical energy conversion and, correspondingly, IM dynamics during stationary (periodical) processes, but load dynamics and transients are not considered as a rule. In some publications analyzed water hammer processes in various environments don't take into account the combined dynamical processes in the pipelines and soft-starter-based pumping units [Çadirci, et al. − 99], [Guevara and Carmona − 90], [Sanks−98] and [Larock, et al. − 00]. This deficiency is caused by the necessity of the complex mathematical model formation that will be discussed in the next chapter.

2.3. Structure of the Mathematical Model of Automated Control System for Soft Starting Induction Motor

At the initial stage of design of an automated control system in particular, the fundamental regularities of dynamic processes are studied including formation of requirements and instructions for the next design stages. The achievement of this purpose supposes development of the mathematical model (MM) reflecting basic behavior of the engineering procedure in various media. The particularity of the soft starting induction machine automation control system of the water supply pumping station consists in that its mathematical model should adequately reproduce the transients in the "power network – soft-starter – induction machine – centrifugal pump – pipeline" system.

The obtained structural schemes of the pump station (see Figure 2.1) and pumping unit (see Figure 2.3) allow representing the mathematical model of soft starting induction machine in the view presented in Figure 2.8.

Two ways to problem approaches are used for modeling dynamical processes of a certain kind of system in dependence on modeling purpose [Larock, et al. − 00], [Kolokolov and Melikhov − 07], [Menon−04], [Solveson, et al. − 06], [Mezani, et al. − 05]: "distributed-based" and "lumped-based" ways.

The distributed problem setting assumes to research not only time-depending but also space-depending dynamical processes.

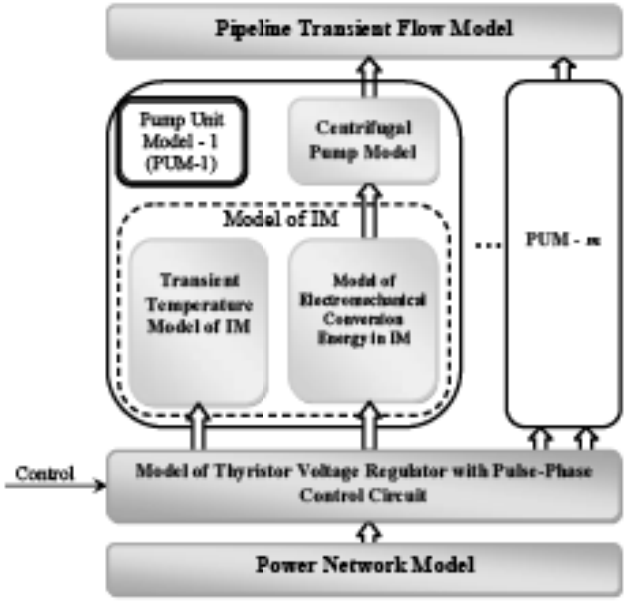

Figure 2.8: Structural scheme of mathematical model of the soft starting induction machine ACS.

The lumped problem setting assumes to research only time-depending dynamic processes. In this case differential equations in partial derivatives are reduced to the ordinary differential equations.

So, processes of the electromechanical energy conversion in IMs are considered usually through a distributed problem setting when dependences between geometrical parameters and transients should be analyzed in dynamics.

The peculiarity of the thesis consists in that IM dynamics is researched together with power converter dynamics including its control system. This circumstance stipulates an application of the lumped model of the subsystem SCRs-IM with the pulse-phase control circuit and the pumping load.

Taking into account the same reason the lumped model is applied to an IM thermal model for determination of maximum temperature rising in stator windings during a transient.

Hereafter, the power supply model includes an ideal model of a voltage transmission line and a model of a power transformer. Meanwhile, induction machines are connected sequentially to the secondary winding of the power transformer during a start of pumping units.

The outside bypass contactor is switched on when the starting process in IM dynamics is finished. Therefore, each induction machine can be represented by the ideal model of electromechanical energy conversion in relation to the operating process.

Design of new control algorithms for the soft starting induction machine ACS requires the usage of such a transient flow pipeline mathematical model that allows taking into account both energy losses decrease and water hammer exclusion. For this purpose, the distributed-based model of unsteady water flow in a pipeline needs to be designed by partial differential equation description.

The difficulties of experimental researches of the energy conversion dynamics in the soft starting induction machine ACS of the pump station are stipulated by the following causes:

(i) The value of surge current amplitude during transients varies from 200 A to 4000 A under voltage changes from 220 to 380 V. Meanwhile, the total consumed power can reach the value of about $2.5 \cdot 10^6 \div 3 \cdot 10^6$ V·A that requires the use of complicated and expensive experimental equipment.

(ii) The possibility of water hammer appearing with column separation effects can lead to destruction of the pipeline in the section with the maximum pressure localization [Chapple−03], [Guevara and Carmona − 90], [Larock, et al. − 00].

Therefore, experimental researches and service staff training are carried out by computer simulators in practice [Seleznov and Aleshin – 07].

Thus, to check-up of a new control algorithm and to develop the PC-based work station of dispatcher for monitoring pump station system it is necessary to design the soft starting induction machine ACS and realize it as an application package.

2.4. Conclusions

Let us mark some general points discussed in this chapter:

1. The pump station general structure for lifting, supply and distribution water systems includes the following major components: intake and elevated reservoirs, a bypass line, trunk pipeline, transforming station and soft starting electrical drives of centrifugal pumps. Due to high reliability requirements to electrical drives of water supply pump stations it is necessary to use the soft starters based on both SCRs with a pulse-phase control circuit and asynchronous protected squirrel-cage machine.
2. The analysis of energy losses changes in the soft starting induction machine windings allows concluding that there are values of duration of the control angle rising t_{ramp}= $t_{ramp,opt}$ =0,02…0,03 sec, at which the energy losses are reduced by about 14-20% during IM soft start in comparison with IM direct start of the IM. So, the problem setting for design of a new control algorithm for the soft start of pumping unit induction machines was formulated in this chapter.
3. The analysis of the requirements to the mathematical model of the "power network – soft-starter – induction machine – centrifugal pump – pipeline" system allows concluding that there is an insistent need to use the distributed-based model of an unsteady water flow in a pipeline with the purpose of transient true mapping. Meanwhile, the descriptions of both electromechanical energy conversion processes and temperature transients in an induction machine can be performed by application of the lumped approach.

CHAPTER 3

Modeling of Energy Conversion Processes in the Automation Soft Start Control System of Pump Station Induction Machines

3.1. Model of SCRs Fed Induction Machines under the Pulse-Phase Control

3.1.1. Unsymmetrical Two-Phase Operation Modeling

An induction motor mathematical model with the Silicon-Controlled Rectifiers (SCRs) and a pulse-phase control circuit are derived taking into account the traditional assumptions of the electromechanical energy conversion theory (for example, neglected by magnetic conductor saturation, an air gap between stator and rotor slots, a mechanical friction, etc.) [Alger, et al. – 76], [Lipo–71], [Zenginobuz and Çadirci – 01], [Melikhov and Hamzaoui – 05], [Melikhov and Loskutov – 05]. In addition, each SCR of the controlled regulator (hereafter, Thyristor Voltage Regulator (TVR)) is represented as an ideal switch without RC-snubber [Deleroi, et al. – 89], [Melikhov and Tsukanov – 04].

A pulse behavior of IM functioning with electronically controlled voltage utilizing series-connected silicon-controlled rectifiers (see Figure 3.1(a)) means the presence of constant structure intervals during the period of voltage supply [Çadirci, et al. – 99], [Hamed and Chalmers – 90], [Zenginobuz and Çadirci – 04].

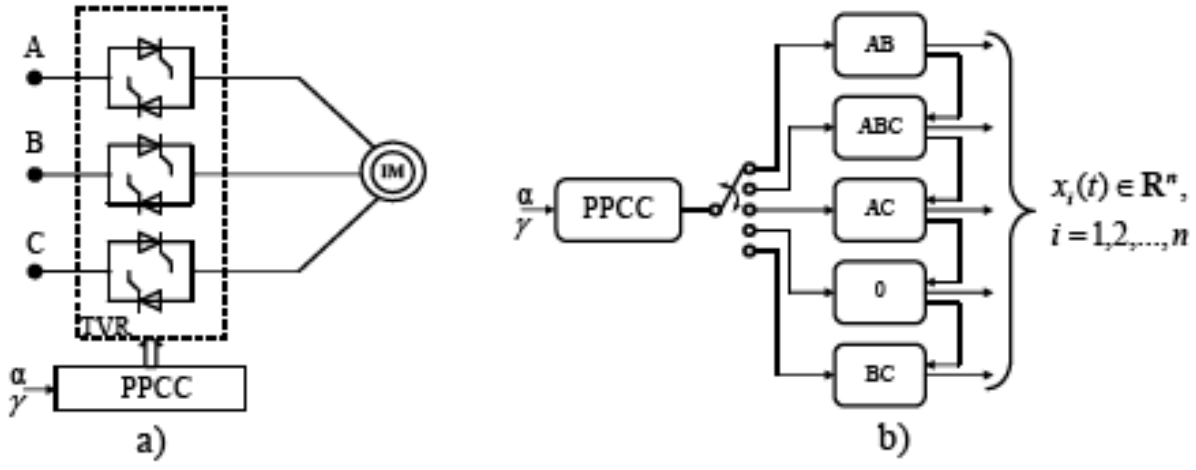

Figure 3.1: Structural scheme of drive (a);
order of IM connections to a voltage supply (b).

Each interval is characterized by the corresponding mode of IM connection to energy supply. In particular, there are three unsymmetrical two-phase operation modes

("AB", "BC", "AC") and two symmetrical three-phase operation modes ("ABC" and "0", where "0" means a disconnection mode) (see Figure 3.1(b)).

The ODE system for *j*-th structure constancy interval (SCI) can be presented in Cauchy normal form:

$$\frac{dx_i(t)}{dt} = f_i[x_1(t), x_2(t), ..., x_n(t), g(t)],\ x_i(t) \in \mathbf{R}^n,\ t \in [t_j, t_{j+1}],\ i = 1,2,...,n; \qquad (3.1.1)$$

$$x_i(0) = x_i^0,\ i = 1,2,..., n,$$

where f_i, i=1…n are non-linear functions; x_i, i=1...n are state variables of IM model (e.g., IM rotor angular velocity; currents and/or flux linkages of stator and rotor windings); $g(t)$ is the supply voltage; n corresponds to a number of the state variables (in particular, n=4 in the case of "0"-mode; n=5 in the case of "AB"-, "BC"-, "AC"-modes, n=7 in the case of "ABC"-mode).

Traditionally, modeling two-phase conduction modes ("AB", "BC", "AC") is carried out as shown in Figure 3.2, i.e., in the sequence of four steps [Hamed and Chalmers − 90], [Lipo−71], [Zenginobuz and Çadirci − 04], [Deleroi, et al. − 89]:

1) Formation of the three-phase IM model in ABC coordinates through Kirchhoff's and Ohm's laws.
2) Transformation of the rotor winding equations from rotating ABC-coordinates to fixed by use of EMF rotation *a*-*b*-*c*-coordinates in the rotor winding equations.
3) Transition to the general two-phase IM model in *a*-*b*-coordinates fixed in relation to a stator.
4) Transformation of the generalized two-phase IM model to a certain unsymmetrical one by applying additional conditions which characterize one of another kind of unsymmetrical model.

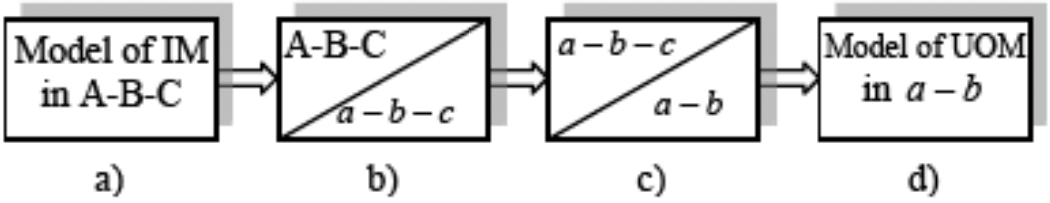

Figure 3.2: Current sequence of transformation applied to formation of simulators unsymmetrical operation modes (UOM) in induction motor.

The approach described above to modeling unsymmetrical operation modes is widely used, because all of the required mathematical transformations can be fulfilled "by hand". However, it has two principal disadvantages: first, the unsymmetrical operation mode is described by the model under the suggestion of symmetrical supply

voltage existence; second, at every listed step, it is necessary to transform the values of stator currents from *a*-*b*-coordinates to *a*-*b*-*c*-coordinates with the purpose to define the turn off moment of the certain thyristor.

Due to the abovementioned disadvantages, a new approach [Kolokolov et al.–06] to modeling an unsymmetrical operation mode is proposed in the thesis. Within this approach the mathematical model of a certain unsymmetrical mode is derived on the basis of Kirchhoff's and Ohm's laws in *a*-*b*-*c*-coordinates, that allows the elimination of periodical coefficients in equations. Meanwhile, intermediate transformations are highly complicated to do "by hand", therefore they carried out by application of Symbolic Math Toolbox (MATLAB 7.4®, The MathWorks, Inc.), [Melikhov and Tsukanov – 04].

In order to demonstrate the proposed approach let us describe the modeling "BC"-unsymmetrical mode.

Equivalent circuits of stator and rotor windings are shown in Figure 3.3. The system of equations describing the voltage balance in stator and rotor windings of the three-phase squirrel-cage IM has the following matrix form [Çadirci, et al. – 99], [Solveson, et al. – 06] and [Novotny and Lipo – 03]:

$$\mathbf{v}^s_{ABC} = R_s \mathbf{i}^s_{ABC} + \frac{d\lambda^s_{ABC}}{dt}; \tag{3.1.2}$$

$$0 = R_r \mathbf{i}^r_{abc} + \frac{d\lambda^r_{abc}}{dt}, \tag{3.1.3}$$

where $\mathbf{v}^s_{ABC}, \mathbf{i}^s_{ABC}(\mathbf{i}^r_{abc})$ are 3×1 vectors of stator voltages and stator (rotor) currents, respectively; $\lambda^s_{ABC}(\lambda^r_{abc})$ is 3×1 vector of stator(rotor) flux-linkages; R_s (R_r) is the resistance of stator (rotor) windings. Here after it is assumed that the stator and rotor resistances are distributed symmetrically.

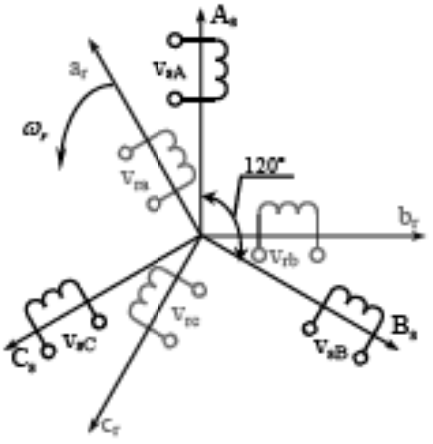

Figure 3.3: The equivalent circuit of three-phase IM.

Where, for example, the stator flux-linkage equation for "A" winding has the following form:

$$\lambda_{sA} = i_{sA}(L_{sA,l} + M_{AA}) + i_{sB}M_{AB}\cos\left(\frac{2\pi}{3}\right) + i_{sC}M_{AC}\cos\left(-\frac{2\pi}{3}\right) + i_{ra}M_{Aa}\cos(\theta) + i_{rb}M_{Ab}\cos\left(\theta + \frac{2\pi}{3}\right) + i_{rc}M_{Ac}\cos\left(\theta - \frac{2\pi}{3}\right), \quad (3.1.4)$$

where i_{sA}, i_{sB}, i_{sC} (i_{ra}, i_{rb}, i_{rc}) are instant stator(rotor) currents of IM windings by "A"("a")-, "B"("b")- "C"("c")-axes respectively; $L_{sA,l}$ is the leakage inductance of "A"- stator winding; θ is the angle between the stator and rotor windings; M_{AA}, M_{AB}, M_{AC}, M_{Aa}, M_{Ab}, M_{Ac} are mutual inductances between "A"- stator winding and other stator and rotor windings. Meanwhile, the values of the listed mutual inductances are accepted to be equal to the maximum mutual inductance IM in any pair of stator and rotor windings [Kolokolov, et al. – 06] and [Novotny and Lipo – 03].

The equivalent circuit of the stator windings corresponding to "BC"-unsymmetrical mode is shown in Figure 3.4.

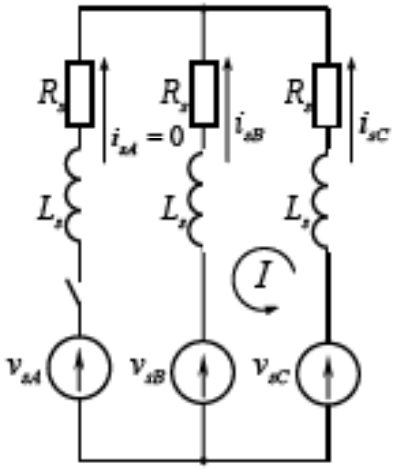

Figure 3.4: The equivalent circuit of stator windings corresponding to "BC"-unsymmetrical mode.

In Figure 3.4, a total stator winding inductance is designated by symbol L_s, where $L_s = L_{sA,l} + M$ for an ideal symmetrical machine. Therefore, the following equations can be written on the basis of Kirchhoff's laws in relation to the loop «I»:

$$i_{sA}(t) = 0; \quad (3.1.5)$$

$$i_{sB}(t) = -i_{sC}(t); \quad (3.1.6)$$

$$v_{sC} - v_{sB} = R_s i_{sC}(t) + \frac{d\lambda_{sC}(t)}{dt} - R_s i_{sB}(t) - \frac{d\lambda_{sB}(t)}{dt}. \quad (3.1.7)$$

Substituting (3.1.6) into (3.1.7) gives:

$$v_{sC} - v_{sB} = 2R_s i_{sC}(t) + \frac{d\lambda_{sC}(t)}{dt} - \frac{d\lambda_{sB}(t)}{dt}. \quad (3.1.8)$$

With the purpose of obtaining a "BC"-mode complete equation system, it is necessary to combine Equation 3.1.8, three equations of the voltage balance in rotor windings and the balance equation of machine shaft moments. The equation of electromechanical energy conversion in "motor" mode is given as [Novotny and Lipo – 03]:

$$\frac{d\omega_r}{dt} = \frac{1}{J_\Sigma}(T_e - T_L), \quad (3.1.9)$$

where ω_r is the angular velocity of the rotor and its rigidly connected load, J_Σ is the total inertia moment in (kg·m^2) of the rotor and associated with other rigidly connected rotating masses, T_e is the electromagnetic torque, and T_L is the load torque including all rotational losses.

On the basis of numerous researches, the authors of publication [Petrov and Petrov – 02] suggest dividing all the mathematical transformations into two groups: equivalent transformations; equivalent transformations in expanded sense. Transformations of the first group are mathematically equivalent, but their usage can change the boundaries of regions of parametric stability. Transformations of the second group are mathematically equivalent also but their usage does not change the regions of parametric stability. The comparison of the parametrical stability regions on an example of the model of "BC"- unsymmetrical mode was described in [Kolokolov, et al. – 07]. The presented results show up the difference between models derived by use of traditional assumptions and a proposed approach. Therefore, one or several intermediate transformations of the traditional approach between the first and the fourth stages (depicted in Figure 3.2) are not equal in a wide sense. So, the transformations 2-4 are not used in the proposed approach, because they can change the boundaries of parametric stability regions regarding the unsymmetrical operation model. Listing of MATLAB script-file describing the unsymmetrical models is presented in APPENDIX B.

3.1.2. Development of Pulse Energy Conversion Systems. Approach to Computation Time Reduction

The models of the constant structure intervals (CSIs) obtained above for SCRs fed

an induction machine is characterized by the following two features:

a) Nonlinearity of ODEs describing constant structure sections (with the exception of "0"-mode model);

b) High order of ODEs increasing four-dimensionality.

The simulation of such models is carried out by the fitting data approach [Banerjee and Verghese – 01]. In this case, an ODE solution at the end of the CSI running is treated as the initial condition for the next CSI. However, it is necessary to choose the stable algorithm of numerical integration which allows the minimization of total computation time under the condition of the required local integration error.

Concerning computation time reduction, several approaches are proposed in the literature, for example: cluster computers based on use of the parallel algorithms theory [Forenc–02]; optimization of algorithms by the integration of the quickest convergence [Butcher–03]; and so on. The minimization of total computation time is a very important problem, especially for the analysis of pulse energy conversion system dynamics. However, an application of the particular simulation algorithm for this purpose is used usually without justified motivation [Hamed and Chalmers – 90], [Barrade–08], [Flaviis–08], [Irwin and Woodford – 08], [Geldhof and Vyncke – 06].

A new approach to computational time reduction [Kolokolov, et al. – 08], [Kolokolov, et al. – 08] for simulation of pulse energy conversion systems is proposed in the thesis. This approach is based on the following propositions:

1) Nonlinear ODEs describing CSI are represented in Cauchy's form. The choice of both integration methods and their parameters (for example, an approximation order and integration step) is justified on the basis of the analysis of the non-linear ODEs stiffness, and also the requirements of this method, stability and the required local error E_{tol}^{local}.

2) Each integration method is realized by an algorithm (hereafter a "sub-algorithm"), which ensures the minimal computational time taking into account the duration of the running CSI.

So, the combination of several sub-algorithms into the generalized algorithm (hereafter a "hybrid algorithm") is proposed with the purpose of the computational time reduction. The hybrid algorithm organizes the choice of suitable sub-algorithms for the running CSI. Let us explain briefly the listed above stages of a hybrid algorithm design.

The ODEs stiffness is determined through the following expression [Butcher–03]:

$$S(t)=\frac{\max\limits_{1\le m\le n}|\mathrm{Re}\,\lambda_m(t)|}{\min\limits_{1\le m\le n}|\mathrm{Re}\,\lambda_m(t)|}, \tag{3.1.10}$$

where $\lambda_m(t)$ are eigenvalues of the matrix *A(t,w(t))*; $m=1,2,...,n$; *A(t,w(t))* is the matrix of invariable coefficients of the first approximation system for ODEs 3.1.1; *w(t)* is the stationary solution of ODEs (3.1.1).

The ODEs (3.1.1) is called "stiffness" on the solution *w(t)* for a certain CSI, if two conditions are satisfied:

1) $\mathrm{Re}\,\lambda_m(t)<0,\ m=1,2,...,n,\ \forall t\in[t_j;t_{j+1}]$;

2) The value of $\sup\limits_{t\in[t_j;t_{j+1}]} S(t)$ is too large.

The dependence of the stiffness (*S*) under variation of the angular velocity $\omega_r\in[0,\omega_r^s]$ is shown in Figure 3.5, where $\omega_{r,s}$ is the synchronous angular velocity of an IM shaft. Simulations are carried out in relation to the parameters of the induction motor "4A225M4Y3" (the rated power P_r=55 kW) under zero initial conditions.

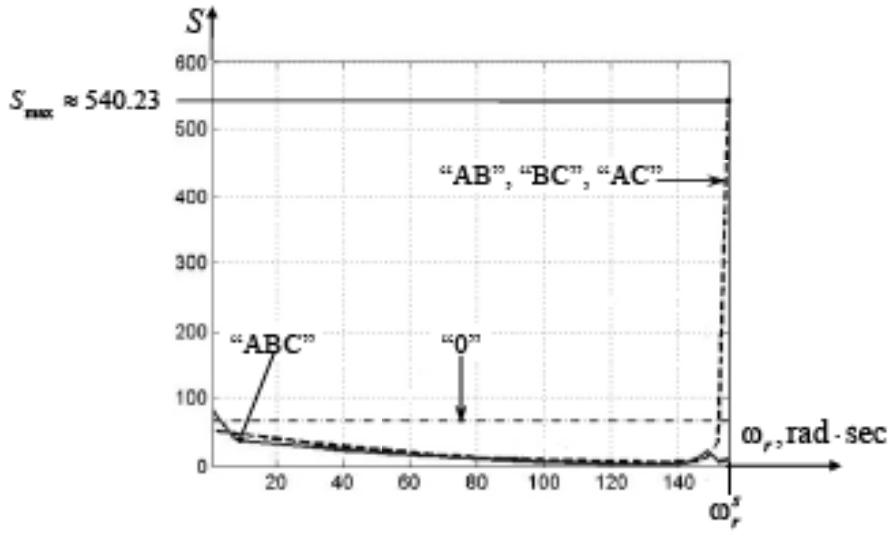

Figure 3.5: Dependence of the stiffness *S* on the angular velocity $\omega_r\in[0,\omega_{r,s}]$.

The analysis of the dependences shown in Figure 3.5 allows making the following conclusion: ODEs of the non-symmetrical modes ("AB", "AC", "BC") are characterized by the maximum value of the stiffness (S_{max}), which is approximated by:

$$S_{max}=\frac{\max\limits_{1\le m\le n}|\mathrm{Re}(\lambda_m)|}{\min\limits_{1\le m\le n}|\mathrm{Re}(\lambda_m)|}=\frac{187.6971}{0.3474}\approx 540.23. \tag{3.1.11}$$

In particular, this value belongs to the range of the non-stiffness ODEs [Butcher−03], [Geldhof and Vyncke − 06].

As presented in [Hoffman−01], [Quarteroni, et al. − 00], [Verner−92] and

[Verner−05], one-step integration methods are preferred for a non-stiffness ODEs integration under the criterion of computational time minimization. Meanwhile, it is well known that the majority of one-step integration methods represent Runge-Kutta methods (RKMs).

Restrictions on the integration step are determined in the RKMs theory in relation to the stability demand. For example, this condition for the second order RKMs (p=2) has the following form:

$$h_{p,\max}\big|_{p=2} \le \frac{2}{|\lambda_{\max}|}, \tag{3.1.12}$$

where $\lambda_{\max}$ is the maximum eigenvalue of the matrix *A(t,w(t))*.

Substituting $\mathrm{Re}(\lambda_{\max})$ from (3.1.11) into (3.1.12) gives:

$$h_{p,\max}\big|_{p=2} \le \frac{2}{187.7} \le 1.07 \cdot 10^{-2}. \tag{3.1.13}$$

So, the stability requirement shows the maximum value of the local step size $h_{p,\max}$.

Integration algorithms of the embedded Runge-Kutta methods (ERKM) calculate the integration step size h_k ($h_k < h_{p,\max}$) automatically guaranteeing the required accuracy. The integration accuracy is determined first by the local integration accuracy $\xi_j \in \mathbf{E}_{tol}^{local}$ which is estimated taking into account the metrological performances of the measuring instruments. Further we consider by an example how this accuracy is estimated in the thesis regarding encoders − ProCoder (BDH, made by Baumer Electric, Germany) which are widely used. It is possible to accept the local accuracy $\xi_j = 1 \cdot 10^{-4}$, which is the double accuracy margin of BDH-encoder [High-grade−08].

Let us determine the range of integration step size variation. The maximal step $h_{\max}$ is equal to the maximum value of the CSI duration ($\tau_{\max}$), which depends on the switching frequency (f_{SW}) of thyristors [Melikhov and Tsukanov − 04]: $\tau_{\max} = \frac{1}{f_{sw}}$, where $f_{SW} = q \cdot f_U$, and q is a number of TVR thyristors; f_U is the frequency of the power supply (f_u=50 Hz). In particular, the maximal value of CSI duration in the case of the model with symmetrical TVR is approximated by:

$$\tau_{\max} = \frac{1}{f_{sw}} = \frac{1}{6 \cdot 50} \approx 3.3 \cdot 10^{-3} \text{ s}. \tag{3.1.14}$$

The minimum value of the integration step h_{min} is determined in the following way: $h_{\min} = \min(h_{\min}^{\alpha}, \forall\alpha)$, where $h_{\min}^{\alpha}$ is the minimum value of the integration step for each

value of the control angle (α).

The simulation results show existence of the dependence between the integration step minimum value $h^{\alpha}_{\min}$ and the control angle α and this dependence has a complex non-linear form (see Figure 3.6).

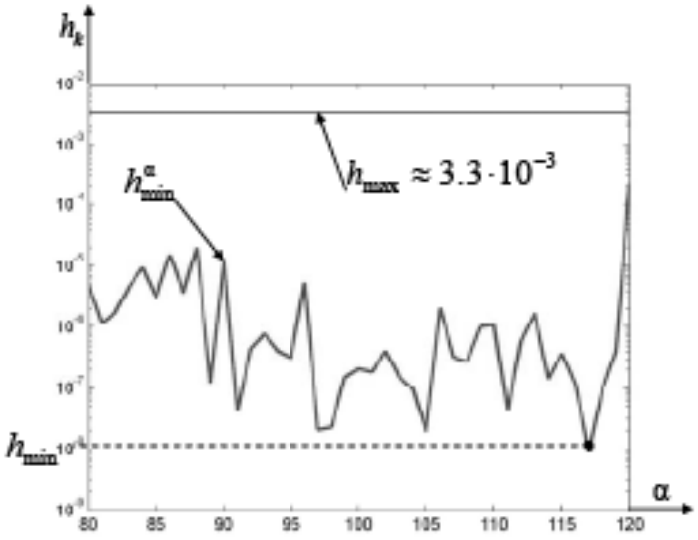

Figure 3.6: Relation between the integration step $h^{\alpha}_{\min}$ and control angle (α).

In Figure 3.6 the range of control angle variation α belongs to (80;120), that can be accepted as a typical one in the case of the symmetrical TVR with voltage synchronization [Hamzaoui, et al. – 04] and [Kolokolov, et al. – 07].

Increasing the approximation order leads to widening of RKM stability domain [Butcher–03]. This regularity allows using ERKM with $p \geq 2$, since their stability is provided by existence of $\tau_{\max} < h_{p,\max}\big|_{p=2}$ (3.1.13, 3.1.14). It relates especially to ERKM of the variable order $p(p+1)$ (hereafter ERKM-$p(p+1)$), since they are characterized by the quickest convergence among other algorithms of the same order [Forenc–02], [Geldhof and Vyncke – 06]. So, ERKM-$p(p+1)$ will be used preferably in the thesis.

The dependences of the total computational time T_{total} on the integration step h_k, where $h_k \in [h_{\min}; h_{\max}]$ are presented in Figure 3.7. These dependences are obtained by integration of (3.1.1) under zero initial conditions within the interval $t \in [0, T_y]$ with the local accuracy $\xi_j \leq 1 \cdot 10^{-4}$ for AB- and ABC-modes.

The analysis of the dependences $T_{total} = f(h_k)$ allows concluding: if both the approximation order (p) and a number of the stages (s) increased, then the total computational time T_{total} increased also. For example, T_{total} for Cash&Karp ERKM-4(5) [Verner–92] is smaller than T_{total} for Butcher ERKM-5(6) [Butcher–03] other equal

conditions.

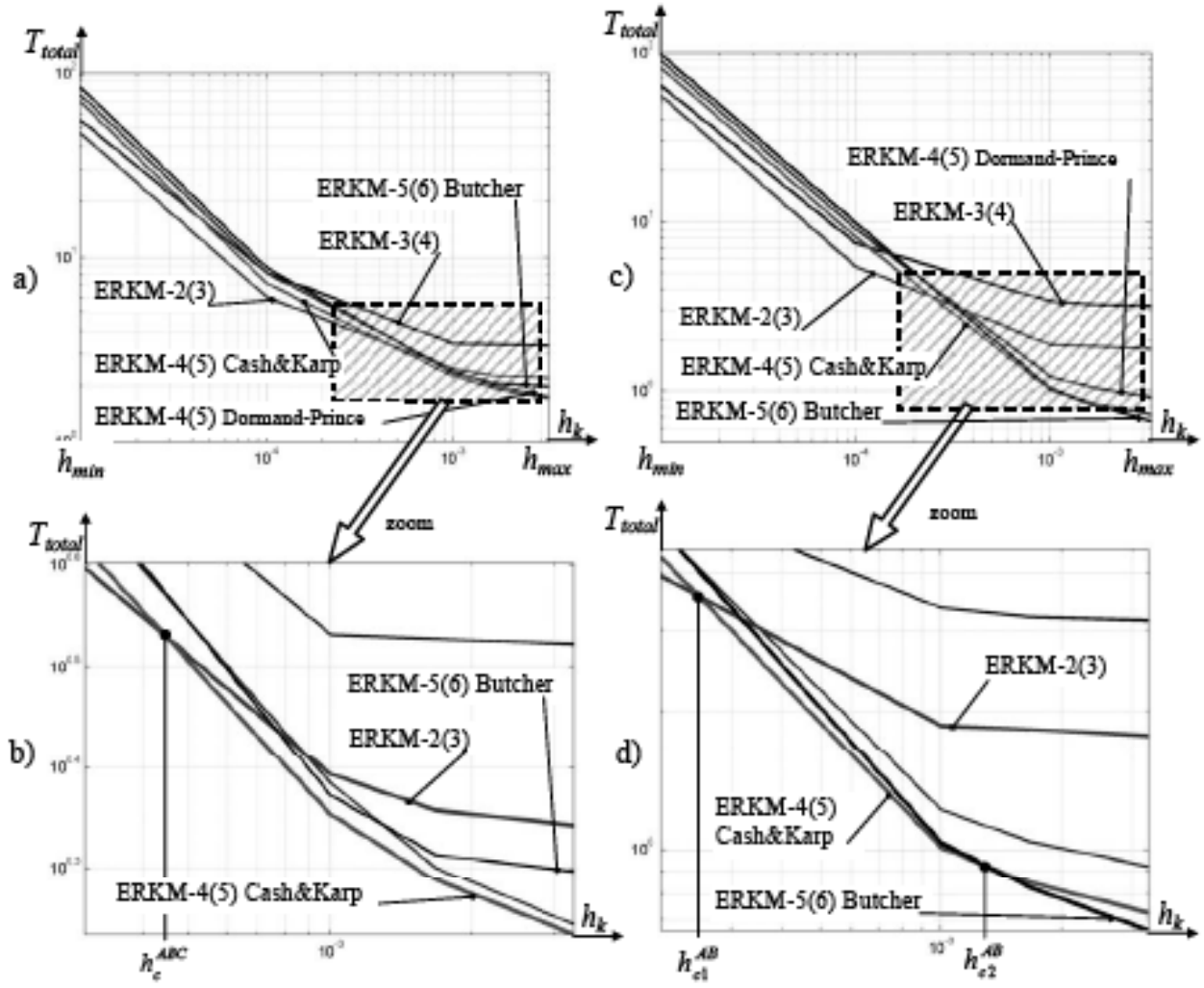

Figure 3.7: Dependences of $T_{total}=f(h_k)$ for BC-modes (a,b) and AB-modes (c,d).

Moreover, there are certain critical values of the integration step (for example, h_c^{ABC} in Figure 3.7(b) and h_{c1}^{AB}, h_{c2}^{AB} in Figure 3.7(d)), which divide the range $[h_{min}; h_{max}]$ into sub-ranges, each of them is optimal from the viewpoint of T_{total} minimization. If the difference between T_{total} values belonging to several integrating algorithms is too small, then it is necessary to prefer the algorithm with the smallest approximation order. For example, usage of ERKM-2(3) will guarantee the minimal T_{total} under $h_k < h_c^{ABC}$; usage of Cash&Karp ERKM-4(5) will guarantee the minimal T_{total} under $h_k > h_c^{ABC}$. Thus, Cash&Karp ERKM-4(5) is chosen as a basis for the development of the hybrid algorithm, because T_{total} value of Cash&Karp algorithm is the smallest or insignificantly exceeds T_{total} for Butcher ERKM-5(6) algorithms within the range $[h_{c1}^{AB}; h_{max}]$.

Being based on the previous analysis, it is possible to develop the "hybrid"

algorithm for simulation of non-linear switched models. The scheme, shown in Figure 3.8 presents the main points of the hybrid algorithm.

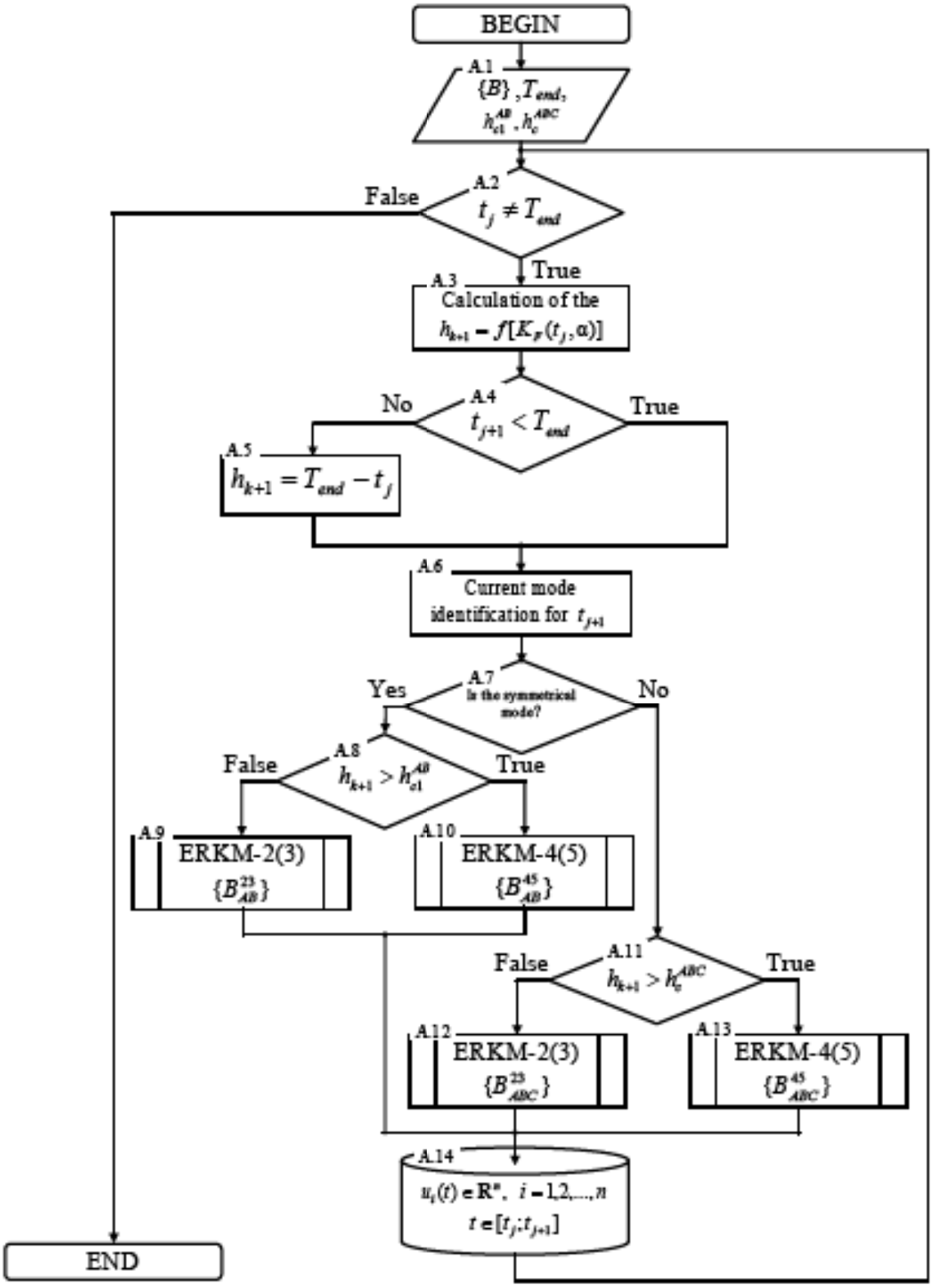

Figure 3.8: Hybrid algorithm for simulation of the SCRs feeding IM with PPCC.

Input data A.1 includes: T_{end} is the moment of integration end; h_{c1}^{AB}, h_c^{ABC} are critical values of the integration step; $\{B_{ABC}^{23}\}, \{B_{ABC}^{45}\}$ and $\{B_{AB}^{23}\}, \{B_{AB}^{45}\}$ are factors which are used

in ERKM algorithms of an integration step control in order to integrate "ABC"- "AB"-model respectively. While running time (t_j) is smaller than T_{end} A.2 the integration step (h_{k+1}) for the next iteration is calculated A.3 as a function of the running control angle (α), running time (t_j) and running value of the pulse commutation function (K_F). While integration in the neighborhood of T_{end} h_{k+1} -value is corrected so that $h_{k+1} \le T_{end}$ A.4, A.5. The running mode is identified at the time moment $t_{j+1} = t_j + h_{k+1}$ A.6. This mode can be symmetric or non-symmetric. If the running mode is non-symmetric and $h_{k+1} > h_{cl}^{AB}$ A.8 then ERKM-2(3) under $\{B_{AB}^{23}\}$-coefficients is applied A.9, else Cash&Karp ERKM-4(5) under $\{B_{AB}^{45}\}$-coefficient is applied A.10. The similar sequence is realized for symmetric mode A.11, A.12, A.13. The computed state variables $u_i(t) \in R^n$ in relation to the interval $t \in [t_j; t_{j+1}]$ are saved into the output matrix A.14.

The dependences of the total computational time T_{total} on the control angle α within the time range $t \in [0, T_{TP}^{max}]$ (where T_{TP}^{max} is the maximal duration of transients under $\alpha \in [80,120]$) is presented in Figure 3.9 for SCRs-IM model. They are obtained by use of the proposed hybrid algorithm and traditional internal algorithm *ode45* ("*MATLAB 7.0*®).

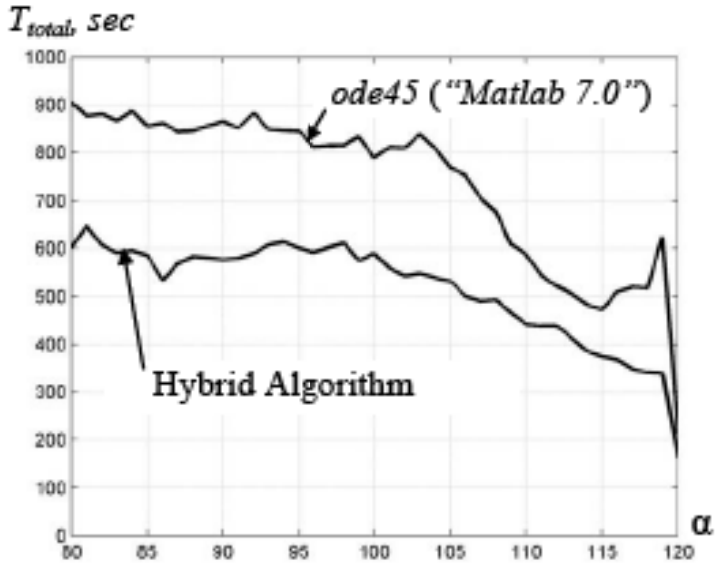

Figure 3.9: Dependences of T_{total} on α by SCRs-IM simulation within the time range $t \in [0, T_{TP}^{max}]$.

The results presented in Figure 3.9 show that the use of the hybrid algorithm allows reducing the total computational time of SCRs-IM simulation in comparison with

the usage of the internal function *ode45*. In particular, for SCRs-IM model T_{total}-value can be reduced from 19,2% to 30%, that is equal to the average value about 27,3%.

Problem setting and fulfillment of experimental researches are carried out in Section 4.1 with the purpose of validation of both SCRs fed IM model and hybrid algorithm adequacy. Meanwhile, the experimental plant, designed and produced in the laboratory of "Pulse Energy Conversion Systems" (Orel State Technical University), will be used.

3.1.3. SCRs-IM with Pulse-Phase Control Circuit and Two Synchronization Types

Two types of synchronization are used usually in SCRs-IM [Bredthauer and Struck – 95], [Kolokolov, et al. − 07]:

(i) Supply voltage synchronization (VS), when the thyristor firing angle (α) is calculated beginning from the point where there is the intersection of the phase voltage curve and abscissa;

(ii) Current synchronization (CS), when the control angle γ is calculated beginning from the moment at which a thyristor is triggered on with respect to the phase-current reaches zero.

Interrelation between the control angles (α and γ) represents the following expression:

$$\alpha = \delta + \gamma. \tag{3.1.15}$$

Simulation of stationary modes in SCRs-IM will be carried out under equal initial conditions for each synchronization types: VS and CS. With this purpose it is necessary to determine (estimate) the angle δ for IM specified parameters.

It means making (drawing) the dependence $\alpha = f(\gamma)$ while stationary mode by numerical simulations of SCRs-IM with PPCC (the dots in Figure 3.10). The shape of the obtained curve allows its approximating by a straight line (the line in Figure 3.10). The equation, corresponding to this line has the following form:

$$\alpha = \gamma + 64. \tag{3.1.16}$$

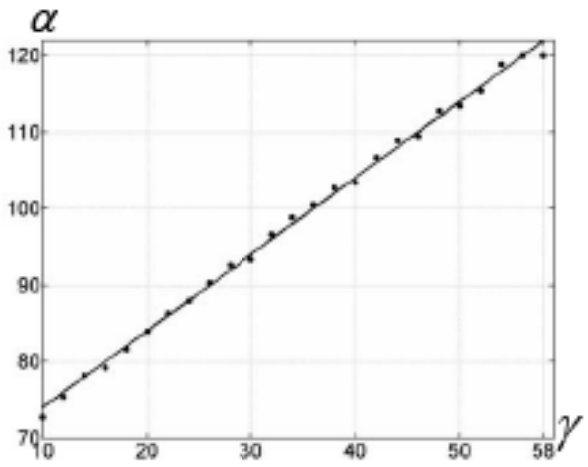

Figure 3.10: Dependence of the control angle α on γ.

The time dependences of both angular velocity $\omega_r(t)$ IM shaft and stator current $i_{sA}(t)$ of "A"-winding are shown in Figure 3.11(a). The control angle α is equal to 89 degrees. A moment of inertia (*J*) on the IM shaft is equal to the rated one ($J=J_{rated}$). The relative deviation of the angular velocity $\omega_r(t)$ from its stationary value is calculated by the expression: $\Delta\omega = \frac{\omega_\sigma}{\overline{\omega}_r}\cdot 100\%$, where $\omega_\sigma = \sqrt{\frac{1}{n-1}\sum_{i=1}^{n}\left(\omega_{r,i}-\overline{\omega}_r\right)^2}$, i=1...n is a mean square deviation of angular velocity $\omega_r(t)$ from the mean angular velocity $\overline{\omega}_r = \frac{1}{n}\sum\omega_{r,i}$ while stationary mode.

The construction of the current envelope $\hat{I}_{sA}$ (see Figure 3.11(a)) allows determining the oscillation period $T\big|_{\alpha=89} = 2.14$ s.

The interrelation between the amplitudes (I_{sA}^{m}) and frequency (*f*) of current sub harmonics $i_{sA}(t)$ shows that the quasi-periodical components (f=3·f_{base},5·f_{base},7·f_{base}...) exist around the fundamental frequency f_{base}=50 Hz. It is necessary to note the considerable peak-to-peak value of IM angular velocity, the relative deviation of which ($\Delta\omega$) reaches till 3%.

Let us draw the similar dependences for SCRs-IM with the current synchronized PPCC. Having expressed (3.1.16) through γ and substituting $\alpha = 89$, we get $\gamma = 35$ degrees. The obtained $i_{sA}(t)$ and $\omega_r(t)$ - graphs while stationary mode and $i_{sA}(t)$ –spectrum are shown in Figure 3.12 for SCRs-IM with the current synchronized PPCC.

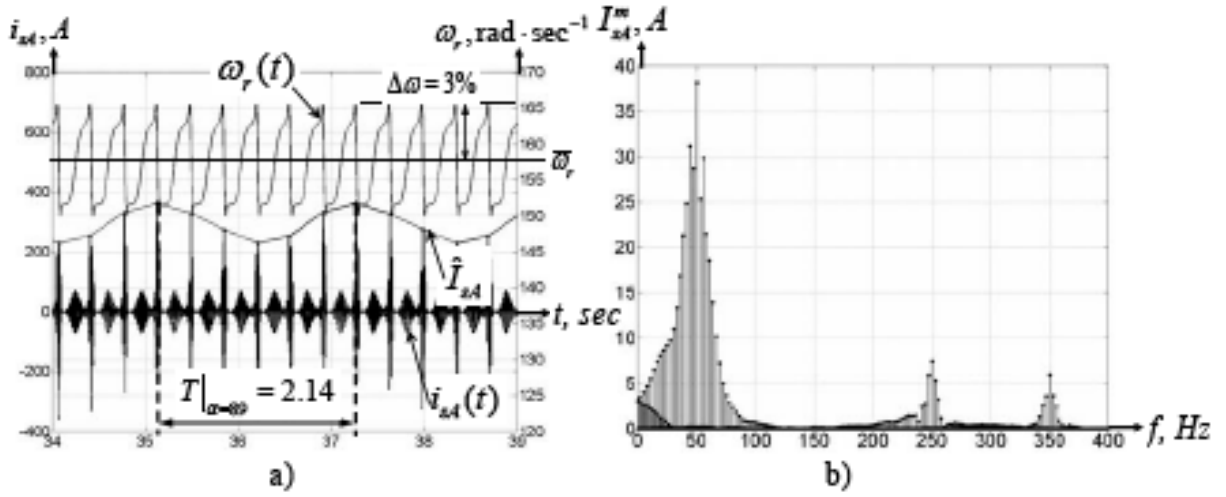

Figure 3.11: Electromechanical processes in SCRs-IM with voltage synchronized PPCC at a stationary state (a); dependence of I^m_{sA} −amplitude on frequency *f* of the current $i_{sA}(t)$ harmonic components (b).

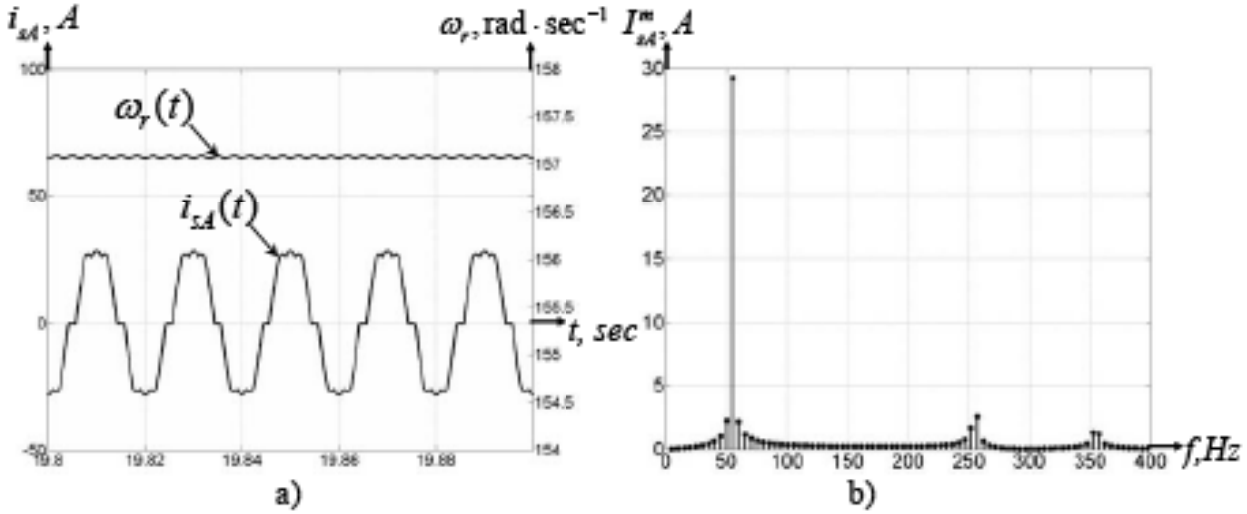

Figure 3.12: Electromechanical processes in SCRs-IM with current synchronized PPCC at a stationary state (a); the dependence of the amplitude I^m_{sA} on frequency *f* of the current $i_{sA}(t)$ harmonic components (b).

The relative deviation of the angular velocity does not exceed the value $|\Delta\omega| = 4.8\cdot10^{-3}\%$ (see Figure 3.12(a)). The frequency spectrum of $i_{sA}(t)$ (see Figure 3.12(b)) shows that the value of quasi-periodical components are too small.

Theoretical analysis of the non-linear switched model stability is a very complicated problem, but it can be carried out numerically. One of the most widespread numerical method is based on monodromy matrix calculation [Banerjee and Verghese −

01]. Meanwhile, the main idea consists in, firstly, derivation of the monodromy matrix of a steady-state model. Secondly, calculation of the matrix eigenvalues allows making the conclusion about stability of the running system state [Banerjee and Verghese − 01].

With the purpose of analysis of the stationary state stability the shift mapping is used [Banerjee and Verghese – 01], [Toyoshima, et al. − 04]:

$$\mathbf{X}_k=\mathbf{F}(\mathbf{X}_{k-1}), \tag{3.1.17}$$

where $\mathbf{X}_k$, $\mathbf{X}_{k-1}$ are phase vectors at the moments T(k-1) and kT, accordingly **F** is the vector function transformed to an autonomous form. The sequence of fixed points $\mathbf{X}_{ck}$, k=1,2,..,m of mapping (3.1.17) corresponds to the periodical process with T_m-period which is multiple in times of T-period of the supply-voltage. As a result, $\mathbf{X}_{ck} = \mathbf{F}^{(m)}(\mathbf{X}_{ck})$, where $\mathbf{F}^{(m)}$ represents m-consecutive iteration of mapping (3.1.17).

Coordinates of the fixed points are determined in the following way: the analyzed model is integrated on T-period with calculation of the maximum distance between the elements of $\mathbf{X}_{k-1}$- and $\mathbf{X}_k$-vectors till this distance is less than the required accuracy.

The local stability of m-cycle $\mathbf{X}_{ck}$, k=1,2,..,m is researched with the use of perturbations equations. In this case it is supposed $\Delta_k=\mathbf{X}_k-\mathbf{X}_{ck}$, k=1,2,..,m is the infinitesimal perturbance of the phase vector $\mathbf{X}_k$ regarding the coordinates of m-cycle**.** Then the disturbance at (k+1)-step has the following form in linear approximation: $\Delta_{k+1}=\mathbf{J}_k\Delta_k$, where $\mathbf{J}_k=\left.\frac{d\mathbf{F}}{d\mathbf{X}}\right|_{\mathbf{X}=\mathbf{X}_{ck}}$ is Jacobian matrix calculated at $\mathbf{X}_{ck}$, k=1,2,.., m. Evolution of Δ_k-disturbance through m iterations of mapping (3.1.17) is calculated as follows: $\Delta_{m+1}=\mathbf{M}\Delta_1$, where $\mathbf{M}=\prod_{k=1}^{m}\mathbf{J}_k$ is the monodromy matrix corresponding to the m-cycle.

So, if the following condition is satisfied then it is possible to conclude that analyzed m-cycle is asymptotically stable [Banerjee and Verghese − 01]:

$$\left|\rho_i\right|<1, i=1,2,...,n, \tag{3.1.18}$$

where $\rho_i, i=1,2,...,n$ are eigenvalues of **M**-matrix.

Let us draw the surfaces formed by changes of the maximum eigenvalue $\rho_{\max}=\max_{1\le i\le n}\left|\rho_i\right|$ as a function of the control angle (α) and IM inertia moment (J). Similar surfaces for SCRs-IM with current and voltage synchronized PPCC are shown in Figure 3.13(a) and 3.13(b), respectively.

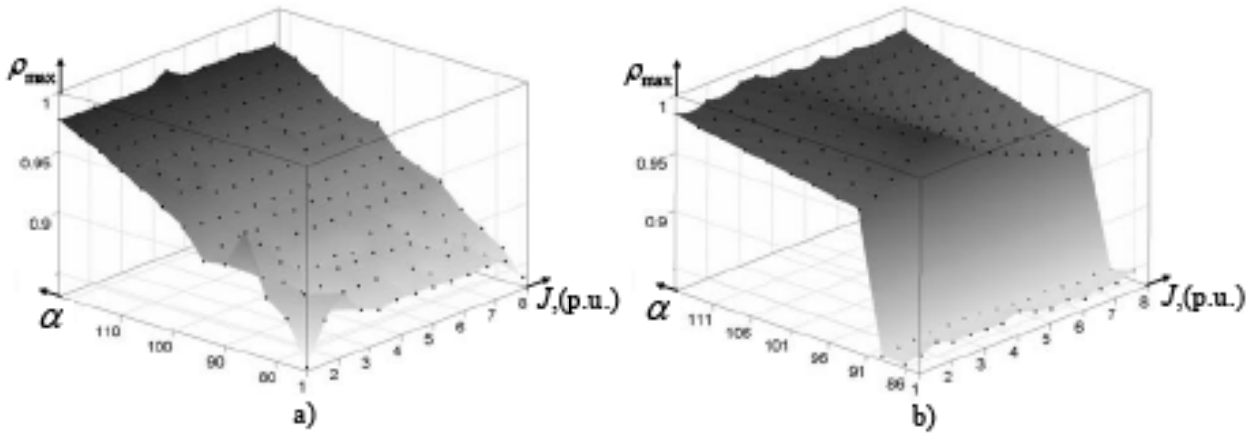

Figure 3.13: The ρ_{max} -surface for SCRs-IM with current synchronized PPCC (a) and SCRs-IM with voltage synchronized PPCC (b).

The analysis of ρ_{max} -surfaces allows making a conclusion, that the periodical processes of the studied models are stable (in terms of Lyapunov), because the condition (3.1.18) is fulfilled within the considered range of parameter variation. However, the amplitudes of angular velocity oscillations can be unacceptable for some applications.

Let us draw the surfaces which represent the evolution of a relative deviation of the angular velocity $\Delta\omega$ as a function of the control angle (α) and the IM inertia moment (J). For example, $\Delta\omega$-surfaces for SCRs-IM with current and voltage synchronized PPCC are shown on Figure 3.14(a) and 3.14(b), respectively.

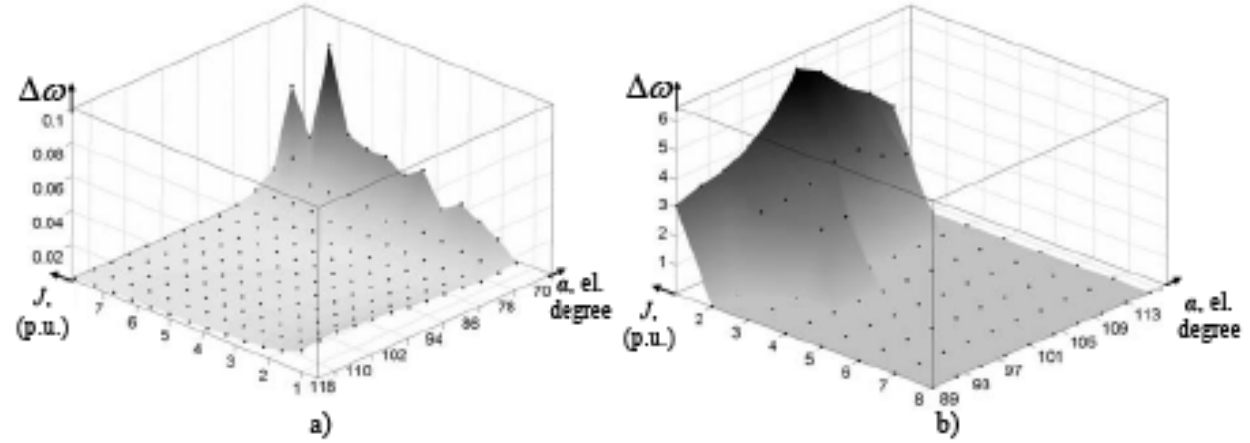

Figure 3.14: The $\Delta\omega$ -surface for SCRs-IM with current synchronized PPCC (a) and SCRs-IM with voltage synchronized PPCC (b).

The analysis of these surfaces allows making the following conclusion: the relative deviation of the angular velocity $\Delta\omega$ can be equal to 6% in the case of the SCRs-IM

with voltage synchronized PPCC; the relative deviation of the angular velocity $\Delta\omega$ is much less and can be equal approximately to $\Delta\omega \approx 0.08\%$ in case of SCRs-IM with current synchronized PPCC.

Now it is necessary to comment one of the ways of oscillation appearance in dynamics of SCRs-IM with voltage synchronized PPCC. With this purpose let us consider the output active voltage of a thyristor voltage regulator (V_{TVR}) under load-on and load dropping conditions. Meanwhile, the dynamics of the SCRs-IM ("4AC132S4Y3") operations with voltage synchronized PPCC is simulated under the control angle α=94 el. degree and total moment of inertia $J_\Sigma = J_r$ (see Figure 3.15).

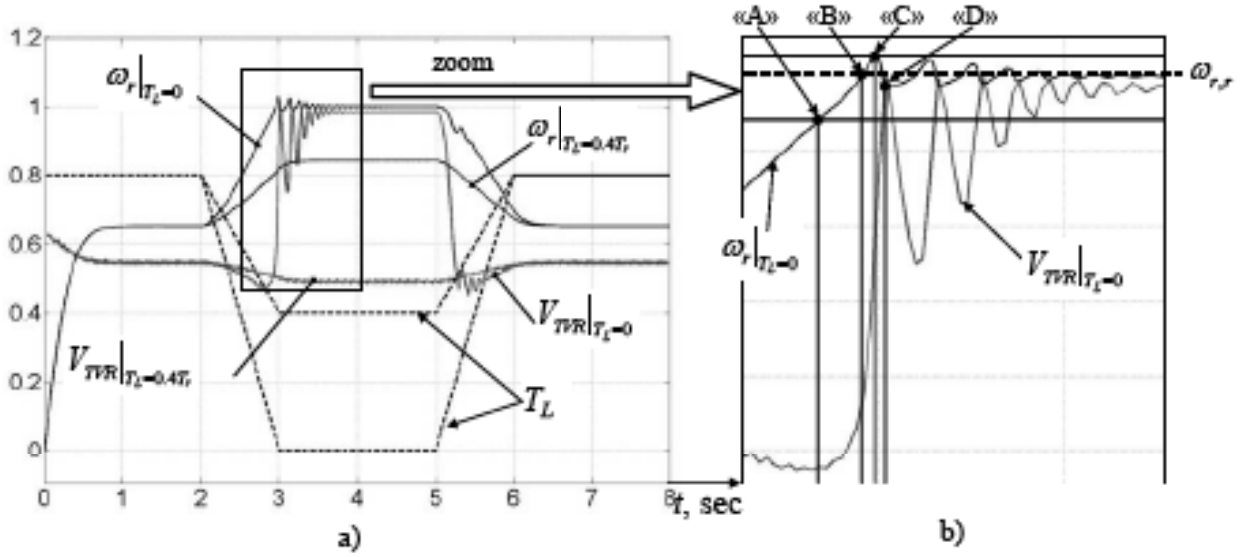

Figure 3.15: Diagrams of start, load surge and load dropping of SCRs with "4AC132S4Y3" IM and voltage synchronized PPCC.

These diagrams illustrate that after load dropping, the angular velocity begins to increase and the output active voltage (V_{TVR}) continues to decrease (see Figure 3.15(a)). Then the angular velocity sets into the region of subsynchronous velocities $\omega_r \geq 0.95\omega_{r,r}$ (interval between "A" and "B" points in Figure 3.15(b)). Meanwhile, V_{TVR}– voltage begins to increase rapidly that leads to getting IM- angular velocity into the regions of the above-synchronous velocities $\omega_r \leq 1.03 \cdot \omega_{r,r}$ (interval between "B" and "C" points in Figure 3.15(b)).

The direction of rotor winding currents changes to the contrary one within the above-synchronous velocity zone and the angular velocity ω_r begins to decrease (interval between "C" and "D" points in Figure 3.15(b)), but V_{TVR} continues to increase while ω_r does not belong to the subsynchronous velocity zone. As a result, an oscillating

process appears. It should be noted that out of the subsynchronous velocity zone under a load drop to T_L=0.4·T_r the similar oscillating processes is absent and the angular velocity increases smoothly up to the value corresponding to the operating mode.

The simulations performed under the same environmental conditions for SCRs-IM with current synchronized PPCC show absence of any oscillating processes (see Figure 3.16).

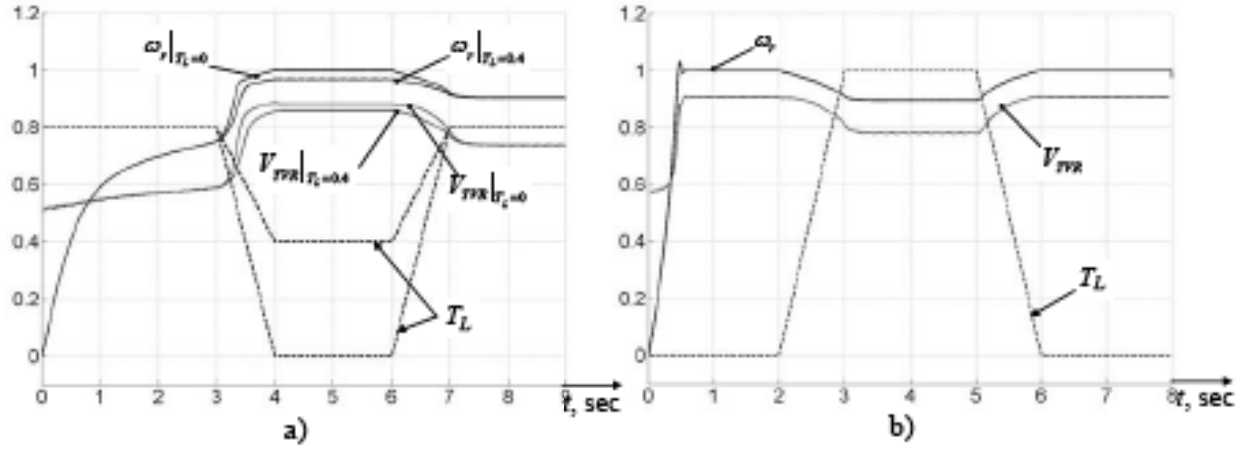

Figure 3.16: Diagrams of start, load surge and load drop of SCRs with "4AC132S4Y3" IM and current synchronized PPCC.

The dynamical processes considered above allow concluding, that the appearance of the internal positive feedback between the angular velocity of the rotor shaft and the output active voltage of the thyristor voltage regulator is a cause of the oscillations in the SCRs-IM with voltage synchronized PPCC.

The oscillations are shown essentially in an electric drive if the middle value of the total inertia moment (J_Σ) belongs to $[J_r;3\cdot J_r]$ and the control angle (α) belongs to (90;117) electrical degree as it is illustrated in Figure 3.14(b).

On the basis of the presented analysis it can be possible to make a conclusion, that SCRs-IM with current synchronized PPCC has better static and dynamical properties in comparison with SCRs-IM with voltage synchronized PPCC. So, soft starters with current synchronization became prevalence in various industrial applications.

3.2. Transformer Substation Mathematical Model

The pump station electrical equipment consists of the step-down transformers provided voltage supply for pump motors and several auxiliary transformers [Chapple –

03], [Martin − 98]. In particular, the pump stations of the first class of reliability are connected to at least two power lines (with rated voltage about 6,3 – 35 kV) and include not less than two auxiliary transformers.

With the purpose of adequacy verification of the adaptive algorithm of the pump motor with a soft starter, the simplified structure of a transformer substation is used. This structure includes one step-down transformer with two windings, which is connected to one power line. Meanwhile, it is possible to neglect the saturation of a transformer magnetic circuit. The simplified circuit of transformer substation together with switching high-voltage equipment (SHVE) and IMs is shown in Figure 3.17.

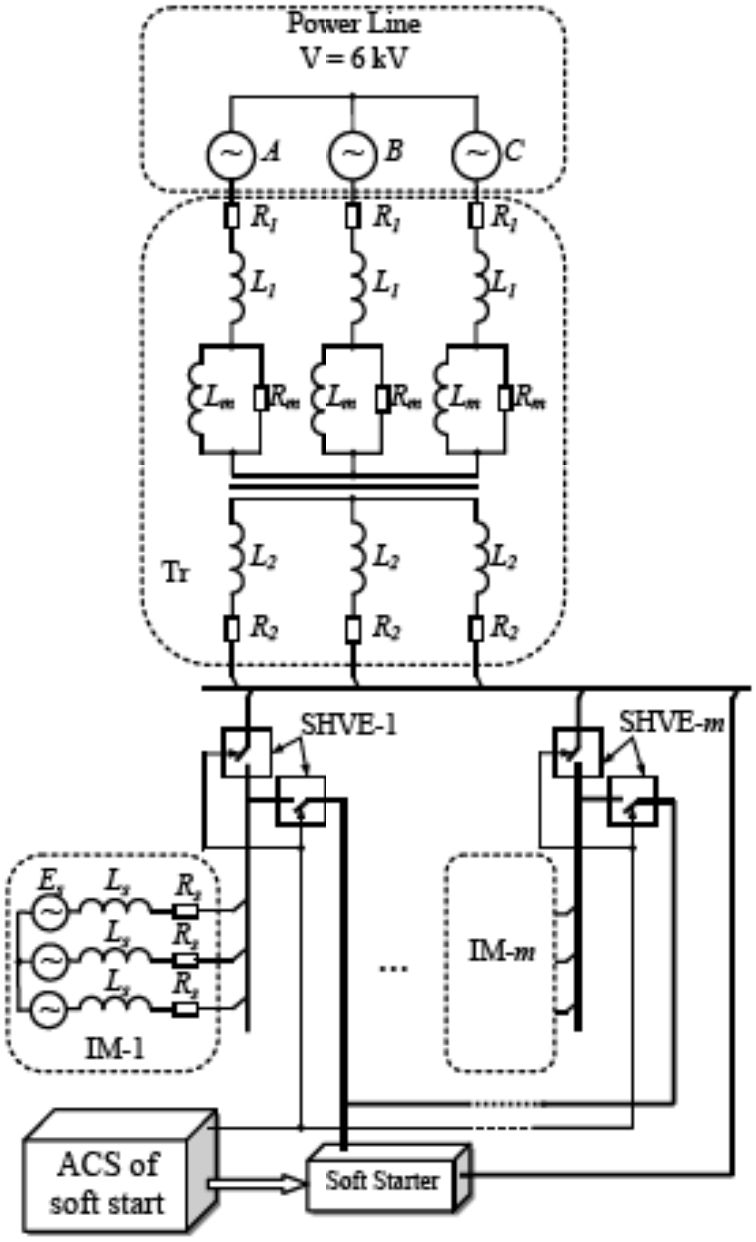

Figure 3.17: Equivalent circuit of the transformer substation including the step-down transformer, switched equipment and induction machines.

The calculation of a transformer capacity is carried out taking into account the number of main pump motors (without standby pump motors) in accordance with the following expression [Martin − 98]:

$$S = k\sum_{i=1}^{m}\frac{P_{r,i}}{\eta_i \cos\varphi_i} + S_{add}\text{, kV·A} \tag{3.2.1}$$

where k is the rate of power request which depends on the number of main pump motors: $k\big|_{i=2} = 1;\ k\big|_{i=3} = 0.9;\ k\big|_{i=4} = 0.8;\ k\big|_{i\geq 5} = 0.7$; $P_{r,i}$, η_i, $\cos\varphi_i$ - the rated power, the factor of mechanical efficiency and power factor, respectively; $S_{add} \approx 10...50$ kV·A is the total power of additional electrical equipment of a pump station.

It is well known that the matrix form is a more convenient for description of a transformer substation model, because it allows forming easily an equivalent circuit including any number of IMs. In particular, let us consider the mathematical model consisting of electrical motors and transformers [Martin − 98]. To unify the form of this model presentation in the cases of stationary states it is proposed initially the use of a two-phase ideal electromechanical energy converter, and then to obtain both an induction motor and transformer models as particular cases of the energy converter operation in certain stationary states. The system of equations of the two-phase ideal electromechanical energy converter becomes:

$$\begin{bmatrix} u_{sd} \\ u_{rd} \\ u_{rq} \\ u_{sq} \end{bmatrix} = \begin{bmatrix} r_{sd} + \frac{d}{dt}L_{sd} & \frac{d}{dt}M & 0 & 0 \\ \frac{d}{dt}M & r_{rd} + \frac{d}{dt}L_{rd} & L_{sq}\omega_r & M\omega_r \\ -M\omega_r & -L_{rd}\omega_r & r_{rq} + \frac{d}{dt}L_{rq} & \frac{d}{dt}M \\ 0 & 0 & \frac{d}{dt}M & r_{sq} + \frac{d}{dt}L_{sq} \end{bmatrix} \times \begin{bmatrix} i_{sd} \\ i_{rd} \\ i_{rq} \\ i_{sq} \end{bmatrix} \tag{3.2.2}$$

In a stationary state, the equation describing the rotor angular velocity has the following form:

$$\omega_r(t) = \omega_e = \frac{\omega_s(1-s)}{p_p}, \tag{3.2.3}$$

where ω_s is the fundamental angular synchronous velocity; s is the rotor slip; p_p is the number of pairs.

Substituting (3.2.3) into (3.2.2) and replacing $j\cdot\omega$ in place of d/dt we obtain:

$$\begin{bmatrix} u_{sd} \\ u_{rd} \\ u_{rq} \\ u_{sq} \end{bmatrix} = \begin{bmatrix} r_{sd} + j\omega L_{sd} & j\omega M & 0 & 0 \\ j\omega M & r_{r\alpha} + j\omega L_{rd} & L_{sq}\omega_c & M\omega_c \\ -M\omega_r & -L_{rd}\omega_c & r_{rq} + j\omega L_{rq} & j\omega M \\ 0 & 0 & j\omega M & r_{sq} + j\omega L_{sq} \end{bmatrix} \times \begin{bmatrix} i_{sd} \\ i_{rd} \\ i_{rq} \\ i_{sq} \end{bmatrix}. \quad (3.2.4)$$

Substituting $\omega_r = 0$ into (3.2.4) the transformer model is obtained. In addition, the angle between fixed windings is equal to 90°, so the magnetic relation between them is absent. It allows considering independently electromagnetic processes along *d*- and *q*-axes in relation to each phase of the three-phase transformer. If the primary winding and its parameters are designated by "1", the secondary winding and its parameters by "2" (as it is accepted in the transformer theory), then it allows rewriting the equation (3.2.4) in the following form:

$$\begin{bmatrix} u_1 \\ u_2 \end{bmatrix} = \begin{bmatrix} R_1 + j\omega L_1 & j\omega M \\ j\omega M & R_2 + j\omega L_2 \end{bmatrix} \times \begin{bmatrix} i_1 \\ i_2 \end{bmatrix}. \quad (3.2.5)$$

To derive the complete model of the electrical circuit shown in Figure 3.17, it is necessary to combine the equations similar to (3.2.5) for each phase of the transformer and equations similar to (3.2.4) for each motor connected to a supply line. The combined integration of such a system and analysis of the obtained results will be discussed in Section 4.2.

3.3. Simplified Induction Machine Thermal Model

There are two widespread approaches to a thermal dynamical process simulation based on the use of lumped and distributed models.

In the case of distributed-based modeling, two-dimensional or three-dimensional temperature field of an induction motor is described by partial differential equations [Mezani, et al. − 05]. Meanwhile, it is necessary first, to specify IM geometric topology. Then, to calculate thermal conductance regarding IM parts. Finally, to define initial and boundary conditions.

The method of finite elements is widely applied to simulate thermal processes in an induction motor by a distributed model usage. It allows getting the high-level accuracy of solutions under a few of accepted simplifications.

Distributed modeling is aimed at the optimization of a motor construction through the minimization of overheating and heating-cooling time constants [Mezani, et al. − 05].

The aim of this chapter consists in the determination of a maximal temperature of IM windings, which can be possible during the controlled start and the application of distributed modeling is not efficient in this case due to laboriousness.

Among the approaches to lumped modeling the thermal transients it is necessary to pick out the approaches based on the use of equivalent thermal circuits as the most popular at present [Boys and Miles – 94], [Mellor, et al. – 91], [Mezani, et al. – 05]. In this case stator and rotor equivalent parameters are represented in terms of lumped elements. No thermal coupling between the rotor and stator is considered. It has been found that an air gap provides a barrier for heat transfer from the stator to the rotor and vice-versa. Therefore, the model utilizes lumped parameters such as thermal conductance or resistances, thermal storage capacitors and heat sources [Boys and Miles – 94], [Lee and Habetler – 03] and [Mellor, et al. – 91]. The equivalent circuit of the thermal model is shown in Figure 3.18.

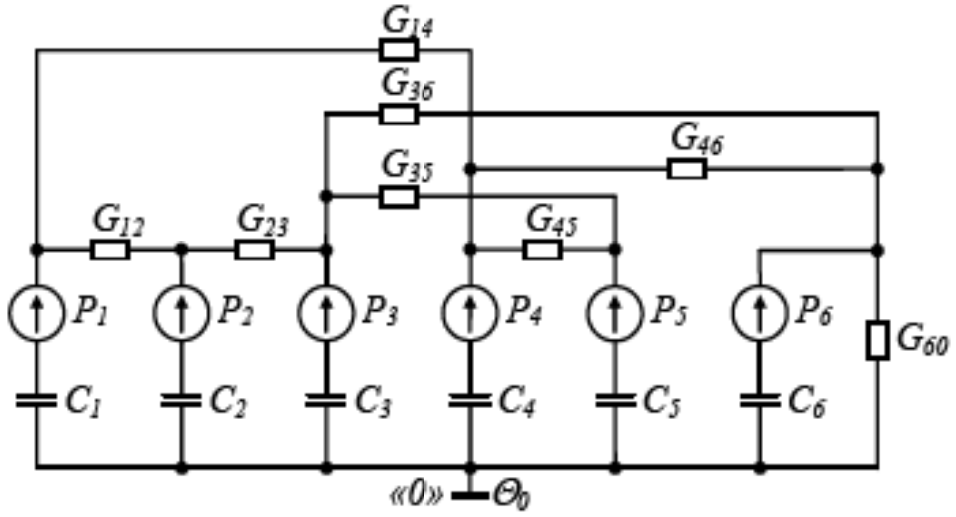

Figure 3.18: The equivalent circuit of IM thermal model.

In this figure the following signs are used:

- P_i – heat sources including end coils of stator windings P_1; slot stator windings P_2; a stator core P_3; an inside air P_4; a rotor core P_5; a motor frame P_6 .
- G_{ij} – thermal conductance between two corresponding surfaces of the heart sources within the motor;
- C_i – thermal capacitances of the heat sources;
- Θ_0 – a temperature of an environment.

Being based on Kirchhoff laws, the system of equations for the circuit shown in Figure 3.18 can be written in the following matrix form:

$$\frac{d\Theta}{dt} = \mathbf{C} \cdot \mathbf{P} - \mathbf{C}^{-1} \cdot \mathbf{G} \cdot \Theta, \quad (3.3.1)$$

where Θ is the temperature rise matrix; C is the thermal capacitance matrix; P is the vector of the heat sources; G is the thermal conductance matrix.

Stator winding data and machine physical data represent the initial information for calculation of C-,G-matrices. The considered model will be studied on adequacy in Section 4.4. In relation to "4A112M4Y3"-IM there will be represented the equation system solution (3.3.1) at the direct start with the purpose of the adequacy verification of the model mentioned above by comparison of numerical and experimental results.

3.4. Pumping Load Mathematical Model

The operating mode of a centrifugal pump is determined through the following parameters: the discharge q (m^3/hour), net head H (m) and speed n (rpm). The required values of the discharge and head $\{Q_{ref}, H_{ref}\}$ during the operating mode are the initial data while the choice of the appropriate pump. This choice is fulfilled from the manufactory series with the use of pump characteristic diagrams under the following condition: the point $\{Q_{ref}, H_{ref}\}$ should be located near the optimal point $\{Q_{p.opt}, H_{p.opt}\}$ corresponding to the maximum value of pump efficiency [Girdhar and Moniz – 05].

The diagrams of pump characteristic curves are shown in Figure 3.19 in relation to one stage of the vertical multistage centrifugal pump CV 400 (n=1450 rpm, Grundfos, Inc.) [Volk–05] for three values of impeller diameters (d = 315, 330, 350 mm).

The point of the maximum efficiency η_{max}, signed in Figure 3.19 for d = 330 mm, will define the optimal pair $\{Q_{p.opt}, H_{p.opt}\}$ and power P_2 required when pump operating at the optimal operating point. The steady-state mode of pump operation under a certain speed n=*const* is defined by a graphical method, through the search of the intersection point between Q-H- and net characteristic curves as it is shown in Figure 3.19. The net head can be written as [Sanks–98]:

$$H_{net} = H_{ST} + k_{net} q^2, \quad (3.4.1)$$

where H_{ST} the a static head in the pipe; k_{net} is the coefficient of pipe losses.

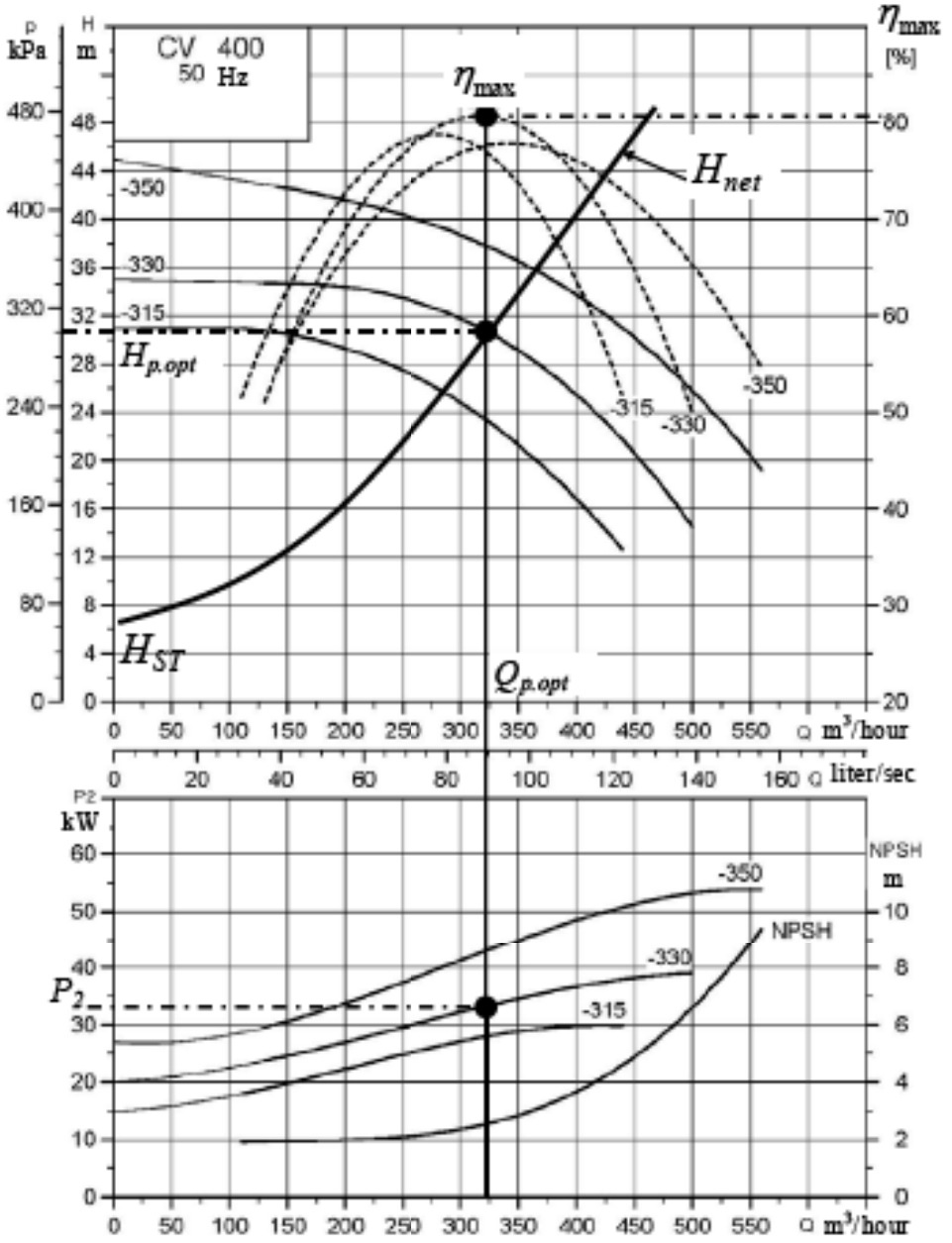

Figure 3.19: Diagrams of pump characteristic curves of CV 400 (Grundfos, Inc.) [Volk−05].

Usually, it is assumed that a pump prototype has homologous features, i.e., there are geometric and kinematic analogies between a model and a prototype.

Let us consider the sets of discharge points $\{q_{0i}\}$ and head points $\{h_{0i}\}$, which are placed on the characteristic curve corresponding to the pump operating mode with the speed n_0. To obtain the sets of the points $\{q_{pi}\},\{h_{pi}\}$, which are placed on the characteristic curve corresponding the pump speed $n_j<n_0$, it is necessary to apply the following equations:

$$q_{pi} = q_{0i}\frac{n_j}{n_0};\quad h_{pi} = h_{0i}\left(\frac{n_j}{n_0}\right)^2, i = 1\ldots m. \tag{3.4.2}$$

To derive the analytical expression of the pump load on an IM shaft, it is necessary to approximate the characteristic curve corresponding to a certain pump speed $n_j<n_0$. With this purpose, the quadratic dependence of the head on the discharge is usually used. Meanwhile, the count sets $\{q_{pi}\}$, $\{h_{pi}\}$, where i=1…3, corresponding to a certain pump speed n_j are obtained with the use of the homologous approach (3.4.2). Further, a matrix equation is derived in the following form:

$$\mathbf{Q}\cdot\mathbf{A} = \mathbf{H}, \tag{3.4.3}$$

where $\mathbf{Q}_{3x3}$ is the matrix of discharge counts:

$$\begin{bmatrix} q_{p1}^2 & q_{p1} & 1 \\ q_{p2}^2 & q_{p2} & 1 \\ q_{p3}^2 & q_{p3} & 1 \end{bmatrix}.$$

$\mathbf{A}_{3x1}$ is the vector of unknown factors: $[a_2 \quad a_1 \quad a_0]^T$ (here T is a transposition symbol); H_{3x1} is the vector of head counts: $[h_{p1} \quad h_{p2} \quad h_{p3}]^T$.

The solution of (3.4.3) is well known from the linear algebra and has the following form [Hoffman−01]:

$$\mathbf{A} = \mathbf{Q}^{-1}\cdot\mathbf{H}. \tag{3.4.4}$$

The calculated vector A allows presenting an analytical expression of pumping head on discharge under some fixed speed n_j=const in the following form:

$$h_p = a_2\cdot q_p^2 + a_1\cdot q_p + a_0. \tag{3.4.5}$$

Then, an available pump capacity is defined as:

$$P_{out} = h_p q_p \rho g, \tag{3.4.6}$$

where ρ is the water density; g is the gravity acceleration, g=9,8 m/sec^2.

The power on the pump shaft is calculated through the following equation:

$$P_c = \frac{h_p q_p \rho g}{\eta_{pump}}. \tag{3.4.7}$$

where η_{pump} is the factor of the pump efficiency.

Therefore, expression of a load torque (moment of resistance) can be written as:

$$T_c = \frac{P_c}{\omega_r}. \tag{3.4.8}$$

Substituting (3.4.7) into (3.4.8) taking into account (3.4.5) in relation to a certain point

$\{q_{p0}, h_{p0}\}$ placed on the nominal characteristic curve gives:

$$T_L = T_{L,e}\left(\frac{\omega_r}{\omega_{r,r}}\right)^2, \tag{3.4.9}$$

where $T_{L,e} = \frac{q_{p0} h_{p0} \rho g}{\eta_{pump} \omega_{r,r}}$ is the load torque corresponding to the rotor speed $\omega_{r,r}$.

If the net head is nonzero $H_{net} = const \neq 0$, then the quadratic dependence of the pump load torque on the speed (3.4.9) will be violated. Meanwhile, an analytical expression of the load torque becomes dramatically complicated, and only graphical methods can be applied for M_L calculation. However, it is possible to define an approximated analytical expression for T_L within the operation ranges of the moment of resistance $T_L \in [T_{L,\min}; T_{L,\max}]$ and the angular velocity $\omega_r \in [\omega_{r,\min}; \omega_{r,\max}]$. With this purpose the parabolic approximation is used in the following way:

$$T_L = T_{L,\max}\left(\frac{\omega}{\omega_{r,\max}}\right)^k, \tag{3.4.10}$$

where k is the parabola index defined through the following expression:

$$k = \frac{\lg\frac{T_{L,\min}}{T_{L,\max}}}{\lg\frac{\omega_{r,\min}}{\omega_{r,\max}}}. \tag{3.4.11}$$

As a result, during a steady state mode, the dependence of the pump head on pump discharge is described by the quadratic form (3.4.5), where the coefficients are defined by means of the rated characteristic curve. The load torque T_L during a transient is described by the parabolic approximation (3.4.10-3.4.11). The dependencies obtained in this chapter will be used further in the course of numerical experiments.

3.5. Transient Water Flow Model

Several assumptions are accepted for modeling hydraulic transients in order to research a water hammer. In particular, if the value of the pipe length L is much more than the value of the pipe radius R ($L>>R$) then liquid is homogeneous and its parameters (for example, viscosity, density, etc.) are equal along all space directions. The use of this assumption allows restricting researches of liquid dynamics by the moving direction only.

The combination of Euler-equation and the law of conservation of mass allow describing the liquid flow transient on a small pipeline section in the following form:

$$\begin{cases} \dfrac{dv}{dt} + g\dfrac{\partial H}{\partial s} + \dfrac{f}{2D} v|v| = 0; \\ a^2 \dfrac{\partial v}{\partial s} + g\dfrac{dH}{dt} = 0. \end{cases} \tag{3.5.1}$$

where a is the wave speed in the pipeline; H is the piezometric head; f is the friction factor (a function of the Reynolds number Re); v is the speed of a liquid flow; t is the time; D is the pipe diameter.

At present the method of characteristics [Chapple−03], [Guevara and Carmona – 90], [Larock, et al. − 00] is the most widely used in the applied hydraulics for the solution of (3.5.1). This method is based on neglecting pressure and speed space-variations, because these variations are too small in comparison with the corresponding variations over time. Such assumptions allow rewriting (3.5.1) as follows:

$$\begin{cases} \dfrac{\partial v}{\partial t} + \dfrac{1}{\rho}\dfrac{\partial p}{\partial s} + g\dfrac{dz}{ds} + \dfrac{f}{2D} v|v| = 0; \\ a^2 \dfrac{\partial v}{\partial s} + \dfrac{1}{\rho}\dfrac{\partial p}{\partial t} = 0. \end{cases} \tag{3.5.2}$$

The essence of the method of characteristics consists in the substitution of the system of partial differential equations for two systems of ordinary differential equations:

$$\begin{cases} \dfrac{dv}{dt} + \dfrac{g}{a}\dfrac{dH}{dt} + \dfrac{f}{2D} v|v| = 0; \\ \dfrac{ds}{dt} = +a. \end{cases} \tag{3.5.3}$$

$$\begin{cases} \dfrac{dv}{dt} - \dfrac{g}{a}\dfrac{dH}{dt} + \dfrac{f}{2D} v|v| = 0; \\ \dfrac{ds}{dt} = -a. \end{cases} \tag{3.5.4}$$

To calculate H- and v-values, it is necessary to preset both the known initial conditions along the s-direction and boundary conditions at s=0 and s=L.

Let us refer to Figure 3.20 where s–t plane is presented. At any point on the s–t plane, for example at the point P, the values of the continuous variables H and V are unique. Let us draw the C^+- and C^--characteristic lines through point P and extend them till intersection with s-axis. As a result there are two points on the left and right of P, $s_{Le}=S_p-\Delta s$ and $s_{Ri}=S_p+\Delta s$, respectively.

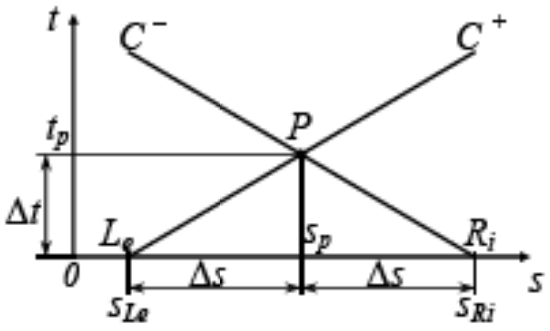

Figure 3.20: The *s*–*t* plane with characteristic lines.

Further, it is necessary to apply (3.5.3) along the C^+-characteristic line, and (3.5.4) along C^--characteristic line. The result of the *H*- and *V*-calculation at *P*-point represents the initial and boundary conditions for *H*- and *V*-calculation at the next time-space point. Meanwhile the primary equation of (3.5.3) and (3.5.4) are written in the finite-difference form:

$$\begin{cases} \dfrac{v_p - v_{Le}}{t_p - 0} + \dfrac{g}{a}\dfrac{H_p - H_{Le}}{t_p - 0} + \dfrac{f}{2D} v_{Le}|v_{Le}| = 0; \\ \dfrac{v_p - v_{Ri}}{t_p - 0} - \dfrac{g}{a}\dfrac{H_p - H_{Ri}}{t_p - 0} + \dfrac{f}{2D} v_{Ri}|v_{Ri}| = 0. \end{cases} \tag{3.5.5}$$

The joint solution of equations (3.5.5) gives:

$$\begin{aligned} v_p &= \frac{1}{2}\left[(v_{Le} + v_{Ri}) + \frac{g}{a}(H_{Le} - H_{Ri}) - \frac{f\Delta t}{2D}\left(v_{Le}|v_{Le}| + v_{Ri}|v_{ri}|\right)\right], \\ H_p &= \frac{1}{2}\left[\frac{a}{g}(v_{Le} - v_{Ri}) + (H_{Le} + H_{Ri}) - \frac{a}{g}\frac{f\Delta t}{2D}\left(v_{Le}|v_{Le}| - v_{Ri}|v_{ri}|\right)\right]. \end{aligned} \tag{3.5.6}$$

With the purpose of (3.5.6) solution getting it is necessary to preset boundary and initial conditions. In particular, it is necessary to obtain *H*- and *V*-values for a steady-state mode at each *i*-point of the net introduced along a pipe. The solution will allow obtaining time moment values and localizing the amplitude of maximum pressure during a transient. To explain the physical essence of appearance and existence of the water hummer process, H_p- and v_p-values are calculated hereafter in Section 4.3 in relation to the simulation task.

3.6. Conclusions

Let us emphasize some general points provided in this chapter:

1. The novel approach to modeling induction motor unsymmetrical operations in $a-b-c$-coordinates, first, satisfies the assumptions used at the lumped approach

to description of electromechanical energy conversion in relation to induction machines. Second, this approach does not require restoration of the values of three-phase stator currents by means of a two-phase-model. Meanwhile, the laboriousness of intermediate transformations can be overcome easily by use of Symbolic Math Toolbox from *MATLAB* 7.x.

2. The novel algorithm for a numerical integration called the hybrid one was developed. The use of a hybrid algorithm allows reducing the total simulation time for the SCRs fed IM with PPCC by 30% in comparison with the widespread algorithm of a numerical integration (for example in comparison with "*MATLAB*"-internal function *ode45*). The choice of integration methods introduced into the hybrid algorithm is justified on the basis of the criterion of integration time minimization taking into account the requirements to integration stability and accuracy.
3. The analysis of periodical processes and transients in dynamics of SCRs fed IM with two types of PPCC synchronization allows showing the following:
   a) Periodical processes are asymptotically stable (in terms of Lyapunov) within all the range of the control angle variation under variation of the inertia moment J_Σ from J_r till 8 J_r.
   b) Periodical processes existed in dynamics of SCRs fed IM with voltage type of PPCC synchronization are characterized by the considerable deviation of the rotor angular velocity from its value during the operating mode and caused by the appearance of the internal positive feedback between the rotor angular velocity and output active voltage of a thyristor voltage regulator. Meanwhile, the oscillations become the most apparent at small values of the summary inertia moment $J_\Sigma \in [J_r; 3 \cdot J_r]$ and control angles corresponding to the turndown $\alpha \in [90;117]$ el. degree. Oscillation parameters depend on a power factor.

So, due to the best steady-state and transient properties, energy-saving potentials and manufacturability, SCRs fed IM with the current type of PPCC synchronization seems to be more attractive as the object for soft-starter design and further researches in the thesis.

Chapter 4

Physical and Numerical Experimental Investigations of Energy Conversion of AC Drive Soft Start Automation Control System of Pump Station

4.1. Formulation and Procedure of Experimental Research of IM Soft Start System Based on Series-Connected Silicon-Controlled Rectifiers Pulse-Phase Control Circuit with Voltage Supply Synchronization

4.1.1. Experimental Research Definition

The mathematical model adequacy check of SCRs-IM-PPCC is the main purpose of physical and numerical experimental investigations. The SCR-IM-PPCC is built by means of asymmetric ac source connection model of the IM (see Section 3.1.1) and the hybrid integration algorithm (see Section 3.1.2).

Two transient process values (amplitude of IM starting high inrush current I_{TSC}, A and transient process duration T_{TP}, s) produce the restrictions of the start-breaking trajectory formation. Consequently, these values are the output parameters of experimental research. The input variable is the SCR control angle α, el. degree.

The value of the IM resisting moment does not affect the function logic of SCR-IM-PPCC. Consequently, IM is started in the idle mode $T_L = 0$ for the elimination of inaccuracy from the realization of an operating moment of inertia in the physical experiment. The summary IM moment of inertia is:

$$J_{\Sigma} = J_{IM} + J_{DCM},$$

where J_{IM} is the IM intrinsic inertia moment, J_{DCM} is the dc motor intrinsic inertia moment. DC motor is in the generator mode. Additionally, it is assumed, that the deviation of the amplitude and frequency of ac source is stochastic and do not affect the investigation results.

The adequacy analysis of the physical and experimental models of the SCR-IM-PPCC is made by means of calculation and estimation of the value of the IM high surge current inaccuracy δI_{TSC} within the range of the control angle variation $\alpha \in [80;116]$, el. degree. The relative inaccuracy of the high surge current is calculated by means of

following equation:

$$\delta I_{TSC} = \frac{I_{TSC,FE} - I_{TSC,NS}}{I_{TSC,FE}} \cdot 100\%, \qquad (4.1.1)$$

where, $I_{TSC,FE}$ ($I_{TSC,NS}$) is the maximum value of the IM stator winding instantaneous current at the physical (numerical) experiment.

The experiment is chosen within the experiment series, which has the maximum value of instantaneous current. The control angle variation step is set to two ($\Delta\alpha$=2) el. degree, that allows getting 19 readings within range $\alpha \in [80;116]$.

The design of algorithm of the SCR-IM-PPCC mathematical model operation and its program realization are the part of the experimental investigation. The flow-block of algorithm operation is shown in Figure 4.1.

The initialization of the dependent variable, SCR control pulse parameters, period counters etc. are made in the first stage at the zero and non-zero initial values; the coefficient matrixes of the sub-algorithm of the hybrid integration algorithm are set; an admissible error, start (t_j) and end (T_{end}) integration moment are set A.1. The numbers of the current period k_a, k_b, k_c A.3, the front and fall time moments $m_{f,i}$, i=1…6 $m_{s,i}$, i=1…6 of the control pulses of each SCR thyristor at the function α, k_a, k_b, k_c and t_j, the current integration step t_{int}=min($m_{f,i}$), the instant connection mode of IM to the source g_j of the $g_j \in$G={AB, BC, AC, ABC, «0»} depending on values $m_{f,i}$, $m_{s,i}$ and the IM stator winder instant current $i_{s\alpha}(t_j)$, $i_{s\beta}(t_j)$, $i_{s\gamma}(t_j)$ A.5 are defined if the value T_{end} is not achieved. The integration on the current stage is made for the model of the regime g_j A.8 if the switching between the regime $g_{j-1} \rightarrow g_j$ was not on the previous step j-1. The integration on the current stage is made for the model of the regime g_{j-1} A.9, which took place at previous time moment if the regimes switching was incorrect on the previous step.

The integration of the models g_j and g_{j-1} is made by means of the hybrid algorithm within the interval $t \in [t_j;t_j+t_{int}]$ or till the moment of the instant current reduce in any phase less than the value of the holding current. This situation corresponds to the thyristor closing and instant connection mode of IM to the source change. The comparison of the current i_{sa}, i_{sb}, i_{sc} polarity with the instant connection mode g_j is made to determine the thyristor voltage shift A.10 if switching between has happened within the integration interval $t \in [t_j;t_j+t_{int}]$. It is made because the thyristor can open at the simultaneous accomplishment of the conditions: (1) existence of the control pulse on the control electrode and (2) existence of the direct shift between the anode and cathode. The current time moment increases for the value $t_j=t_j+t_{int}$ A.12 if the mode switching has not

happened, where t_{Int} is the integration step of instant iteration of the A.5.

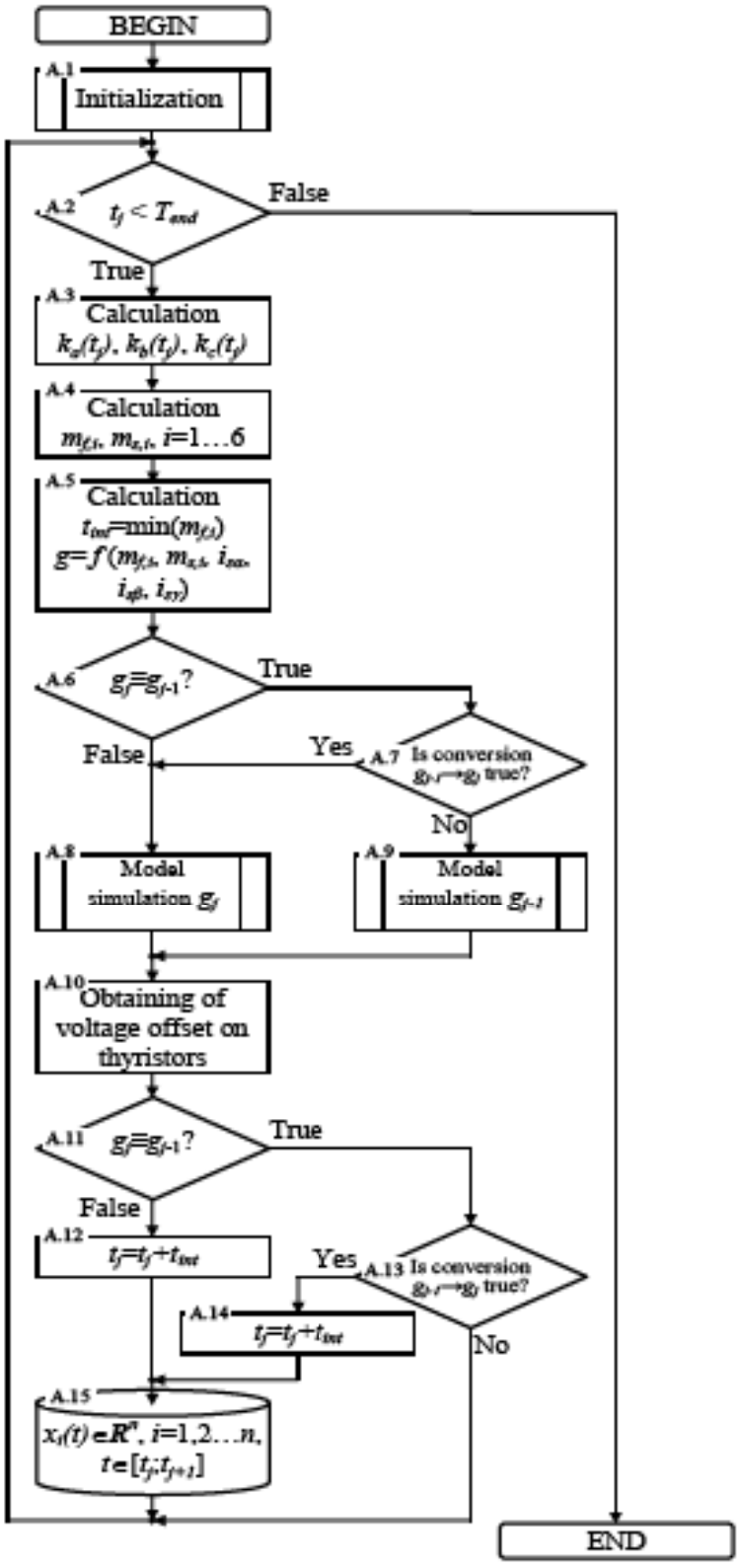

Figure 4.1: Flow-block of algorithm of SCR-IM-PPCC.

The current time moment increases for the value $t_j=t_j+t_g$ A.12 if the regime switching is not happen correct, where t_g is a time interval from the beginning of instant iteration to the mode switching moment. The state variables $x_i(t) \in R^n$, i=1,2…n are

integration results. They are stored in the output data array A.15. The algorithm stops its work, if condition $t_j=T_{end}$ is fulfilled.

The mathematical computer-aided design (mathematical CAD) was chosen to realize the thesis algorithms beacuase universal programming languages do not have essential mathematical functions and that's why are not effective. There are free widely used mathematical CADs: *"Mathcad"*® (The MathSoft, Inc.), *"Maple"*® (The Waterloo Maple, Inc) and *"MATLAB"*® (The MathWorks, Inc.). The mathematical CAD was chosen is conditioned on its purposeful trend. *"Mathcad"*® was designed for the education area that caused its functional limitations. *"Maple"*® was designed for the symbolic analytic mathematical computing. "*MATLAB*"® was designed for the numerical calculation with the use of matrices. At present "*MATLAB 7.4*"® is a leader within the similar mathematical CAD due to the its functional possibilities and additional bump packs. However, the "*MATLAB 7.4*"® core is oriented mainly to the numerical calculation. The additional bum pack of symbolic computation (Symbolic Math Toolbox) allows the automation of the labor-intensive computer operations having included the Maple core. "*MATLAB 7.4*"® specified for 64-bit operation system (with the package of Distributed Computing Toolbox) allows increase significantly the speed of complicated problem solutions [Kolokolov, et al. – 04]. The circumstances mentioned lead to choose the mathematical CAD "*MATLAB*"® for the realization of the designed algorithms. The part of program listing in the language of "*MATLAB 7.4*"® of the model operation algorithm of SCR-IM-PPCC is shown in the appendix C.

The mathematical CAD "*MATLAB 7.4*"® is stipulated by requirements to the computer configuration. Table 4.1 contains the requirements to the computer and operation system for the 32-bit and 64-bit version of "*MATLAB 7.4*"® [The MathWorks – MATLAB and Simulink for Technical Computing – 08].

Table 4.1: Software and hardware requirement of "*MATLAB 7.4*"®

Digit capacity of OS	Operation system	Processor	Hard disk drive space	RAM
32 bit	Windows XP (Service Pack 1 or 2)	Intel Pentium (Pentium IV and later)	510 Mb (MATLAB kernel)	512 Mb (1024 Mb recommended)
	Windows Vista	AMD Opteron		
64 bit	Windows XP x64 (Service Pack 1 or 2)	Intel Pentium (Pentium IV and later)	510 Mb (only MATLAB kernel)	512 Mб (1024 Mb recommended)

4.1.2. Experimental Research of Induction Motor Start With Soft-Start System. Comparison of Experimental and Modeling Results

The functional scheme and the photo of the experimental plant components are shown in Figure 4.2. The experimental plant is mounted in the laboratory of pulse system dynamics the Orel State Technical University.

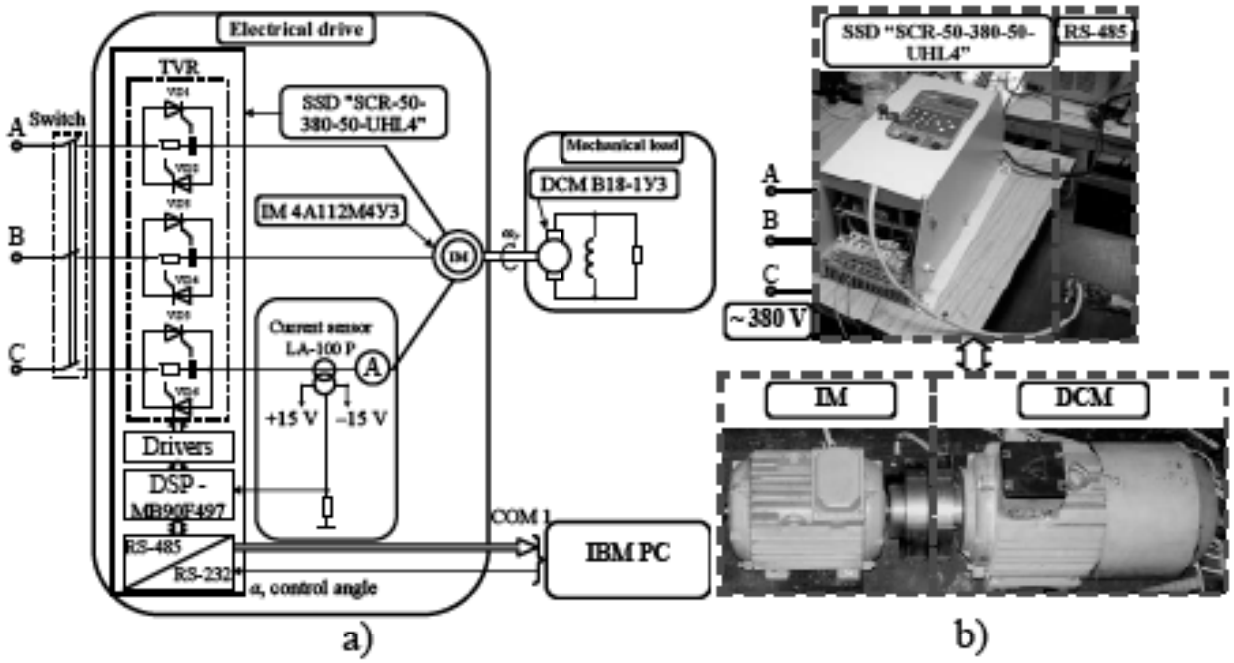

Figure 4.2: Soft-start experimental plant: structure scheme (a); components photo (b).

Experimental plant contains three functional parts:

1. AD and control equipment. AD is an off-the-shelf product of the JSC "Proton-Electroteks" the city of Orel Soft Starts SCR-50-380-5-UHL4, based on the symmetric SCR with PPCC with voltage synchronization; IM A112M4Y3 (P_I=5,5 kW, I_I=11,5 A, the repetition factor of starting current k_I=7, J_Σ =0,077 kg·m^2).
2. DC motor is B18-1U3 (P_I=5,5 kW), operated in the generator mode.
3. Information control computer based system.

A symmetric scheme of SCR stipulates symmetric currents in IM windings. On that ground for data registration of the surge starting current $i_{SC}(t)$ in the course of experiment carrying out there were taken readings of the instant current of the phase C with the use of the current sensor LA-100 P [LEM Holding SA − 08] having the instrument range ±150 A, relative error δ_I=±0,45% (Θ=25 °C) [LEM Holding SA − 08]. The current sensor output is connected to the input of 10-bit ADC of microcontroller Fujitsu MB90F497. The controller RS-485 based on ADM485 is used for data exchange with PC. The transfer rate of ADM485 is up to 5 Mb/s (signal reception delay is 10 ns,

signal transmission delay is 25 ns).

The transient duration was determined by means of the instant current $i_{sC}(t)$ reading processing by means of PC. The duration of transient process was considered to be equal to the time lag passed since the IM start to the moment at which an effective value of current in stator winding "C" I_{sC} fell into and then would not leave the range $I_{sC} \in [0{,}95 \cdot I_{sC,ss}; 1{,}05 \cdot I_{sC,ss}]$, where $I_{sC,ss}$ is the steady state value of the root-mean-square current of the stator phase C.

In Figure 4.3(a,b) (4.3(c,d)) there are shown the physical (numerical) experimental diagrams of the instant phase C stator current at the IM idle start from the braking mode with the control angle α = 100 el. degree at the time lag from zero to the steady state.

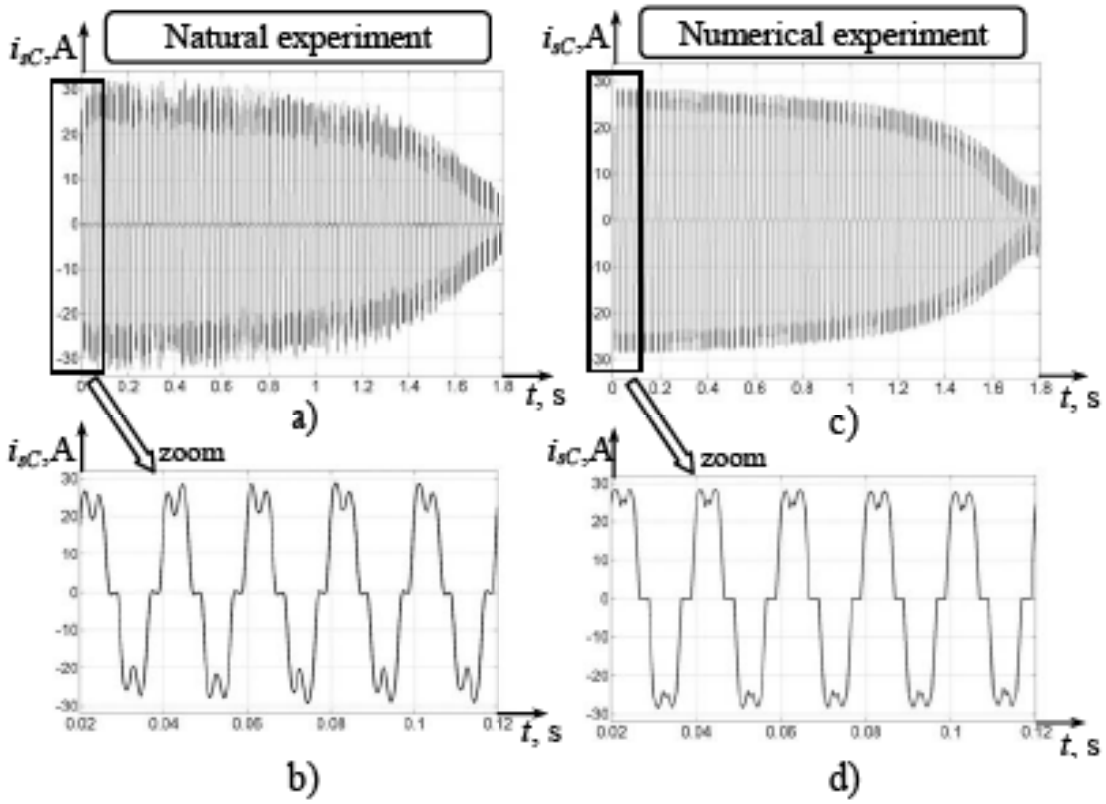

Figure 4.3: Physical and numerical experimental results of start IM 4A112M4Y3 with Soft Starts-SCR-50-380-59-UHL4.

In Figure 4.4a there are shown the diagrams of dependences for the repetition factor of surge current of stator winding "C" to IM rated current (k_I) at control angle variation within the range $\alpha \in [80;116]$ el. degree obtained in the course of physical and numerical experiments. The dependence diagram of $k_I = f(T_{TP})$ is shown in Figure 4.4(b) formed on the basis of data of the physical experiment, which is approximated through the exponent function:

$$k_I = 6{,}77 \cdot \exp(-2{,}01 \cdot T_{TP}) - 2{,}54 \cdot \exp(-0{,}06 \cdot T_{TP}) \qquad (4.1.2)$$

for which the boundaries of the 95% confidence interval were plotted. For the approximation obtained the correlation coefficient is R^2≈0,991, the sum of error squares is SSE≈0,25. These values confirm the adequate exponent function description (4.1.2) of the investigated dependence $k_I = f(T_{TP})$.

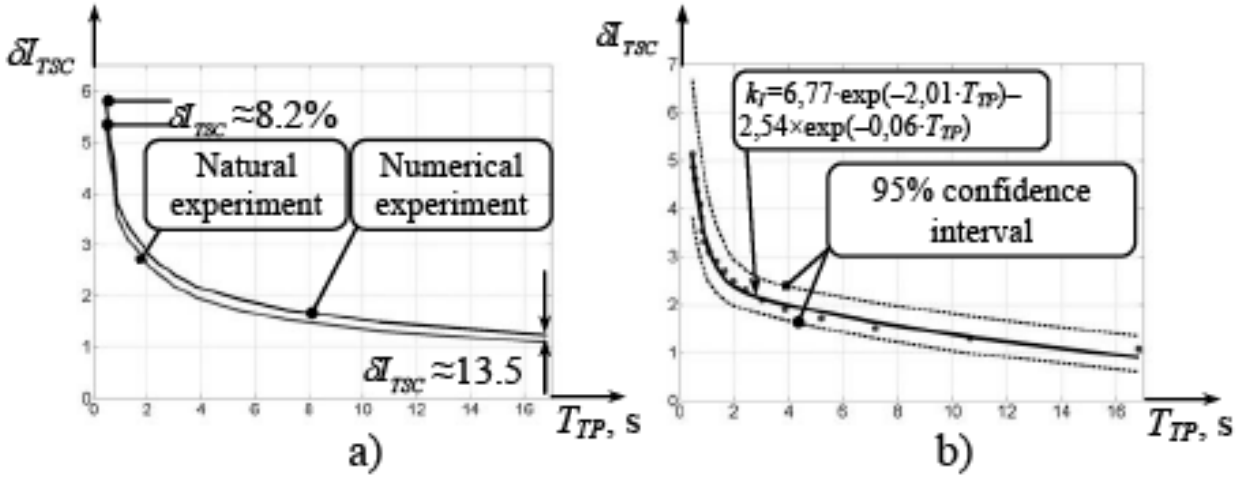

Figure 4.4: The dependence of k_I on the IM start duration T_{TP}.

The analysis of diagrams shown in Figure 4.3 and 4.4 is a satisfactory coincidence of numerical and physical experimental results for the lumped model SCR-IM-PPCC. The relative error of the maximum stator current determination is equal to δI_{TSC}≈8,2% (4.1.1) within the small transient process duration (Figure 4.4(a)). The relative error of the maximum stator current determination increases with the start time increase and at α=116 el. degree the maximum value is equal to δI_{TSC}≈13,5%.

The calculation error of dependent variable could not be obtained less than 12-15% at modeling the power conversion in IM in transients for the lumped model [Solveson, et al. − 06]. Consequently, the achieved result can be assumed satisfactory and confirm the adequacy of the designed mathematical model and integration algorithm.

The dependency $k_I = f(T_{TP})$ (Figure 4.4) has a monotonous feature and does not have limitations to the constant coefficients of the approximation function (4.1.2). Consequently the minimum number of the points $\{k_{I,i}; T_{TP,i}\}$ for the determination of the approximation function coefficients by the numerical modeling of SCR-IM-PPCC is equal to the number of these coefficients [Hoffman − 01]. This fact will be used to design the adaptive control algorithm for the soft start automation control system of IM of the pumping station in Section 5.1.

4.2. Energetic Subsystem of Soft Start Automation Control System of IM

The limitation of the start-brake trajectory formation procedure of the IM pump machine can be analyzed by means of the results of Chapter 3. The limitations list in the thesis was considered in Section 2.2.1. It includes four items. The first two items will be described below. They are related to the energy aspect of the electro-magnetic conversion in IM.

In [Pozdeev and Erezeev − 06] were ascertained the normal permissible and maximum permissible values of the voltage fluctuation $\Delta V_{max,perm}$ in the output of the electric energy source, these value are accordingly ±5 and ±10% of rated voltage. The negative voltage deviation $\Delta V_{max,perm}$ for a value of more than 10% is considered as a voltage depression, which is characterized by a maximum permissible value of duration equal to 30 sec in the electrical supply network up to 20 kW.

The modeling of the energy system (power line, transformer substation and pump IM) will be made to ascertain the conditions of transients. The model structure scheme is shown in Figure 3.17.

A pump station contains three IM 4AS250M4Y3 (power rating P_r=63kW). The expression (3.2.1) with the IM parameters leads to the following:

$$S = 0{,}9 \cdot \sum_{i=1}^{3} \frac{63000}{0{,}87 \cdot 0{,}93} = 233{,}59 \cdot 10^3 \text{ V·A.} \qquad (4.2.1)$$

The power transformer TM-250/6-10 was chosen by the value of additional load power $S_a \approx 16$ kV·A and the value of S. The power rating of power transformer is S_r=250 kV·A.

Figure 4.5 contains the results of modeling the direct start of the first IM in the pump station. The parameters of the equivalent circuit of the transformer TM-250/6-10 were computed by means of methods [Martin − 98] with respect to the referenced data. The diagram of Figure 4.5 corresponds to the direct start with the zero initial value from the brake state. The resist torque changes through the expression (3.4.10) and at the steady state is equal to nominal value. The top diagram of Figure 4.5 shows change of the angle velocity of IM rotor within the start ($\omega_r(t)$, rad·s^{-1}); the middle diagram shows changes of the linear root-mean-square voltage at the connection point of IM to the supply (V_L); the bottom diagram shows changes of the instantaneous IM stator current phase "A" $i_{sA}(t)$.

The motor starts at the moment t_{start}=0,3 s. The stator windings current decreases after approximately 0,35 s. This interval corresponds to the transition of the IM the angle velocity to the area of the subsynchronous values. The transient stops after approximately 0.85s and IM comes to a steady state.

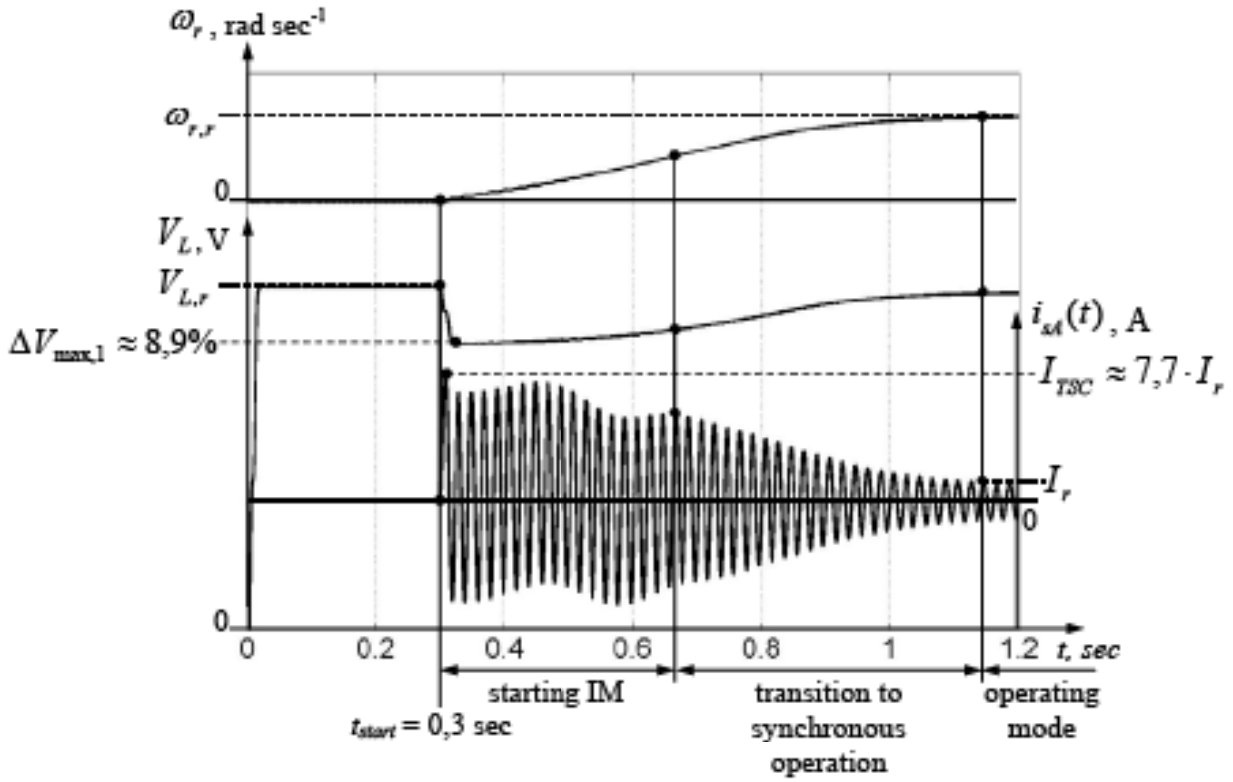

Figure 4.5: Electromechanical process at the direct start of IM 4AS250M4Y3 of pumping station.

The amplitude of the instantaneous current of the stator winding of the phase "A" achieves the high inrush current value I_{TSC}, which is greater than nominal current value in 7,7 times. The occurrence of a large current value leads to the increase of resistance voltage drop of the primary and secondary windings. The analysis of the root-mean-square linear voltage ascertains that the maximum deviation of the root-mean-square linear voltage of the supply is equal to $\Delta V_{max,1}$≈8,9%. This value is less than overload capacity of standard [Pozdeev and Erezeev – 06].

Figure 4.6 contains the diagram of the change of the root-mean-square linear voltage in the investigated supply network under conditions of all IM start at the moment $t_{start,1}$, $t_{start,2}$ and $t_{start,3}$ consequently.

The diagram analysis of Figure 4.6 gives the conclusion that the error of the root-mean-square voltage from the nominal one does not exceed the normally permissible value. At the end of the third IM start the error is equal to 3%. However, the maximum

error of the root-mean-square voltage within the third IM start is equal to 10,6%, that exceeds maximum allowable deviation for 0,6%.

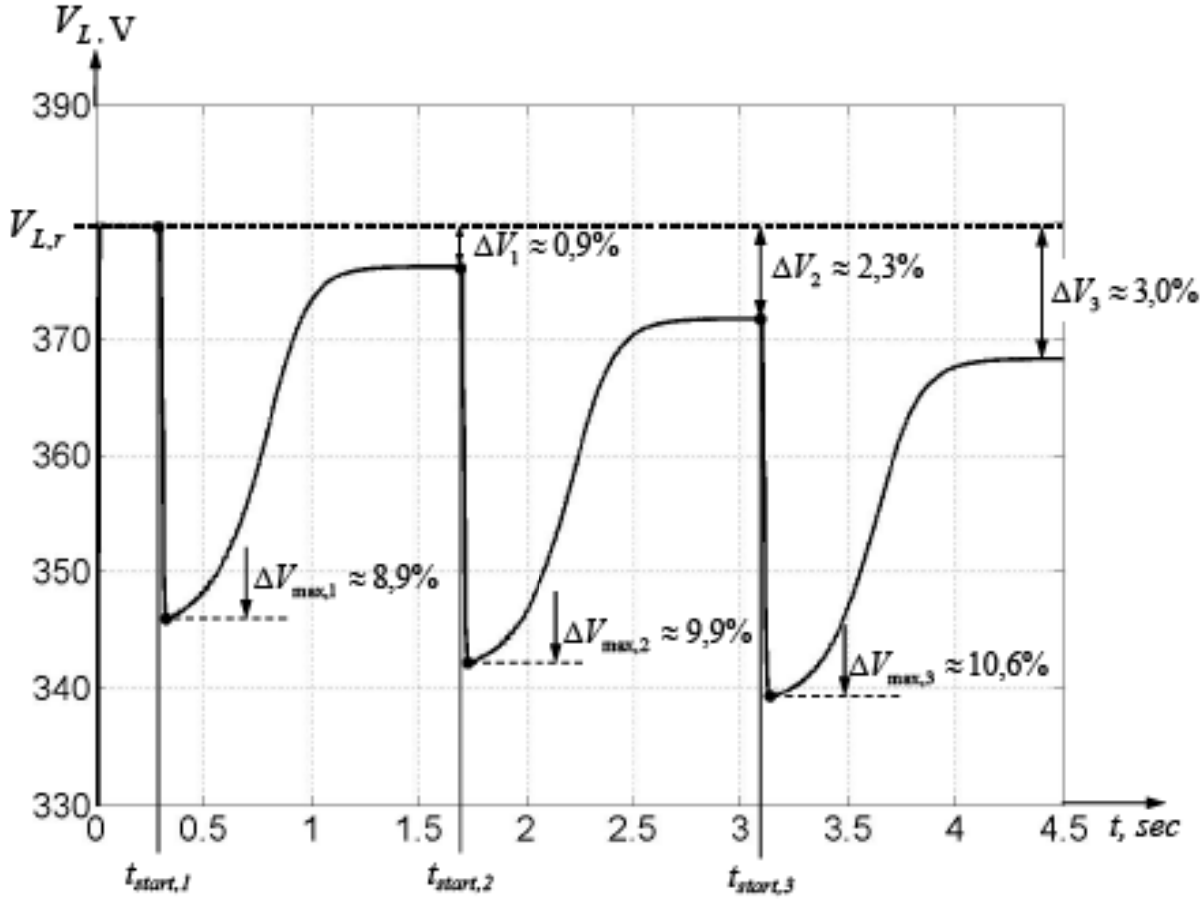

Figure 4.6: Diagram of root-mean-square linear voltage.

The above mentioned results allow making a conclusion about the necessity of transient limitations at the IM start. The mathematical model of the power subsystem of the pumping station formed in the previous chapter allows carrying out the computation of maximum allowable current. This current value at the IM start does not provide the voltage drop less than a maximum allowable value. This fact will be used in Section 5.1 in the stage of design of the adaptive algorithm of the IM soft star control at the pump station of the water supply system.

The second restriction of high surge current regards the constructional behavior of IM. It is well known, that large start current is dangerous due to its mechanical and thermal influences (non-stationary winding heat will be considered at Section 4.4).

The mechanical influence of transient current relates to the significant mechanical effort in the frontal winding part. For example, the effort in the powerful IM achieves 75 kg/sm on the frontal winding part at 15-fold surge currents [Lihachev – 02]. That is why, a frequent transient is the reason of deforming vibration, which leads to untimely

winding breakage. It is the reason of taking into account high surge current of the normal start at the estimation of the frontal winding mount. The value of the maximum high surge current I_{SC} is set by the motor producer and is normally permissible, which guaranty is minimum 23000 hours of mean time between failures [Lihachev − 02]. The maximum value of the high surge current deviation from the maximum start current is 20% of the normally permissible value.

The ratio of the start current amplitude I_{SC} to the nominal value I_r will be designated as follows:

$$k_{I,S} = \frac{I_{SC}}{I_r}$$

Figure 4.7 contains the plot of the $k_{I,S}$ in the function of IM nominal power with the nominal rotor speed n_r=3000 и n_r=1500 rpm of the series 4A 5A, with the protection level IP44 and IP54 correspondently [Lihachev − 02].

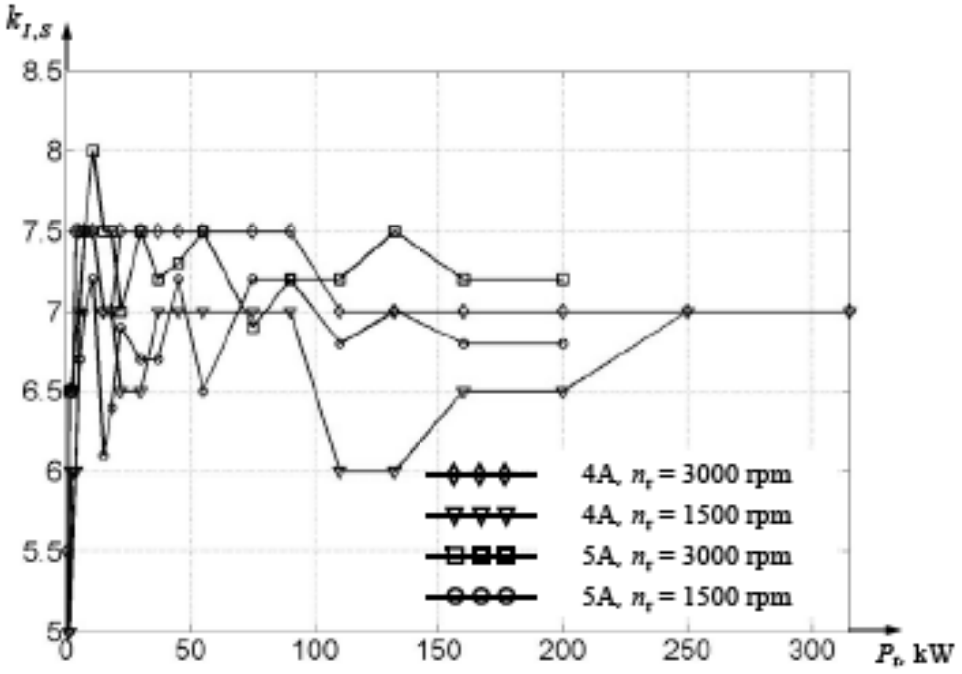

Figure 4.7: Ratio of the start current amplitude I_{SC} to the nominal value I_r for the IM 4A and 5A series.

In Figure 4.7 the plot analysis allows making a conclusion, that the average value of $k_{I,S}$ is in the range 6.5–7.5. Meanwhile, this value increases with the IM angle velocity increase. Consequently, a soft start device protects the structure of IM from the mechanical influences at the start mode by means of limitation of high surge current with the value which is recommended by the motor producer. The coefficient $k_{I,S}$ will be

used in the formation of the adaptive control algorithm of the soft start device of IM in the pump station. The coefficient $k_{l,S}$ is defined by means of reference data.

4.3. Hydraulic Subsystem of Induction Motor Soft Start Automation Control System

The rapid development of the liquid non-steady motion theory was in the late 1960. It is closely connected with the development of computer numerical methods. A lot of papers are devoted to the problems of modeling and analysis of the mechanism occurrence and operation of a hydraulic hammer in the system of water supply [Chapple – 03] and [Larock, et al. − 00]. The first work about a hydraulic hammer was carried out by N.E. Zhukovsky. He proved the wave behavior of the pressure distribution and ascertained the increase of the water head for the ideal incompressible liquid in the non-elastic pipeline under the condition of instantaneous gate close through the following expression:

$$\Delta H = -\frac{a\Delta v}{g}. \tag{4.3.1}$$

where a is the wave speed, depends on physical properties of the pipe (modulus of elasticity E, Poisson ratio μ); geometric properties of the pipe (diameter D, thickness of the pipe e); density ρ and the bulk modulus of elasticity of the liquid K.

The speed of wave propagation does not depend on the direction of liquid movement. This fact leads to the special method in hydraulics, which consists in the analysis of liquid dynamics for non-steady liquid under the condition of the valve closing process. The liquid speed changes from the steady value v_0 to the zero value [Chapple – 03], [Larock, et al. − 00].

The transient of valve closing in the hydraulic system will be considered for the check of the adequacy of the pressure increase estimation. The scheme of the hydraulic system is shown in Figure 4.8.

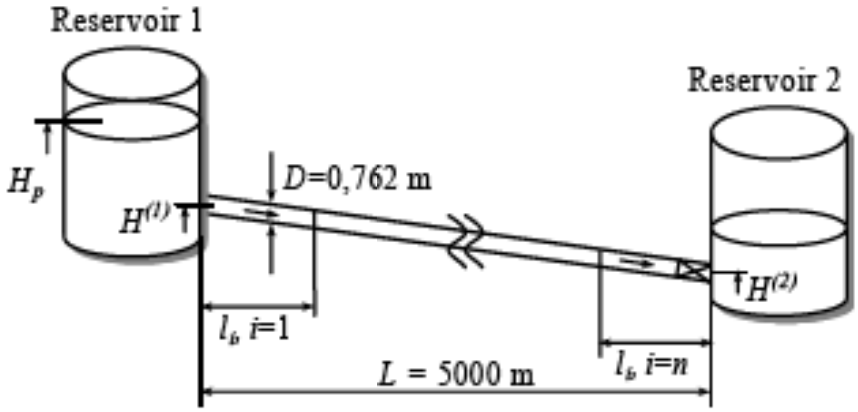

Figure 4.8: The scheme of a model hydraulic system.

A steel pipeline is used in the hydraulic system (see Figure 4.8) and provides the liquid movement from the tank "1" to the tank "2". The temperature of the liquid is 4 °C (ρ = 1000 kg/m^3). The scheme has the following boundary conditions [Larock, et al. – 00]:

– for the last section counter the stream:

$$H_1 = H_p;$$

– for the last section with stream:

$$H_n = H_p - (n-1)\cdot\frac{12\cdot f\cdot\Delta L\cdot v_0^2}{64{,}4\cdot D}$$

where f is the Darcy friction factor.

The initial data, calculation results in the steady state for the hydraulic system of Figure 4.8 are shown in Table 4.2.

Table 4.2: Initial data and parameters of steady state for studied hydraulic systems

Parameter name	Symbols	Value
Elevation of the first reservoir [m]	$H^{(1)}$	30,5
Elevation of the second reservoir [m]	$H^{(2)}$	15,25
Pipe length [m]	L	1524
Pipe diameter [m]	D	0,762
Darcy friction factor	f	0.02
Thickness of the pipe [m]	e	$2.54\cdot10^{-3}$
Modulus of elasticity [Pa]	E_{steel}	$207\cdot10^{9}$
Poisson ratio	μ	0.3

Parameter name	Symbols	Value
Density of the liquid (water at 4 °C) [kg/m^3]	ρ	1000
Bulk modulus of elasticity of the liquid [Pa]	K	$2{,}2 \cdot 10^9$
Initial fluid velocity [m/s]	v_0	1,5
Wave speed [m/s]	a	751

Figure 4.9(a) contains the diagram of water head in the section, which joins the valve for two positions of closing duration: T_1=1 and T_2=10 s. Figure 4.9(b) shows the surface of the water pressure in piping gate for the case of gate closing during T_1=1 s.

The analysis of Figure 4.9(a) shows, that maximum water head is equal to H_{max}= H_0+ΔH, where ΔH – the water head increase, which is determined through the expression (4.3.1) and is equal to H_{max}=336,4 m (1.5·H_0). This value conforms to the maximum water head value, which is calculated by means of the whole equation system integration (3.5.3)-(3.5.4).

The water head wave form H (see Figure 4.9(a)) under condition T_1=1 s has a sharp edge. It conforms to the theoretical process data at a hydraulic hammer [Chapple – 03], [Larock, et al. – 00], [Menon − 04]. The wave shape transforms to a more flat form and the maximum amplitude of water head decreases to the H_{max}=262,1 m (1.3·H_0) if the gate closing duration decreases by T_2.

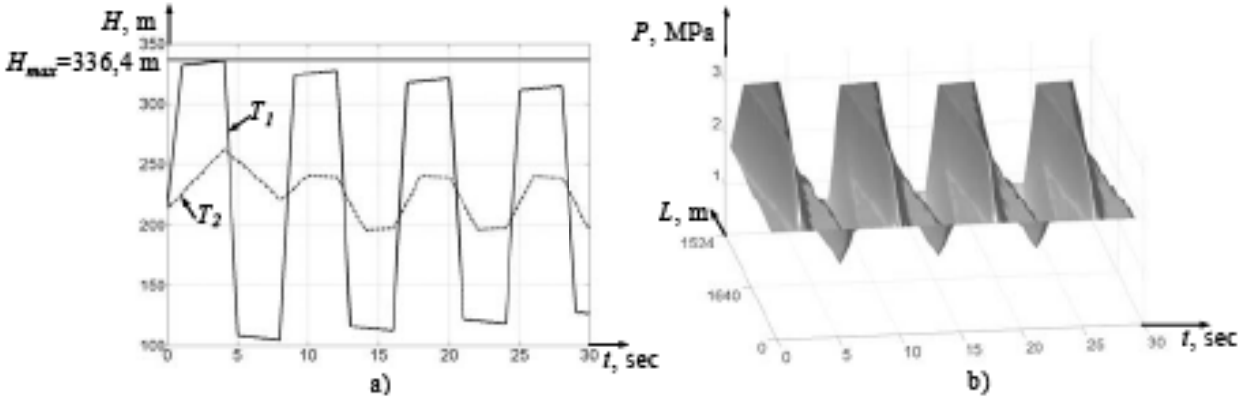

Figure 4.9: Wave processes in the pipeline section joined to the gate: head change (a); surface of water pressure (b).

The modeling of the start and brake of the pump station IM will be made later under conditions of an open gate. The system structure is shown in Figure 2.1. The main pump station parameters are as follows: the value of concatenated pipe-line sections is n=3; the water head in the tank is $H^{(1)}$=120,4 m, $H^{(2)}$=256 m; the value of the parallel pump device is m=4 (all pumps are identical to the rotary pump Ingersoll-

Dresser 15H277 and have the behavior shown in [Larock, et al. − 00]). The moments of pump start are: $t_{start,j}$={100, 400, 500, 600}, j=1…4. The moments of pump brake are: $t_{stop,j}$={800, 900, 1000, 1100}, j=1…4. The duration of a transient is equal to T_S=20 s. The parameter of an equivalent circuit is equal to 4AN280M4Y3. The physical behavior of liquid and pipe-line material are shown in Table 4.2.

Figure 4.10(a) contains the diagram of total water head H change in the first section of the pipe-line. Figure 4.10(b) shows the diagrams of the maximum P_{max} and minimum P_{min} water pressure within all pipe-line sections relative to the time.

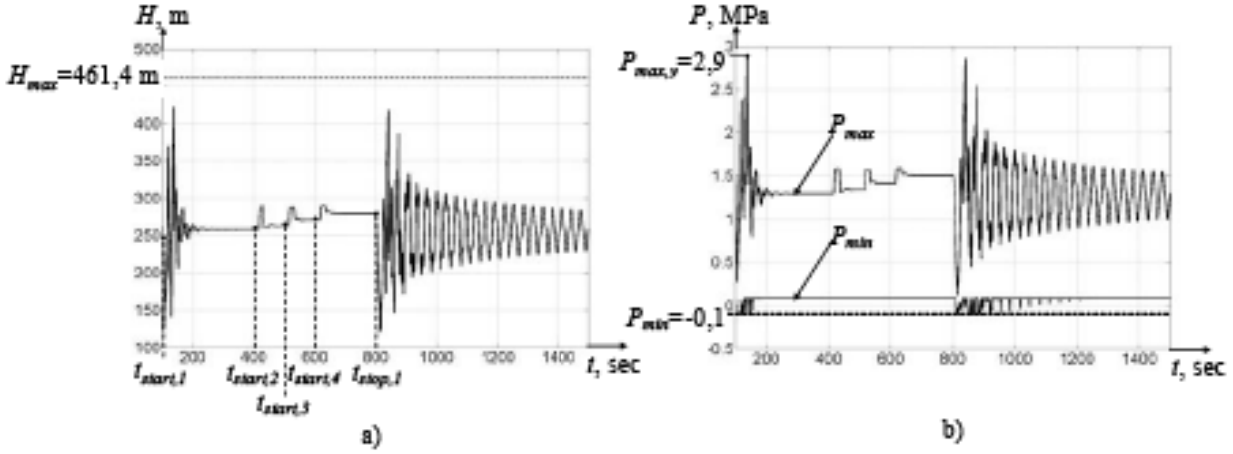

Figure 4.10: Results of the modeling of transient of the start and stop of a standard pump station.

Figure 4.10(a) diagram analysis shows, that the maximum head in the pipe-line is not greater than value H_{max} = 461,4 m. The value H_{max} was calculated by means of the expression (4.3.1). Figure 4.10(a) diagram analysis ascertains that the impact pressure in the system $P_{max,s}$ = 2,9 MPa. This value is significantly less than the impact pressure for the steel pipe-line ($P_{s,steel}$ = 10 MPa [Menon − 04]). At the same time, the minimum pressure in the pipe-line P_{min}=-0.1 MPa is less than atmospheric one. If the drop of pressure is considerable enough to cause the local pressure reached the saturated vapor pressure of liquid, then the liquid boils (cavitates, vaporizes) forming large pockets of undissolved gases and vapor. This phenomenon is called a column separation. Excessively low pressures can lead to the release of large amounts of dissolved air, and extensive vaporization of the liquid can occur if the pressure drops to the liquid vapor pressure. The resulting low pressures, possibly enhanced by external pressures, could cause the pipe destruction. Also, a vapor cavity closure event occurred at some point in the pipeline can produce high shock pressures which could lead to failure of a pipe. These cavity closure shocks are difficult to predict owing to the difficulty of simulating the actual physical phenomena occurred in the pipe. Therefore, the

simplest approach to simulate column separation phenomena described in [Larock, et al. – 00] is used in this thesis.

The simplest model of column separation ignores the existence of dissolved gases that might come out of the solution at low pressures. Instead it is assumed that the liquid remains intact until the vapor pressure is reached. When that point is reached, it is postulated that the vapor cavity will grow at a constant cavity pressure equal to the vapor pressure. Eventually, when the cavity closes, it is presumed that the vapor is re-absorbed so that it disappears at the instant of cavity closure. In effect, the vapor cavity is treated much like vacuum.

The determination of the consequences of cavity closure is an important prediction of the model. To analyze this feature we apply conservation of momentum to the collision of the two collapsing cavity walls that are moving at different velocities. The result is an equation for the water head increase which results from the collision [Larock, et al. – 00]:

$$\Delta H = \frac{a}{2g}(v_1 - v_2). \qquad (4.3.2)$$

Figure 4.11 contains the counts of the maximum increase of pipe-line pressure ΔP_{max}. Figure 4.11 contains the diagram of relation $\Delta P_{max}=f(T_{TP})$, which is approximated by means of the following exponential function:

$$\Delta P_{max}=2{,}22\cdot\exp(-0{,}02\cdot T_{TP})-0{,}69\cdot\exp(-0{,}08\cdot T_{TP}) \qquad (4.3.3)$$

Figure 4.11 has the boundaries of the confidence interval 95%. The correlation coefficient is equal to $R^2\approx 0{,}964$, the square sum of errors is equal to SSE≈0,04. It confirms the adequacy of the exponential function (4.3.3) to the investigated function $\Delta P_{max}=f(T_{TP})$.

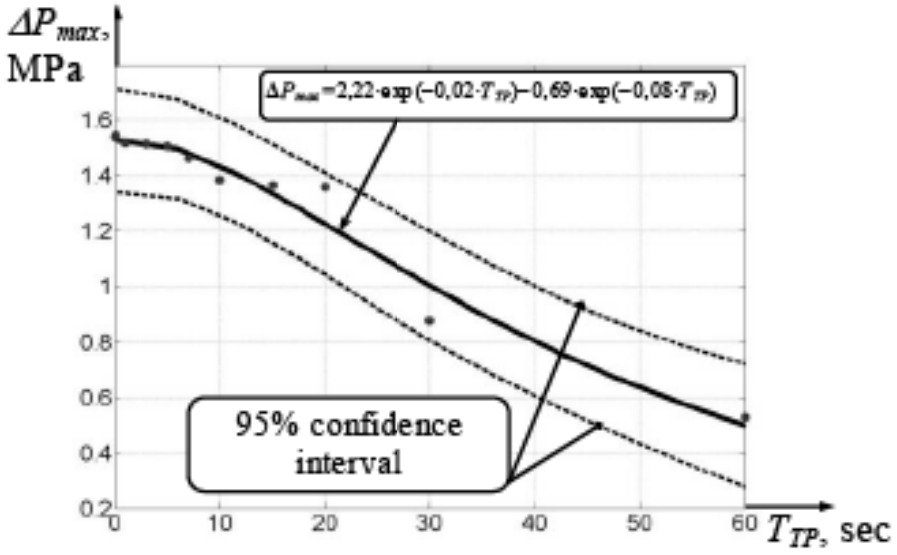

Figure 4.11: Dependence of the pressure in a pipeline of a pump station on motor start process.

The dependence $\Delta P_{max}=f(T_{TP})$ has the monotonous feature and does not have the limitation to the constant coefficients of the approximation function (4.3.3). Consequently the minimum value of the points $\{\Delta P_{max,i};T_{TP,i}\}$ for the determination of approximation function coefficients through numerical modeling a hydraulic system is equal to the value of these coefficients [Hoffman − 01]. This fact will be used to design the adaptive control algorithm for the soft start automatic control system IM of the pumping station in Section 5.1.

4.4. Modeling of Non-Stationary Heat of IM Windings

The heat energy output in the construction elements is an undesirable result of IM operation. The winding isolation is the most vulnerable part for thermal load. The irreversible physicochemical processes occur if the temperature exceeds the maximum permissible value $\Theta_{max.perm,}$ which accelerates the aging. The levels of heat resistance are shown in [Boys and Miles − 94] for electro-technical device electric isolation. These levels are shown in Table 4.3.

Table 4.3: Levels of heat resistance and corresponded maximum temperature

Insulation class	Θ_{max}, °C
Y	90
A	105
E	120
B	130
F	155
…	…

The squared matrices of heat capacity and heat conductivity of IM in the non-stationary model of heat and cooling have the following form for the equivalent circuit of Figure 3.18:

$$\mathbf{C} = \begin{bmatrix} C_1 & 0 & 0 & 0 & 0 & 0 \\ 0 & C_2 & 0 & 0 & 0 & 0 \\ 0 & 0 & C_3 & 0 & 0 & 0 \\ 0 & 0 & 0 & C_4 & 0 & 0 \\ 0 & 0 & 0 & 0 & C_5 & 0 \\ 0 & 0 & 0 & 0 & 0 & C_6 \end{bmatrix}; \quad (4.4.1)$$

$$\mathbf{G} = \begin{bmatrix} G_{11} & -G_{12} & 0 & -G_{14} & 0 & 0 \\ -G_{21} & G_{22} & -G_{23} & 0 & 0 & 0 \\ 0 & -G_{32} & G_{33} & 0 & -G_{35} & -G_{36} \\ -G_{41} & 0 & 0 & G_{44} & -G_{45} & -G_{46} \\ 0 & 0 & -G_{53} & -G_{54} & G_{55} & 0 \\ 0 & 0 & -G_{63} & -G_{64} & 0 & G_{66} \end{bmatrix}. \quad (4.4.2)$$

The heat conductivities of the main diagonal of the matrix (4.4.2) are calculated by means of following expression:

$G_{11} = G_{12} + G_{14}$;

$G_{22} = G_{21} + G_{23}$;

$G_{33} = G_{32} + G_{35} + G_{36}$;

$G_{44} = G_{41} + G_{45} + G_{46}$;

$G_{55} = G_{53} + G_{54}$;

$G_{66} = G_{63} + G_{64} + G_{60}$.

The method of [Boys and Miles − 94] was used for the calculation of heat conductivities and capacity of elements of an equivalent heat network of Figure 3.18. The results of calculation are summarized in Table 4.4.

Table 4.4: Value of elements of equivalent heat network of IM 4A112M4Y3

Specific thermal capacity	J/(kg·°C)	Specific thermal conductivity	W/(m·°C)
C_1	539,9	G_{12}	5,71
C_2	423,4	G_{14}	0,53
C_3	4450,6	G_{23}	28,12
C_4	0,99	G_{35}	7,41

Specific thermal capacity	J/(kg·°C)	Specific thermal conductivity	W/(m·°C)
C_5	1006	G_{36}	64,77
C_6	18446,6	G_{45}	1,07
		G_{46}	24,04
		G_{60}	66,67

Figure 4.12(a) contains the diagrams of a stator winding front part heat of the IM 4A112M4Y3, which was built by means of the model (3.3.1). Figure 4.12(b) contains the analogues diagrams, which was built experimentally (dotted line) in [Mezani, et al. – 05] and by means of the calculation of the temperature field by means of finite elements method (continuous line).

The analysis of Figure 4.12 allows making a conclusion about satisfactory convergence of the modeling results by the (3.3.1) and the experimental data. The difference in the temperature increase speed is compensated by good coincidence of the steady state value, $\Theta_{ss} \approx 120$ °C.

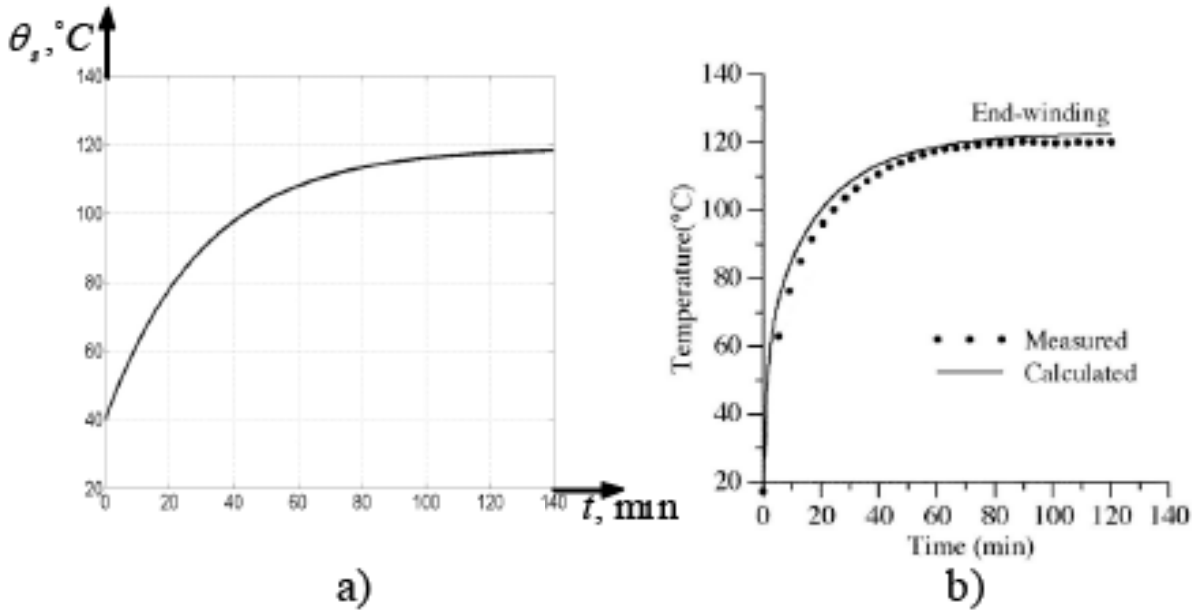

Figure 4.12: Stator winding front part heat of the IM 4A112M4Y3: modeling result (a); experimental result and finite elements method calculation result in [Mezani, et al. – 05] (b).

The controlled start of IM with soft start system leads to the increase of duration within the area of a large slide and consequently additional heat release in windings through the non-sinusoidal power supply. The long start of the loaded IM leads to the exceeding of the temperature at the direct start. It results in the necessity of the temperature check by means of a sensor or by means of the inclusion of a thermal model of the IM in the software of soft start system microcontroller. That is why the thermal model of the IM of a non-stationary model will be used for the design of an adaptive control algorithm of a pump station IM soft start. This algorithm will be considered in Section 5.1.

The theoretical results were confirmed experimentally. It confirms the adequacy of designed mathematical models and the efficiency of the integration algorithm. These results were used for design of the instrumental and program-algorithmic base for an effective control algorithm of the IM soft start system of the pump station. They will be considered in the next chapter.

4.5. Conclusions

1. It is reasonable to use the computer mathematic system "*MATLAB 7.4*®" for realization the function algorithm of the model SCRs-IM with the voltage synchronized PPCC of Section 3.1.2. "*MATLAB 7.4*®" permitting to automate numerical and analytic calculations.
2. The results of the physical experiment of IM soft start system satisfactory correspond to the numerical experiment results. Particularly, the maximum stator current estimation error is close to $\delta I_{TSC} \approx 13{,}5\%$ for IM at α=116 el. degree. These results allow to use of the designed mathematical model of SCRs-IM with voltage synchronized PPCC in the control algorithm of a soft star automation control system.
3. The dependence of a current repetition factor on the starting current $k_I = f(T_{TP})$ can be authentically approximated by means of the exponential function (4.1.2). The calculation of constant rates can be made by means of four points.
4. The breach of the standard mentioned in [Pozdeev and Erezeev – 06] was ascertained by means of the pump station modeling. The breach consists in the decrease of voltage in the secondary winding of the power transformer by 10% less than rated root-mean-square linear voltage. This fact amplifies the necessity of the limitation by means of a soft start system the transition surge current of IM.

The mathematical model of the energetic subsystem of the previous chapter allows the estimation to be carried for the maximum permissible current value, which does not provide the voltage drop of the supply less the permissible value within the IM start.

5. The modeling of the water hammer in the pipe-line with two tanks was made by means of numerical integration of the equation of a non-steady movement of non-ideal liquid. The comparison of the theoretical and numerical researches [Larock, et al. – 00], [Menon − 04] confirms the adequacy of designed mathematical model and integration algorithm.
6. The dependence of maximum pressure increase in the pipe-line from the IM start tie moment in the pump station $\Delta P_{max}=f(T_{TP})$ can be authentically approximated by means of an exponential function (4.3.3). The calculation of the constant rates can be made by means of four points.

CHAPTER 5

The Development of Adaptive Algorithm for Soft Start Control Pump Station Induction Machines. Numerical Experiment Setting and Carrying Out

5.1. Development of Adaptive Algorithm of Soft Start Control of Pump Station Induction Machines

The analysis of the mathematical model of IM automatic control system carried out in the previous Section allows the development of the discrete algorithm for adaptive control with an identifier and predictor considering computer operation model of the IM automatic control system as a controlled object.

The analysis results of the IM energy losses during the controlled start (see Section 2.2.3) as well as the analysis of the operation scheme (see Figure 2.7) make it possible to conclude that the application of the fixed current setting for all pump station IMs is not effective because the choice of the underrated I_{SCS} value leads to a baseless start increase and energy losses (as it follows from graphic analysis of Figure 2.6); the choice of the overrated I_{SCS} value (see Figure 4.6) leads to the voltage drops lower than maximum allowable value and can be the reason of a water hammer in the pipeline (see Figure 4.11).

The adaptive algorithm has been developed to avoid the above-mentioned drawbacks. This algorithm allows formation of the maximum allowable current setting I_{SCS} on the base of a current energy conversion process state in the system "power network-soft starter-IM-pump-pipeline". An application of formed reference makes it possible to fulfill the required specifications during the IM controlled start. The adaptive algorithm logic diagram of the soft start control of the pump station IM of the water supply system is depicted in Figure 5.1.

The basic information is added to the database at the stage of computer program introduction, which realizes the automatic control system of the IM soft start. This information concerns the electrical subsystem (transformer substation and IM parameters including IM material thermal parameters); the mechanical subsystem (centrifugal pump parameters); the hydraulic subsystem (parameters of a trunk pipeline, by-pass line, reservoirs) (see Figure 5.2).

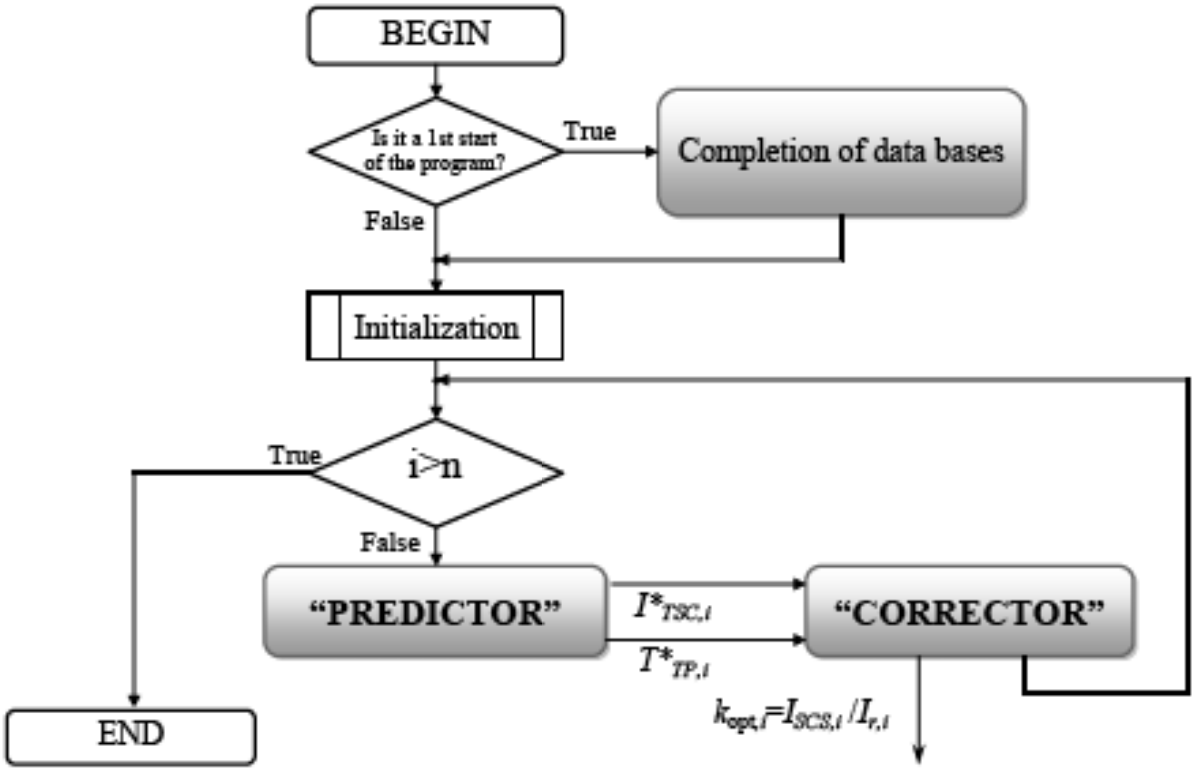

Figure 5.1: Logic diagram of soft start control of pump station IM in water supply system.

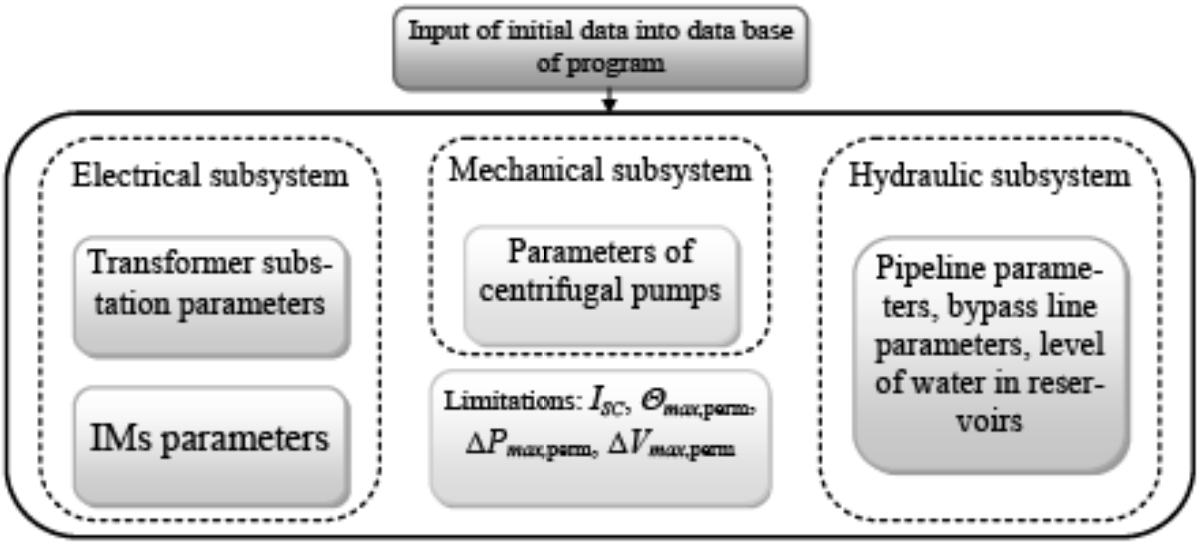

Figure 5.2: Structure of basic data of adaptive algorithm for IM soft start control.

The constraints applied to the start-stop processes of the pump station IM have the particular meaning for basic data. These constraints can be divided into two groups: the fixed constraints that are stipulated by a type of the IM used (I_{SC}, $\Theta_{max,perm}$) and those varied depending on pump station operating conditions ($\Delta V_{max,perm}$, $\Delta P_{max,perm}$).

The initialization procedure of the program variables and parameters takes place, when all initial data have been introduced and checked. Then control is given to the predictor according to the adaptive algorithm (see Figure 5.3), which has two functions:

1. Acquisition of j readings of the maximum hydraulic increase $\Delta P_{max,ij}$ in the pipeline in the function of the start duration of the i-th IM $T_{TP,ij}$. The readings are calculated automatically by means of the numerical integration of a hydraulic subsystem model. The dependence of the type $\Delta P_{max}=f(T_{TP})$ (see Figure 4.11) makes it possible to apply the exponential approximation with the accuracy sufficient for a practice (4.3.3):

   $$\Delta P_{max}=a_1 \cdot exp(a_2 \cdot T_{TP})+a_3 \cdot exp(a_4 \cdot T_{TP}), \qquad (5.1.1)$$

   where a_j, j=1,2…4 are constant rates. The monotonous property of the function (5.1.1) allows the assertion that the minimum required point quantity $\{\Delta P_{max,ij};T_{TP,ij}\}$ corresponds to the number of unknown quantities, i.e. n = 4. If reading acquisition of the function $\Delta P_{max}=f(T_{TP})$ for the hydraulic subsystem of random configuration was already realized, then the values of the function (5.1.1) constant rates would be taken from the program database. The value $T^*_{TP,i}$ corresponding to the constraint $\Delta P_{max,perm}$ is determined as a result of the above-mentioned approximation.
2. The equivalent electrical circuit is composed. It includes the sinusoidal voltage source of infinite power with the power line rated voltage; step-down power transformer and already started IMs (if there are such IMs) for which the simplified equivalent circuit is used (this circuit corresponds to the nominal operation mode). The calculations of the maximum allowable current magnitude $I_{TSC,perm}$ that corresponds to the constraint $\Delta V_{max,perm}$ are realized for this circuit. The value of $I^*_{TSC,i}=\min(I_{TSC,perm},I_{SC,i})$ is determined also, where $I_{SC,i}$ is the start current of i-th IM and corresponds to the producer's data in a catalogue.

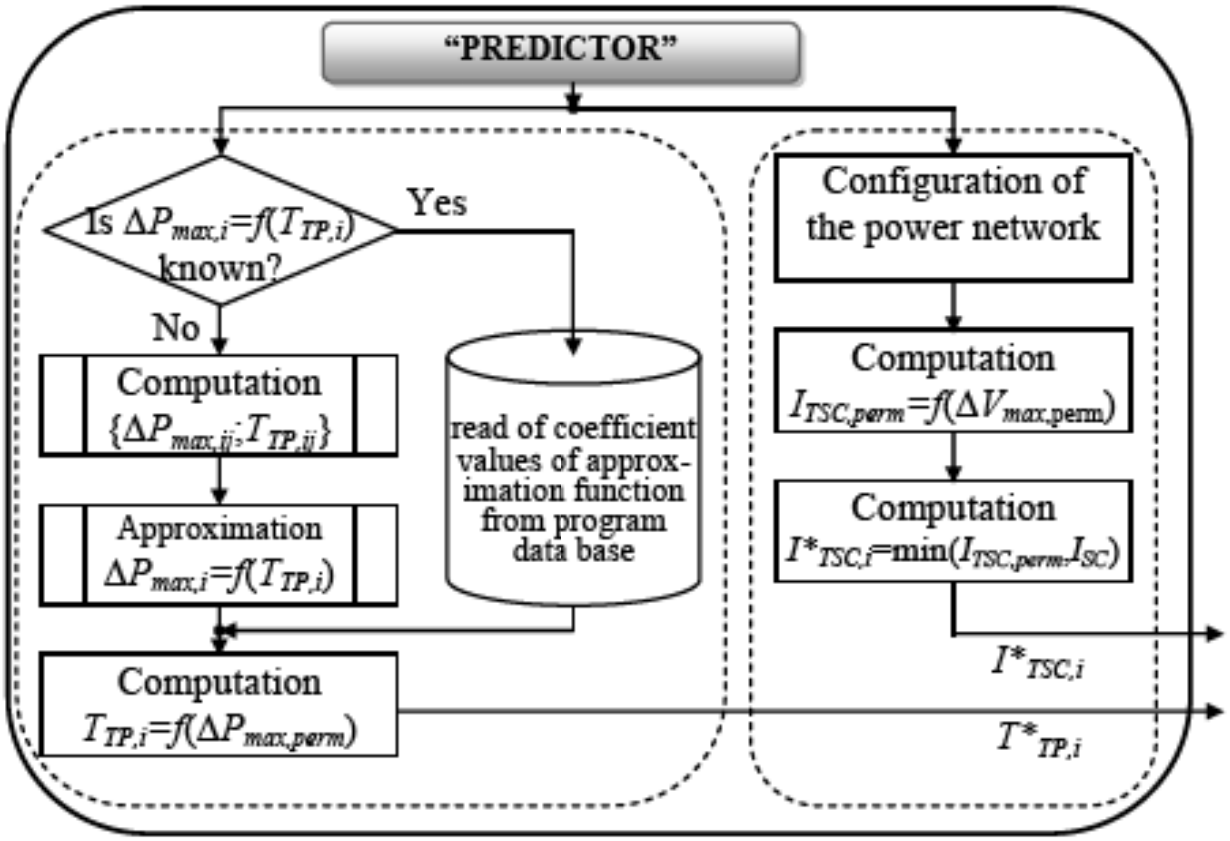

Figure 5.3: Logic diagram of predictor block of adaptive algorithm of IM soft start control.

So, the results of the predictor operation are values of the start duration $T^*_{TP,I}$ and start current $I^*_{TSC,I}$, with which the i-th pump station IM can be started along with the fulfillment of the constraints $\Delta V_{max,perm}$ and $\Delta P_{max,perm}$.

Then the control is transferred to a corrector (see Figure 5.4), which, as the predictor, has two functions:

1. An acquisition of j readings of the start current $I_{TSC,ij}$ in the start duration function $T_{TP,ij}$ for each i-th IM takes place. The readings are taken automatically by means of the numerical integrating of pulse-phase control system with IM model. The dependence type $I_{TSC}=f(T_{TP})$ (see Figure 4.4) as well as for $\Delta P_{max}=f(T_{TP})$ makes it possible to use the exponential approximation. It limits the quantity of the numerical experiments that are necessary for a constant rate calculation in the equation (4.1.2).
2. If the acquisition of the function $I_{TSC,I}=f(T_{TP,I})$ readings for i-th IM with the current resistance torque $T_{L,I}$ is already formed, then the constant rate values of the approximating function (4.1.2) are taken from the program database. The optimal current reference $I_{SCS,i} = f\left(T_{TP,opt}\Big|_{t_{ramp}=0.025} \right)$ is determined for the value $T^*_{TP,I}$,

which is less or equal to $T_{TP,opt}\big|_{I_{ramp}=I_{ramp,opt}}$. Otherwise, i.e. for $T^*_{TP,i}>T_{TP,opt}$, the value of $I_{SCS,I}$ is determined with the application of the approximating function $I_{TSC,I}=f(T_{TP,I})$. Two conditions $I_{SCS,I}\le I^*_{TSC,I}$ for $T_{TP,I}=f(I_{SCS,I})\ge T^*_{TP,I}$ take place for the value of $I_{SCS,I}$.

3. The calculation of the maximum temperature $\Theta_{max,I}$ of the frontal parts of the stator windings of the *i*-th IM is realized for the values of $I_{SCS,I}$, $T_{TP,I}$. If the condition $\Theta_{max,i}>\Theta_{max,perm}$ is satisfied, then the corresponding message concerning the inadmissible start conditions of the current IM is displayed. An opportunity of the varied constraint $\Delta P_{max,perm}$ and $\Delta V_{max,perm}$ decrease is considered in this case.

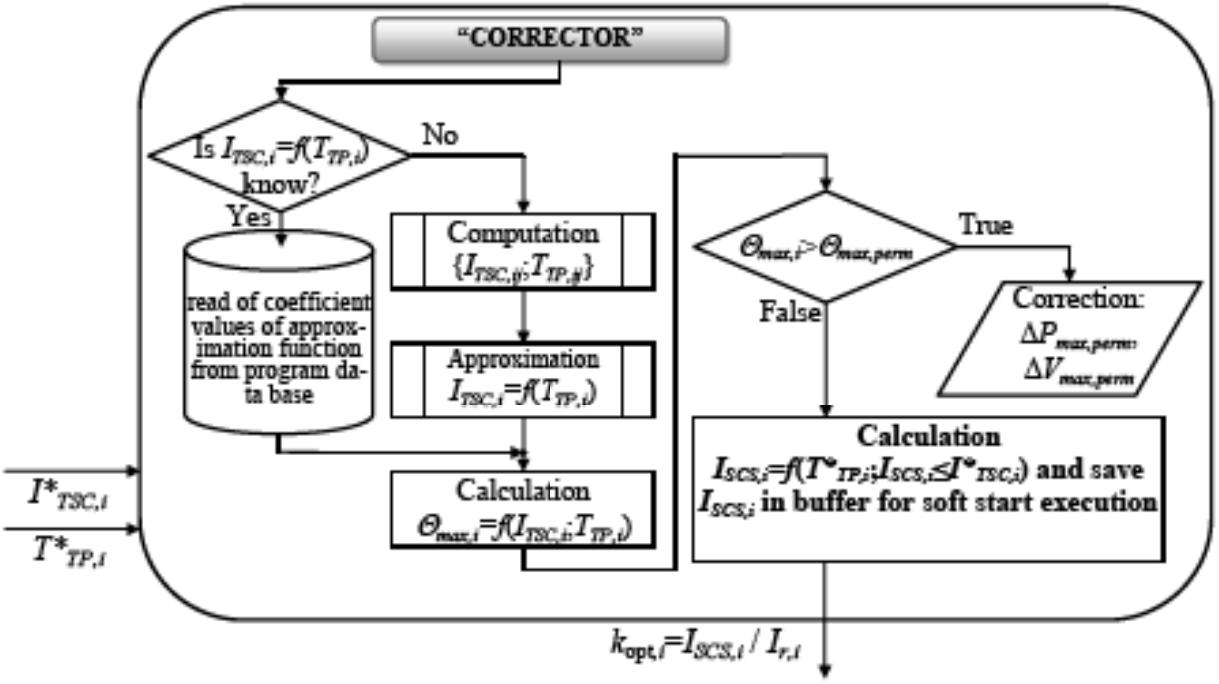

Figure 5.4: Logic diagram of corrector block of adaptive algorithm of IM soft start control.

If not all motors are started, then the return takes place and the control is given to the predictor. The calculated optimal values of $k_{opt,I}=I_{SCS,I}\,/\,I_{r,I}$ for each IM are sent sequentially to the soft starter for an execution of the algorithm with the current limitation (see Section 2.2.2).

There is no need to control mains voltage and motor windings during the soft start, therefore one can use the simplified variant of the above-mentioned algorithm of $k_{opt,I}$ calculation.

An advantage of the above-mentioned adaptive algorithm consists in the fact that it does not contain iterations; it allows securing the performance sufficient for an

interactive control.

The above-mentioned algorithm structure accelerates calculations and makes it possible to use the distributed computing network by means of paralleling of two most resource-consuming groups of predictor operations, which are circled by a dot line in Figure 5.3. This is urgent for a great number of IMs of large pump stations. That is why it is recommended to use the functions of the Distributed Computing Toolbox that is a component of "*MATLAB 7.4*"® environment.

5.2. Software Development of Control System and Monitoring of IM Soft Start Automatic Control System. Numerical Experiment Setting and Realization

An analysis of the composition and general requirements to the automatic control system software presented in Section 1.5 "Requirements to automatic control system software" allows the concretization of requirements to the automatic control system of a pump station IM soft start. In particular, the program and technical complexes of automatic control system of soft start of pump station of water supply must promote simultaneously with other technical means the following:

– Providing an efficient control of water supply and distribution.
– Increase of an operation safety of the automated equipment of pump station.
– Efficient control of the automated equipment parameters.
– Efficient control of the automated equipment economy.
– Increase of the automated equipment reliability.
– Comfort increase for staff operations.
– Providing staff with information.
– Objective evaluation of the efficiency of equipment application and staff operation.

The program and technical complex must provide with an opportunity of development of one- and multilevel hierarchical systems of the distributed and centralized control that corresponds to the structure of a technological object and character of its control. The technical and program means must provide with the development opportunity of automatic control system of technological processes, which are open for an upgrade and development without a necessity for changes of technical solutions realized earlier.

One can emphasize the following functional subsystems in the functional structure of an automatic control system of IM soft start:

- Acquisition, primary processing and information distribution taken from the sensors of heat and electrical engineering parameters in the form of analog, discrete and digital signals including a reception-transmission of information from other automatic control systems as well as formation of arrays of current information for its subsequent processing by other subsystems.
- Representation of information and user interaction with program and technical complexes.
- Remote control for an actuating device driving gears.
- Computer system that realizes the algorithms of accumulation, averaging, information archiving etc.
- Information exchange between the program and technical complexes of an automatic control system of a pump station.
- Self-control and self-diagnostics of the program and technical complexes, adjustment of the applied programs and filling a database, acquisition and information processing concerning the program and technical complex diagnostics (instrumental subsystem).
- Realization of the service function algorithms.

The united system within the framework of the automatic control system and its program and technical complexes must be used to encode the technological equipment, physical and virtual automatic devices, algorithms and programs. It is allowed the use of technological semantic encoding with the application of terms and abbreviations commonly used in water supply for a convenient perception of information presented on the screens and printers.

The general software requirements follow from the corresponded standards and satisfy the principles [Wang and Tan − 06]:

- Modularity of all the software components.
- Software and data hierarchy.
- Efficiency (the minimum resource consumption to develop and maintain the software).
- Integration simplicity (an opportunity for expansion and upgrade).
- Flexibility (an opportunity of change introduction and readjustment).
- Reliability (a correspondence to the given algorithm, an absence of false actions), unauthorized access secure and either destruction programs and data.

– Survivorship (an execution of the required functions in the full or partial scope after failures, restoration after errors).
– Solution unification.
– Simplicity and clearness of the composition, structure and source program codes.

The structure of the program module of an automatic control system of IM soft start (see Figure 5.5) is developed and realized in "*MATLAB 7.4*"® environment taking into account the above-mentioned requirements.

The menu structure of the program module of an automatic control system of IM soft start of pump station is presented in Figure 5.6.

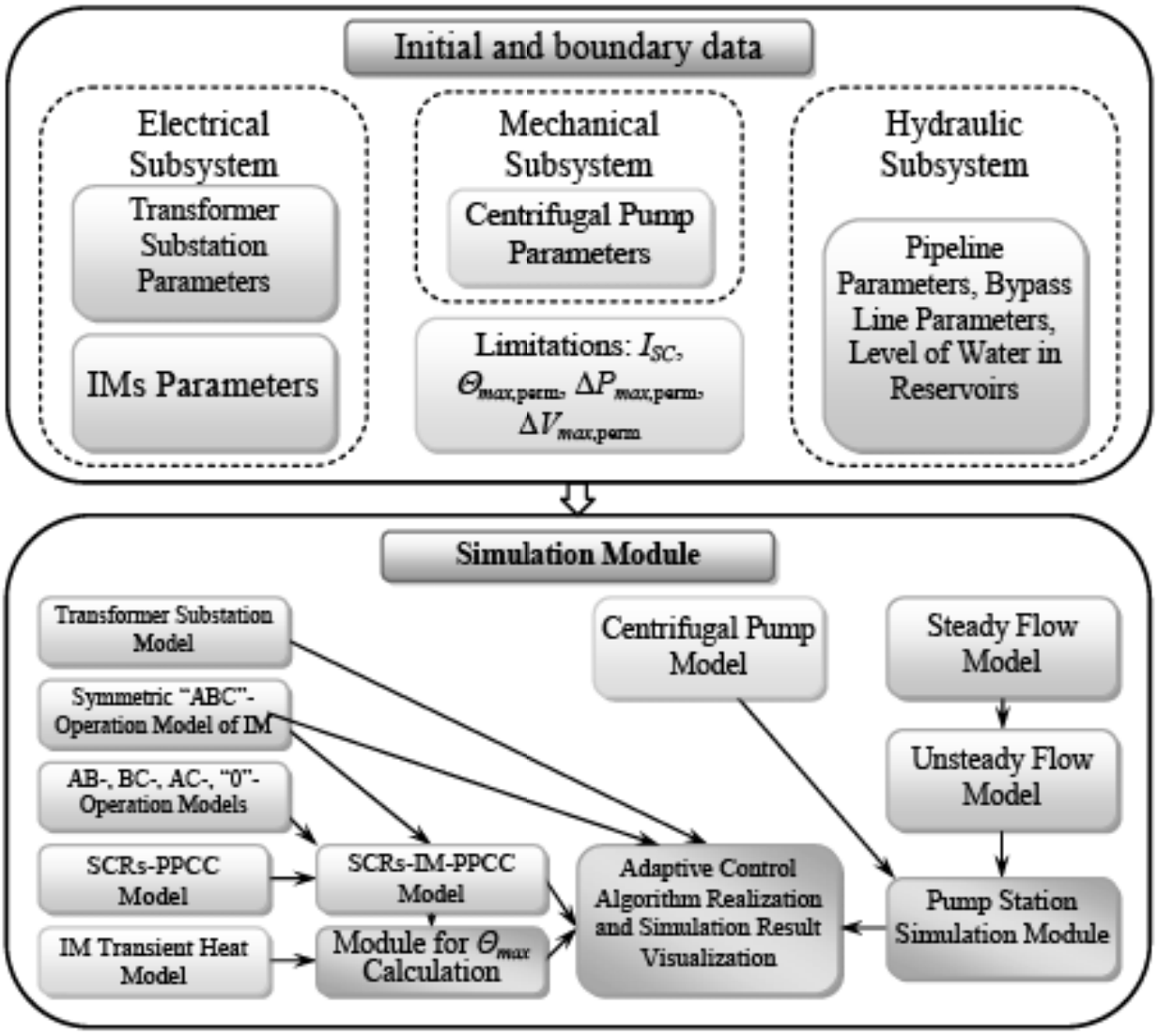

Figure 5.5: Structure of program module of automatic control system of IM soft start for pump station supervisor.

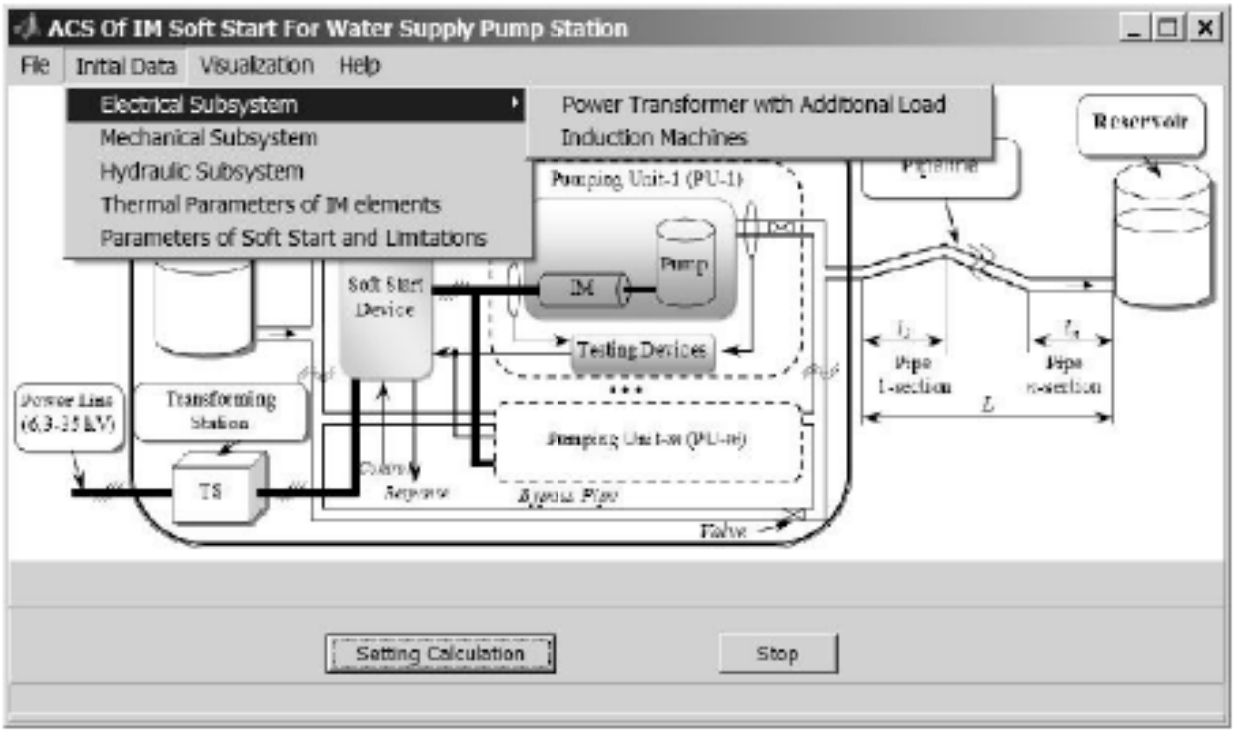

Figure 5.6: Menu structure of program module of automatic control system of pump station IM soft start.

According to the operation logic of the adaptive control algorithm of an IM soft start, the initial data introduction and check take place with an application of the menu item "Initial data" after the program module start (see Figure 5.7).

A calculation of the coefficient $k_{opt.i}$ takes place for each *i*-th pump station IM after data introduction by means of the button "Reference calculation" taking into account the predetermined constraints. The form with the summary results appears on the computer screen (see Figure 5.8) after the calculation completion.

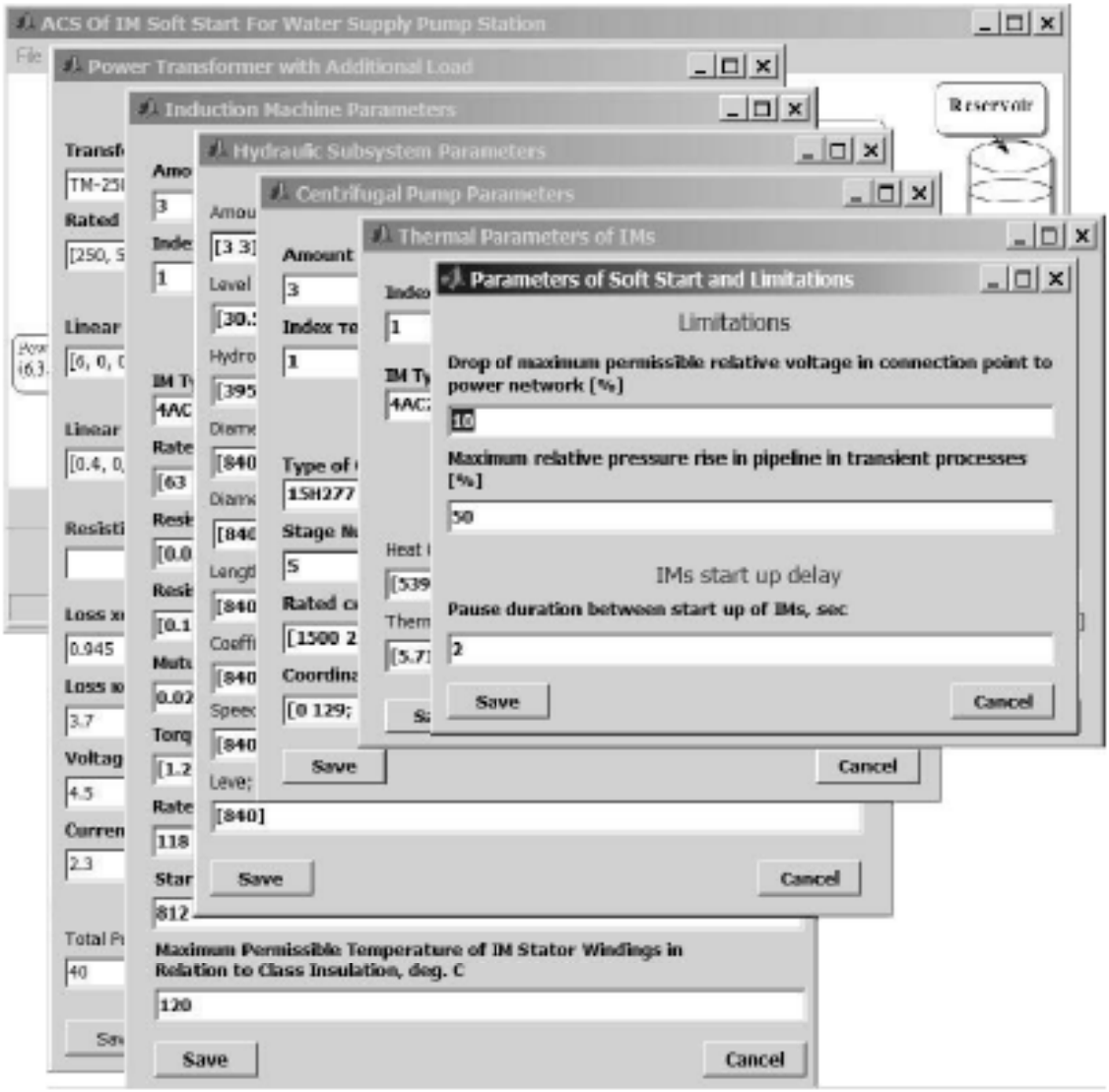

Figure 5.7: Initial data screen of the program module of automatic control system of pump station IM soft start.

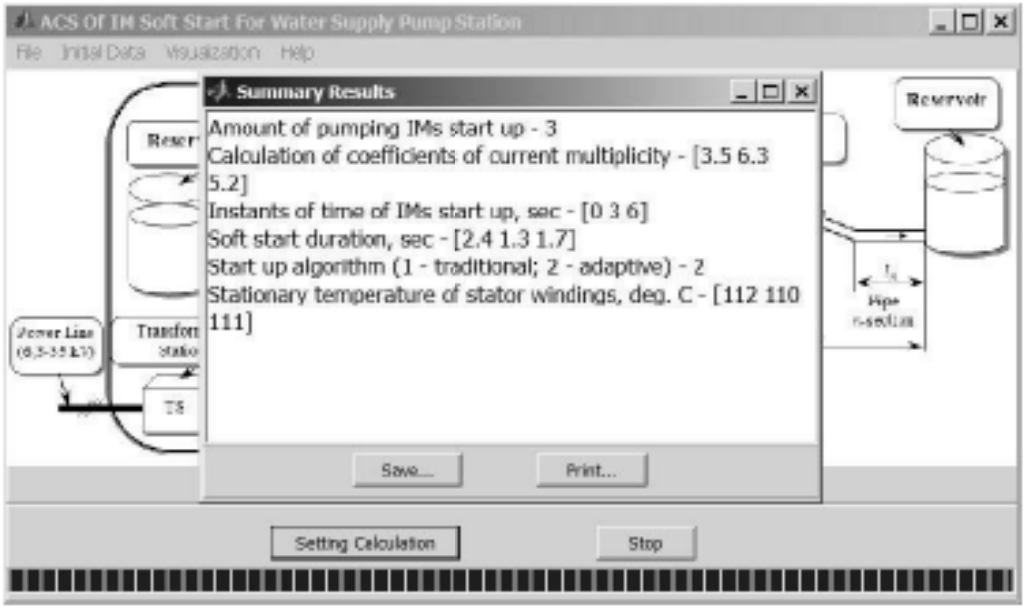

Figure 5.8: Calculation result screen.

A user can output the graphics of the interested dependences on the computer screen after the calculation completion (see Figure 5.9) via the menu item "Visualization".

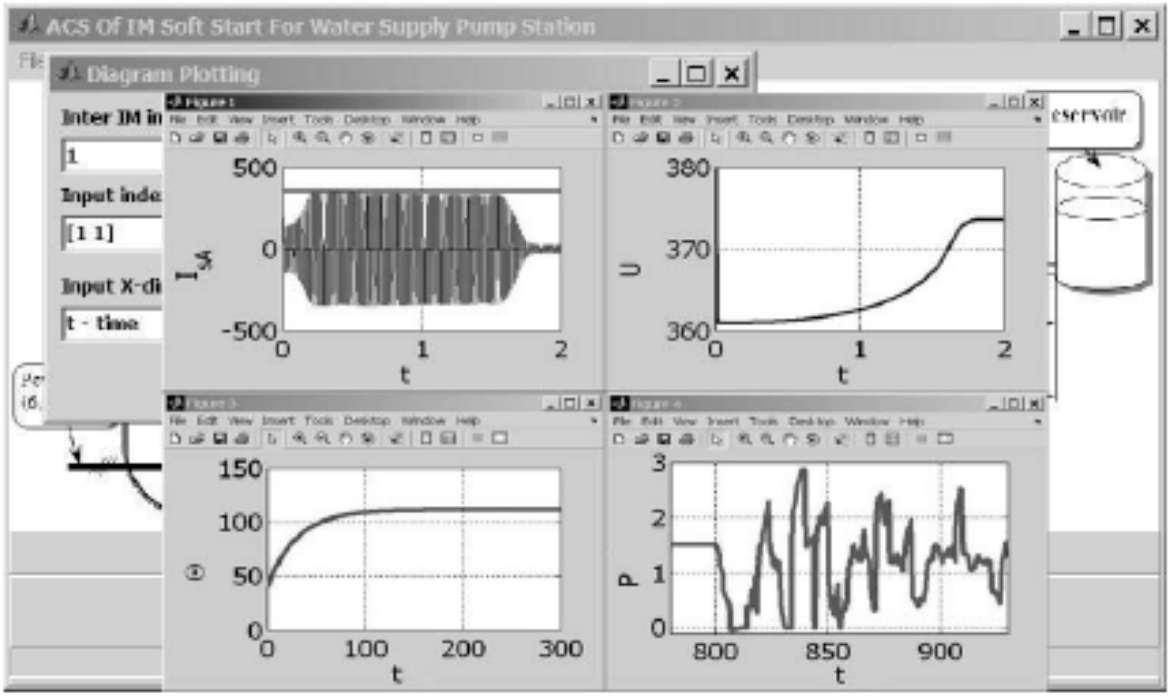

Figure 5.9: Appearance of state variable graphics of automatic control system of IM soft start plotted with application of the developed program module.

The numerical experimental investigation of an adequacy of the adaptive control algorithm for an automatic control system of IM soft start of pump station with the structure depicted in Figure 2.1 was carried out with an application of the developed program module.

The parameters of the hydraulic and electrical subsystems correspond to the parameters defined in Section 4.3. In particular, it is supposed that a pump station is completed with three IMs of type 4AC250M4У3; the characteristic curves of the centrifugal pumps correspond to the pump Ingersoll-Dresser 15H277 [Larock, et al. – 00]; the two-winding transformer TM-250/6-10 with the power rating S_r=250 kV·A is used in a transformer substation, the total power of the auxiliary equipment is $S_a \approx 16$ kV·A. The values of the fixed constraints correspond to: (1) the multiplication factor coefficient of the IM 4AC250M4У3 $k_{I,S} = 7$ start current; (2) the maximum allowable winding temperature with the isolation class of heat resistance B $\Theta_{max,perm} = 130$ °C.

The varied constraints had the following values during the experiment: maximum allowable relative voltage decrease in the secondary transformer circuit $\Delta V_{max,perm} =$ 10%; maximum allowable pressure increase in the pipeline with respect to the steady

state mode $\Delta P_{max,perm}$ = 50%.

The data for comparison of energy loss in IM windings determined by an application of the conventional soft start algorithm with the fixed setting k_I for all pump station IMs and adaptive algorithm developed in the thesis are summarized in Table 5.1. The maximum values of relative voltage ΔV_{max} decrease and pressure increase in the pipeline ΔP_{max} determined during the transient process of all pump station IM start are presented in Table 5.1. The maximum temperature value of the IM stator winding front parts Θ_{max} is given for a steady mode.

Table 5.1: Modeling results of pump station IM soft start during conventional and adaptive algorithm application

Conventional algorithm					Adaptive algorithm	Relative energy loss decrease value	Energy loss decrease value per day for 30 start cycles per hour
k_I	ΣW, kilojoule	ΔV_{max}, %	ΔP_{max}, %	Θ_{max}, °C	ΣW, kilojoule	δW, %	ΔW, kilowatt-hour
2,5	252	4,7	43	122,3	140,25 $k_{opt,i}$={4,1 6,2 4,8}, i = 1…3	44,3	22,35
3,0	171	6,2	49	118,1		17,9	6,15
4,0	141,57	8,1	49,8	116,0		0,9	0,26
5,0	139,59	9,9	50,3	115,8		–	–
6,0	139,59	10,1	50,6	115,7		–	–

The soft starter manufactures recommend to set the value of k_I equal to 2,5; 3 during the pump station IM start [Çadirci, et al. – 99], [Zenginobuz and Çadirci – 04], [Zenginobuz and Çadirci – 01].

One can conclude on the base of the results in Table 5.1 that an IM soft start with an application of the adaptive algorithm allows the decrease by 17,9% of the total energy loss in the IM windings with respect to the energy loss while applying the conventional algorithm with the fixed setting k_I = 3. It follows from the modeling results that the value k_I decrease by 0,5 leads to the loss increase by $\frac{\left|\sum W|_{K_I=3.0} - \sum W|_{K_I=2.5}\right|}{\sum W|_{K_I=3.0}} \cdot 100 \approx 47\%$. Increase of the value k_I up to k_I = 5 leads to the maximum exceeding the pressure increase in the pipeline higher than the constraint $\Delta P_{max,perm}$ = 50%. In addition, the voltage drop in the transformer windings corresponding to the value k_I = 6 leads to the voltage decrease in the secondary circuit by the relative value ΔV_{max} = 10,1%, it violates the predetermined constraint $\Delta V_{max,perm}$ =

10%.

The adaptive algorithm application makes it possible to avoid an appearance of the similar modes because the value of k_I is considered individually for each starting drive taking into account the corresponding constraints. The optimal values of the current repetition factor $k_{opt,I}$={4,1 6,2 4,8} are calculated through the adaptive algorithm in the above-mentioned example taking into account the predetermined constraints. It follows from the results presented in Table 5.1 that the temperature exceeding the IM stator winding coil ends higher the maximum allowed value $\Theta_{max,perm}$ = 130 °C had not been revealed during the experiment carrying out.

The modeling duration of a soft start of a pump station IM during the first program execution was 14 minutes for PC equipped with Pentium 4 processor and 1 GB RAM. The modeling duration did not exceed 1 minute each subsequent time thanks to an application of the approximating dependences determined during the first iteration.

The carried out numerical investigation made it possible to confirm an efficiency of the developed adaptive algorithm of a soft start of pump station IM of water supply system. This algorithm allows the decrease of electrical energy losses in drive windings taking into account the constraints imposed on transients in the system "power network-soft starter-IM-pump-pipeline".

5.3. Conclusions

1. The new algorithm for an adaptive formation of start-stop trajectories of pump aggregate IM that provides with an efficiency increase of energy conversion electromechanical process has been developed. An essence of the proposed algorithm consists in determination of optimal energy loss according to the criterion of energy loss minimization of soft start program parameters for each IM individually taking into account the constraints imposed on the maximum IM stator winding current, a maximum stator winding temperature and maximum pressure increase in pipeline during transients.
2. The complex of mathematical models and modeling method that includes the adaptive control algorithm of an IM soft start and optimal integration algorithm of the "pulse-phase control system – series-connected silicon-controlled rectifier – IM" has allowed development of the software for an automated control system of a pump aggregate IM soft start. This software satisfies the requirements of [Wang and Tan − 06] and is recommended for an application as a part of the automated workplace for a pump station supervisor.
3. The numerical investigation of a IM soft start with the application of conventional and adaptive control algorithm of an IM soft start and the developed program module have been carried out. The results are shown in Table 5.1.

The adequacy check of the developed algorithm of IM soft start adaptive control has shown its efficiency in comparison with the traditional soft start control, which consists in random choice of the stator current repetition factor value k_I and this value application for all pump station drive start. In particular, the generally accepted value k_I=2.5÷4 choice leads to a baseless start deceleration and energy losses that exceed losses, which take place when the developed in this thesis algorithm is used. If k_I=5÷7, then one may observe a pressure increase in pipeline higher than the maximum allowed value and, in addition, the transient current can lead to the voltage drop up to the value allowed by [Pozdeev and Erezeev − 06].

The adaptive algorithm proposed in the thesis eliminates an appearance of the similar modes because the value of k_I is calculated individually for each starting drive taking into account corresponding constraints.

Summary and Future Research Directions

The task of electrical energy loss decrease in IM windings of a pump station of water supply system during the controlled formation of start-stop trajectories has been solved.

Meanwhile, the pump station mathematical model has been developed, constraints and efficiency criterion of electromechanical energy conversion in IM soft starter of pump station of water supply system have been determined.

The IM soft start adaptive algorithm has been developed on the base of the carried out analysis. This algorithm allows the decrease of electrical energy losses in IM windings and satisfaction of the constraints imposed on quality of transient processes of electromechanical energy conversion in a pump station IM of a water supply system.

The adequacy experimental investigations of "power network – soft starter – IM – pump – pipeline" model and efficiency of the developed adaptive algorithm of IM soft start control have been carried out.

The main results and conclusions of the thesis are the following:

1. The new algorithm of adaptive forming of start-stop trajectories of a pump aggregate IM has been developed. It provides electrical energy loss decrease in IM windings of a pump station of a water supply system. An essence of the proposed algorithm consists in a determination of optimal (according to energy loss minimization criterion) program parameters of a soft start for each IM taking into account the constraints on the maximum pressure increase in pipeline, maximum current and IM stator winding temperature during transient process. An adaptation of the proposed algorithm is provided by means of an individual start program formation sequentially for each pump station IM taking into account the current state variable values of electrical and hydraulic pump station subsystems. The calculated setting increase of the maximum allowable transient current individually for each IM had led to electrical energy loss decrease in windings during the numerical experiment from 1% to 44% in comparison with analogous losses, which take place during an application of the traditional soft start control algorithm with the fixed current reference.
2. The approach proposed in the thesis to electrical energy loss decrease in pump station IM windings of a water supply system has been formed on the base of a complex mathematical model development that includes a power line with transformer substation, "pulse-phase control system – series-connected silicon-

controlled rectifier – IM" with a pump load, IM thermal model, and model of liquid movement in pipeline. It allows reproduction and investigation of the energy conversion processes in "grid – soft starter – IM – pump – pipeline" system in transient and steady-state modes.

3. The new "hybrid" algorithm of numerical integrating that adapts an integration method to the current model state has been proposed. This algorithm makes it possible to decrease computer time consumption during the integration equation systems that correspond to the transient and steady operating modes of pulse energy converters. A model nonlinearity of structure constancy intervals and a high order are characterized for pulse energy converters. The integration method choice is justified in agreement with the criterion of computer time minimization taking into account the stability requirement fulfillment of the differential scheme and given modeling accuracy. The hybrid algorithm realization in "*MATLAB 7.4*®" environment and its efficiency analysis have shown the computer time consumption decrease during modeling "pulse-phase control system – series-connected silicon-controlled rectifier – IM" system (up to 29%) in comparison with the conventional approach to the analogous problem.
4. The modeling method that includes mathematical models, an adaptive control algorithm of IM soft start and an optimal integrating algorithm of "pulse-phase control system – series-connected silicon-controlled rectifier – IM" model composes a base of the application package. The last one is recommended for an interactive control, monitoring and diagnostics of automated control system of a IM soft start for a standard pump station in water supply system.

As a rule, electrical drives of a pump station include both soft starters and induction motor drives based on PWM rectifier-inverter for accurate control of specified water delivery. Scientific research, aimed at the search of power efficient control of all induction motors of a pump station in the modes of both energy and water consumption overflow is a promising direction for the further researches.

Appendices

A. Parameters of Equivalent Scheme of IMs

Parameters of IM	Units	Types of IMs				
		4A112M4Y3	4A225M4Y3	4AC132S4Y3	4AC250M4Y3	4AH280M4Y3
p	–	2	2	2	2	2
m	–	3	3	3	3	3
f	Hz	50	50	50	50	50
P_r	kW	5.5	55	8.5	63	160
$cos\varphi$	–	0.85	0.91	0.85	0.93	0.9
η	–	0.855	0.925	0.825	0.87	0.935
$V_{r.t.}$	V	220	220	220	220	220
$I_{r.t.}$	A	11.5	99.0	18.4	117.9	288.1
r_s	Ohm	1.164	0.032	0.574	0.034	0.017
r_r	Ohm	0.645	0.017	0.850	0.123	0.012
M	Henry	0.171	0.0217	0.107	0.0231	0.009
L_s	Henry	0.176	0.0221	0.110	0.0236	0.0102
L_r	Henry	0.179	0.0222	0.111	0.0235	0.0103
$T_{L,r}$	N·m	36.4	355.9	58.2	429.4	1041.6
J_r	kg·m^2	0.017	0.621	0.028	1.2	2.1

B. MATLAB-Scripts of Models of Induction Machine Unsymmetrical Operations

```
function y_out = ad_3f_ab(t,y)
%
global Rs Ls Rr Lr Lm P_n p_p;
global J E_n f F k_Mc;
global k_mc_d T_i;
s_m=whos('k_mc_d');
omega_s=2*pi*f;Fi=0;
%
i_su=y(1);
i_sv=y(2);
i_sw=y(3);
i_ru=y(4);
i_rv=y(5);
i_rw=y(6);
omega_r=y(7);
```

```
%
if s_m.class=='struct' %
  k_mc_d_i=1;
  if find((k_mc_d.t-T_i)>=0)
    tmp=find((k_mc_d.t-T_i)>=0);
    if k_mc_d.t(tmp(1))-T_i==0
      k_mc_d_i=k_mc_d.e(tmp(1));
    else k_mc_d_i=k_mc_d.e(tmp(1)-1);end;
  end;
  Mc=k_mc_d_i*k_Mc*(omega_r/(omega_s/p_p))^2;
else Mc=0;%
end;
%
u_su=E_n*sin(omega_s*t+Fi);
u_sv=E_n*sin(omega_s*t-2*pi/3+Fi);
u_sw=E_n*sin(omega_s*t+2*pi/3+Fi);
%
u_sA=u_su;u_sB=u_sv;u_sC=u_sw;
omega_r_out = 1 / J *(-0.8660254038e0 * p_p * Lm * i_sv * (0.2e1 * i_rw - 0.1e1 * i_ru -
0.1e1 * i_rv)-omega_r*F - Mc);
i_rv_out = -0.8333333333e-1 * (0.36e2 * Lm ^ 3 * Rs * i_sv - 0.1385640646e2 * p_p *
omega_r * Lr ^ 3 * i_ru * Lm + 0.4156921938e2 * Lr ^ 2 * p_p * omega_r * Lm * i_sv * Ls
+ 0.2771281292e2 * Ls * p_p * omega_r * Lr ^ 3 * i_rw + 0.1558845727e2 * Lr * p_p *
omega_r * Lm ^ 3 * i_rv - 0.2078460969e2 * Ls * Lr * Lm ^ 2 * p_p * omega_r * i_rw +
0.1385640646e2 * p_p * omega_r * Lr ^ 3 * i_rw * Lm + 0.6e1 * Rr * i_ru * Lm ^ 3 -
0.5196152423e1 * Lr * Lm ^ 3 * p_p * omega_r * i_ru - 0.2078460969e2 * Ls * Lm ^ 3 *
p_p * omega_r * i_sv - 0.2078460969e2 * Lr * Ls * p_p * omega_r * Lm ^ 2 * i_sv +
0.24e2 * Rr * i_ru * Lm * Lr * Ls + 0.24e2 * Rr * i_rw * Ls * Lr * Lm - 0.1212435565e2 *
Lm ^ 4 * p_p * omega_r * i_ru - 0.1039230485e3 * Lr * Lm ^ 3 * p_p * omega_r * i_sv +
0.12e2 * Lr * Lm ^ 2 * Rr * i_rw - 0.12e2 * Ls * Lm ^ 2 * Rr * i_rv - 0.54e2 * Lr * Lm ^ 2 *
Rr * i_rv + 0.24e2 * Rr * i_rv * Lm * Lr ^ 2 + 0.48e2 * Ls * Rr * i_rv * Lr ^ 2 -
0.3117691454e2 * Lr ^ 2 * Lm ^ 2 * p_p * omega_r * i_rv - 0.6928203230e1 * Ls * Lm ^
3 * p_p * omega_r * i_rw + 0.1558845727e2 * Lm ^ 4 * p_p * omega_r * i_rv -
0.3464101615e1 * Lm ^ 4 * p_p * …

function y_out = AD_3F_ac(t,y)
…
i_sw_out = -0.2500000000e0 * (0.3464101615e1 * p_p * omega_r * Lm ^ 2 * i_rv +
0.6928203230e1 * Lr * p_p * omega_r * Lm * i_rv + 0.6e1 * Rr * i_ru * Lm -
0.1732050808e1 * p_p * omega_r * Lm ^ 2 * i_rw - 0.3464101615e1 * p_p * omega_r *
Lr * i_rw * Lm - 0.1732050808e1 * p_p * omega_r * Lm ^ 2 * i_ru - 0.3464101615e1 *
p_p * omega_r * Lr * i_ru * Lm + 0.4e1 * Lr * u_sA - 0.2e1 * u_sC * Lm - 0.4e1 * Lr *
u_sC + 0.4e1 * Rs * i_sw * Lm + 0.8e1 * Lr * Rs * i_sw - 0.6e1 * Lm * Rr * i_rw + 0.2e1 *
Lm * u_sA) / (Ls * Lm + Lr * Lm + 0.2e1 * Lr * Ls - 0.4e1 * Lm ^ 2);
i_rw_out = 0.8333333333e-1 * (-0.1385640646e2 * p_p * omega_r * Lr ^ 3 * i_ru * Lm +
0.2078460969e2 * p_p * omega_r * Lm ^ 2 * i_sw * Lr ^ 2 - 0.2078460969e2 * Ls * Lr *
Lm ^ 2 * p_p * omega_r * i_sw - 0.2078460969e2 * Ls * Lm ^ 3 * p_p * omega_r * i_sw
+ 0.2771281292e2 * p_p * omega_r * Lr ^ 3 * i_rv * Ls - 0.1039230485e2 * Lr * p_p *
omega_r * Lm ^ 3 * i_rv + 0.1385640646e2 * p_p * omega_r * Lr ^ 3 * i_rv * Lm - 0.48e2
* Lr ^ 2 * Rr * i_rw * Ls - 0.36e2 * Lr * Lm ^ 2 * Rs * i_sw - 0.2078460969e2 * Ls * Lm ^
2 * Lr * p_p * omega_r * i_rv - 0.6e1 * Rr * i_ru * Lm ^ 3 - 0.5196152423e1 * Lr * Lm ^ 3
* p_p * omega_r * i_ru - 0.24e2 * Rr * i_ru * Lm * Lr * Ls - 0.6928203230e1 * Ls * Lm ^ 3
```

```
* p_p * omega_r * i_rv + 0.18e2 * Lm ^ 3 * u_sC - 0.24e2 * Lr ^ 2 * Rr * i_rw * Lm -
0.1212435565e2 * Lm ^ 4 * p_p * omega_r * i_ru + 0.54e2 * Lr * Lm ^ 2 * Rr * i_rw -
0.12e2 * Ls * Lm ^ 2 * Rr * i_rv - 0.12e2 * Lr * Lm ^ 2 * Rr * i_rv - 0.3117691454e2 * Lr ^
2 * Lm ^ 2 * p_p * omega_r * i_rw - 0.3464101615e1 * Lm ^ 4 * p_p * omega_r * i_rv +
0.1558845727e2 * Lm ^ 4 * p_p * omega_r * i_rw + 0.3117691454e2 * Lr ^ 2 * Lm ^ 2 *
p_p * omega_r * i_ru + 0.1558845727e2 * Lr * Lm ^ 3 * p_p * omega_r * i_rw -
0.1039230485e3 * Lr * Lm ^ 3 * p_p * omega_r * i_sw + 0.8313843876e2 * Lm ^ 4 * p_p
* omega_r * i_sw - 0.12e2 * Rr * i_ru * Lm ^ 2 * Ls + 0.42e2 * Rr * i_ru * Lm ^ 2 * Lr -
0.18e2 * Lm ^ 2 * Lr * u_sA + 0.4156921938e2 * Ls * p_p * omega_r * Lm * i_sw * Lr ^ 2
+ 0.6928203230e1 * Ls * Lm ^ 3 * p_p * omega_r * i_ru - 0.18e2 * Lm ^ 3 * u_sA +
0.6e1 * Lm ^ 3 * Rr * i_rw + 0.12e2 * Ls * Lm ^ 2 * Rr * i_rw + 0.2078460969e2 * Ls *
Lm ^ 2 * p_p * omega_r * Lr * i_ru - 0.2771281292e2 * p_p * omega_r * Lr ^ 3 * i_ru * Ls
+ 0.72e2 * Lr ^ 2 * Lm * Rs * i_sw + 0.18e2 * Lr * Lm ^ 2 * u_sC - 0.36e2 * Lr ^ 2 * Lm *
u_sC + 0.48e2 * Lm ^ 3 * Rr * i_rv - 0.24e2 * Lr * Ls * Rr * i_rv * Lm - 0.36e2 * Lm ^ 3 *
Rs * i_sw + 0.36e2 * Lr ^ 2 * Lm * u_sA) / (-0.3e1 * Lr * Lm ^ 2 * Ls + 0.4e1 * Lm ^ 4 +
0.2e1 * Lr ^ 3 * Lm + 0.4e1 * Lr ^ 3 * Ls - 0.9e1 * Lr ^ 2 * Lm ^ 2 + 0.3e1 * Lr * Lm ^ 3 -
0.1e1 * Ls * Lm ^ 3);...

function y_out = ad_3f_bc(t,y)
i_rv_out = 0.8333333333e-1 * (-0.6e1 * Lm ^ 3 * Rr * i_rw + 0.36e2 * Lr * Lm ^ 2 * Rs *
i_sw - 0.72e2 * Lr ^ 2 * Lm * Rs * i_sw + 0.48e2 * Rr * i_ru * Lm ^ 3 - 0.24e2 * Lr * Ls *
Rr * i_rw * Lm - 0.24e2 * Rr * i_ru * Lm * Lr * Ls - 0.1212435565e2 * Lm ^ 4 * p_p *
omega_r * i_rw - 0.8313843876e2 * Lm ^ 4 * p_p * omega_r * i_sw + 0.1558845727e2 *
Lm ^ 4 * p_p * omega_r * i_rv - 0.3464101615e1 * Lm ^ 4 * p_p * omega_r * i_ru +
0.6928203230e1 * Lm ^ 3 * Ls * p_p * omega_r * i_rw - 0.2078460969e2 * Lr ^ 2 * p_p *
omega_r * Lm ^ 2 * i_sw - 0.2771281292e2 * p_p * omega_r * Lr ^ 3 * i_rw * Ls +
0.18e2 * Lr * Lm ^ 2 * u_sB - 0.18e2 * Lr * Lm ^ 2 * u_sC + 0.36e2 * Lr ^ 2 * Lm * u_sC -
0.36e2 * Lr ^ 2 * Lm * u_sB - 0.12e2 * Lm ^ 2 * Ls * Rr * i_rw + 0.12e2 * Lm ^ 2 * Ls * Rr
* i_rv + 0.54e2 * Lr * Lm ^ 2 * Rr * i_rv - 0.24e2 * Lr ^ 2 * Rr * i_rv * Lm - 0.48e2 * Lr ^ 2
* Rr * i_rv * Ls - 0.3117691454e2 * Lr ^ 2 * Lm ^ 2 * p_p * omega_r * i_rv +
0.1039230485e3 * Lr * Lm ^ 3 * p_p * omega_r * i_sw + 0.1385640646e2 * p_p *
omega_r * Lr ^ 3 * i_ru * Lm + 0.6e1 * Lm ^ 3 * Rr * i_rv - 0.1385640646e2 * p_p *
omega_r * Lr ^ 3 * i_rw * Lm + 0.2771281292e2 * p_p * omega_r * Lr ^ 3 * i_ru * Ls +
0.18e2 * Lm ^ 3 * u_sB - 0.18e2 * Lm ^ 3 * u_sC + 0.42e2 * Lr * Lm ^ 2 * Rr * i_rw -
0.6928203230e1 * Lm ^ 3 * Ls * p_p * omega_r * i_ru + 0.3117691454e2 * Lr ^ 2 * Lm ^
2 * p_p * omega_r * i_rw - 0.1039230485e2 * p_p * omega_r * Lr * i_ru * Lm ^ 3 +
0.36e2 * Lm ^ 3 * Rs * i_sw - 0.2078460969e2 * Lm ^ 2 * Ls * p_p * omega_r * Lr * i_ru -
0.5196152423e1 * Lr * Lm ^ 3 * p_p * omega_r * i_rw + 0.2078460969e2 * Lm ^ 3 * Ls *
p_p * omega_r * i_sw + 0.2078460969e2 * Lr * Ls * p_p * omega_r * Lm ^ 2 * i_sw -
0.4156921938e2 * Lr ^ 2 * p_p * omega_r * Lm * i_sw * Ls - 0.12e2 * Rr * i_ru * Lm ^ 2 *
Ls - 0.12e2 * Rr * i_ru * Lm ^ 2 * Lr + 0.2078460969e2 * Lm ^ 2 * Ls * p_p * omega_r *
Lr * i_rw + 0.1558845727e2 * Lr * Lm ^ 3 * p_p * omega_r * i_rv) / (-0.9e1 * Lr ^ 2 * Lm ^
2 + 0.2e1 * Lr ^ 3 * Lm + 0.4e1 * Lr ^ 3 * Ls + 0.3e1 * Lr * Lm ^ 3 - 0.1e1 * Lm ^ 3 * Ls -
0.3e1 * Lr * Lm ^ 2 * Ls + 0.4e1 * Lm ^ 4);
i_rw_out = -0.8333333333e-1 * (-0.6e1 * Lm ^ 3 * Rr * i_rw + 0.36e2 * Lr * Lm ^ 2 * Rs *
i_sw - 0.72e2 * Lr ^ 2 * Lm * Rs * i_sw + 0.24e2 * Lr * Lm * Ls * Rr * i_rv - 0.48e2 * Rr *
i_ru * Lm ^ 3 + 0.24e2 * Rr * i_ru * Lm * Lr * Ls + 0.1558845727e2 * Lm ^ 4 * p_p *
omega_r * i_rw + 0.8313843876e2 * Lm ^ 4 * p_p * omega_r * i_sw - 0.1212435565e2 *
Lm ^ 4 * p_p * omega_r * i_rv - 0.3464101615e1 * Lm ^ 4 * p_p * omega_r * i_ru +
0.2078460969e2 * Lr ^ 2 * p_p * omega_r * Lm ^ 2 * i_sw + 0.6928203230e1 * Ls * Lm
^ 3 * p_p * omega_r * i_rv + 0.18e2 * Lr * Lm ^ 2 * u_sB - 0.18e2 * Lr * Lm ^ 2 * u_sC +
0.36e2 * Lr ^ 2 * Lm * u_sC - 0.36e2 * Lr ^ 2 * Lm * u_sB - 0.12e2 * Lm ^ 2 * Ls * Rr *
```

```
i_rw + 0.12e2 * Lm ^ 2 * Ls * Rr * i_rv - 0.42e2 * Lr * Lm ^ 2 * Rr * i_rv +
0.3117691454e2 * Lr ^ 2 * Lm ^ 2 * p_p * omega_r * i_rv - 0.1039230485e3 * Lr * Lm ^
3 * p_p * omega_r * i_sw + 0.1385640646e2 * p_p * omega_r * Lr ^ 3 * i_ru * Lm +
0.6e1 * Lm ^ 3 * Rr * i_rv + 0.2771281292e2 * p_p * omega_r * Lr ^ 3 * i_ru * Ls +
0.18e2 * Lm ^ 3 * u_sB - 0.18e2 * Lm ^ 3 * u_sC - 0.54e2 * Lr * Lm ^ 2 * Rr * i_rw +
0.48e2 * Lr ^ 2 * Ls * Rr * i_rw + 0.24e2 * Rr * i_rw * Lm * Lr ^ 2 - 0.6928203230e1 * Lm
^ 3 * Ls * p_p * omega_r * i_ru - 0.3117691454e2 * Lr ^ 2 * Lm ^ 2 * p_p * omega_r *
i_rw - 0.1039230485e2 * p_p * omega_r * Lr * i_ru * Lm ^ 3 + 0.36e2 * Lm ^ 3 * Rs *
i_sw - 0.2078460969e2 * Lm ^ 2 * Ls * p_p * omega_r * Lr * i_ru + 0.1558845727e2 * Lr
* Lm ^ 3 * p_p * omega_r * i_rw - 0.2078460969e2 * Lm ^ 3 * Ls * p_p * omega_r * i_sw
- 0.2078460969e2 * Lr * Ls * p_p * omega_r * Lm ^ 2 * i_sw + 0.4156921938e2 * Lr ^ 2
* p_p * omega_r * Lm * i_sw * Ls + 0.12e2 * Rr * i_ru * Lm ^ 2 * Ls + 0.12e2 * Rr * i_ru *
Lm ^ 2 * Lr - 0.2771281292e2 * Ls * p_p * omega_r * Lr ^ 3 * i_rv - 0.1385640646e2 *
p_p * omega_r * Lr ^ 3 * i_rv * Lm + 0.2078460969e2 * Ls * Lr * Lm ^ 2 * p_p * omega_r
* i_rv - 0.5196152423e1 * Lr * Lm ^ 3 * p_p * omega_r * i_rv) / (-0.9e1 * Lr ^ 2 * Lm ^ 2
+ 0.2e1 * Lr ^ 3 * Lm + 0.4e1 * Lr ^ 3 * Ls + 0.3e1 * Lr * Lm ^ 3 - 0.1e1 * Lm ^ 3 * Ls -
0.3e1 * Lr * Lm ^ 2 * Ls + 0.4e1 * Lm ^ 4);
i_sw_out = 0.2500000000e0 * (-0.1732050808e1 * p_p * omega_r * Lm ^ 2 * i_rw -
0.2e1 * Lm * u_sB + 0.2e1 * Lm * u_sC - 0.6e1 * Lm * Rr * i_rv - 0.3464101615e1 * Lm
* p_p * omega_r * Lr * i_rw - 0.1732050808e1 * p_p * omega_r * Lm ^ 2 * i_rv -
0.3464101615e1 * p_p * omega_r * Lr * i_rv * Lm + 0.6928203230e1 * p_p * omega_r *
Lr * i_ru * Lm + 0.4e1 * Lr * u_sC - 0.4e1 * Lr * u_sB + 0.3464101615e1 * p_p *
omega_r * Lm ^ 2 * i_ru + 0.6e1 * Rr * i_rw * Lm - 0.4e1 * Lm * Rs * i_sw - 0.8e1 * Lr *
Rs * i_sw) / (Lm * Ls - 0.4e1 * Lm ^ 2 + Lr * Lm + 0.2e1 * Lr * Ls);
```

C. MATLAB-Script of SCRs-IM Model with Pulse-Phase Control Circuit

```
function
[T_rez,Y_rez,m_em]=trn_real_3d_17(alfa,k_i,t_base,w_nu,NU_i,c_par,par_contrl,time_
contrl,flag_stop)
global I_nom;
% par_contrl - [i_min t_cos]
% k_i - (0)
% flag_stop - 1
% t_base
% w_nu (if w_nu==0 then NU_i- active)
% time_contrl
% vector_impuls
global f p_p T_i AlfaContr U Omega_ref_ W;
s_g=whos('AlfaContr');
s_g_om=whos('Omega_ref_');
if s_g.class=='struct' %
    alfa_c=(100-20*AlfaContr.v(1))/(f*360); %
    U.t=AlfaContr.t(1);U.v=AlfaContr.v(1);
else alfa_c=(100-20*alfa)/(f*360); %
end;
if s_g_om.class=='struct' %
  Omega_ref.t=Omega_ref_.time;
  Omega_ref.v=Omega_ref_.signals.values;
  W.t=Omega_ref.t(1);W.v=Omega_ref.v(1);
end;
%
i_min=par_contrl(1)*I_nom*k_i;%
```

```
t_cos=par_contrl(2);%
i_y=I_nom*k_i;%
s_i=1;%
mas_t_sin=0;
err_i=[0 0]; %
m_em=0;%
k_T_i=0;%
graf=0;%graf (2 Simulinkom, 0)
f=50;%
Fi=0;%
I_kr=1e-7;%
T=1/f;%
omega_s=2*pi*f;
w_s=omega_s/p_p;%
imp_a_pr=0;imp_a_inv=0;%
imp_b_pr=0;imp_b_inv=0;%
imp_c_pr=0;imp_c_inv=0;%
regim_nom=0;%
regim_real=0;%
regim_i(1)=0;%
%
T_i=t_base(1);%
t_base=t_base(2);%
%
if T_i~=0
  %
  for i=1:6
    if abs(NU_i(i))<=I_kr NU_i(i)=0;end;
  end;...
```

D. MATLAB-Script of Optimal Algorithm for Control of Pumping IM Soft Start

```
function [h_rez,head_rez,rpm_rez,m_h,max_head]=pipelin_trans_1(intr_pip)
%
Pip_Trans_Ini;
%
% intr_pip
% h_rez
% head_rez
% rpm_rez
% m_head
% max_head
global N_pips N_parts H_res H_sump Z_end H_atm Q_try Q_acc T_max DT_new
Re_run D_b KL_b;
global D L F A Pipez Air_vac;
%
global N_pumps N_stage Rpm WR_sq N_start Qn HN_sq TN_sq;
%
global T_start T_stop T_ramp Rpm_strt Rpm_end;
n_p=N_pips;%?
i=1;
i_count=0;
```

```
d_n=100000;
r_start=0;%
bypass=0;%
r_stop=0;%
rpm_s=zeros(1,10);
qp=zeros(1,10);
pinert=WR_sq/32.2;
if F(1)>10, n_exp=0.85;else n_exp=1; end;
%
if Q_try<0.001, Q_try=Qn(4);end;
if F(1)>10
  coef=3.03*(12^4.87)*(N_pumps/(449*0.7854))^1.85;
else
  coef=12*144^2*16*N_pumps^2/(64.4*449^2*pi^2);
end;
for nz=1:20
  flag_1=0;flag_2=0;
  for i=1:5
    if (Q_try>Qn(i))&&(Q_try<=Qn(i+1)), flag_1=1;break;end;
  end;%for i=1:5
  if flag_1==1
    h_n=HN_sq(i)+(Q_try-Qn(i))*(HN_sq(i+1)-HN_sq(i))/(Qn(i+1)-Qn(i));
    sum=0;
    for j=1:N_pips
      if F(1)>10, sum=sum+L(j)*Q_try^1.85/((F(j)^1.85)*(D(j)^4.87));
      else sum=sum+F(j)*L(j)*Q_try^2/D(j)^5;end;
    end;%for
    func_t=H_sump-H_res+N_stage*h_n-coef*sum;
    f_prime=N_stage*(HN_sq(i+1)-HN_sq(i))/(Qn(i+1)-Qn(i))-2*coef*sum/Q_try;
    qn_ext=Q_try-func_t/f_prime;
    if abs(qn_ext-Q_try)<Q_acc, flag_2=1;break;end;
    Q_try=qn_ext;
  else
    error('');
  end;%if flag_1==1
end;%for nz
if flag_2==0, error('');end;
q_line=qn_ext*N_pumps;
q=qn_ext;
h_pump=N_stage*h_n+H_sump;…
```

References

[Alger − 76] Alger, P. L., I. V. Ingvarsson, and W. R. Oney. "Saturistor motor for pump drive with SCR speed control." *IEEE Transaction on Power Apparatus and Systems*, no. 3 (1976): 766–772.

[Altmann − 05] Altmann, W. *Practical Process Control for Engineers and Technicians*. Oxford: IDC Technologies, 2005.

[Banerjee, et al. − 01] Banerjee, S., and G. Verghese. *Nonlinear Phenomena in Power Electronics. Attractors, Bifurcation, Chaos, and Nonlinear Control*. New York: IEEE Press, 2001.

[Barrade − 08] Barrade, P. "Simulation tools for power electronics: teaching and research." *Laboratoire d'Electronique Industrielle Departement Electricite Ecole Polytechnique Federale de Lausanne*. 2008. http://www.epfl.ch/ publications/ barrade_workshop_simplorer_01.pdf.

[Berezin − 08] Berezin, S., and Z. Chernota. "Size minimization of sewage immersible pumps." *Northwest Office of Public Corporation Leasing of Ecological Projects, St. Petersburg*. 2008. http://www.pump.ru/ images/ stories/ Articles/ optimal_construction.pdf (accessed In Russian).

[Blaabjerg − 97] Blaabjerg, F., and J. K. Pederson. "Can soft-starter help save energy." *IEEE Industry Applications Magazine*, no. 4 (1997): 56–66.

[Boys − 94] Boys, J. T., and M. J. Miles. "Empirical thermal model for inverter-driven cage induction machines." *IEE Proc.-Electr. Power Appl.*, 1994: 360–372.

[Bredthauer − 95] Bredthauer, J., and N. Struck. "Starting of large medium voltage motors: design, protection, and safety aspect." *IEEE Transactions on Industry Applications*, no. 5 (1995): 1167–1176.

[Butcher − 03] Butcher, J. C. *Numerical Methods for Ordinary Differential Equations*. Chichester: John Wiley & Sons, 2003.

[Çadirci − 99] Çadirci, I., M. Ermiş, and E. Nalçaci. "A solid state direct on line starter for medium voltage induction motors with minimized current and torque pulsations." *IEEE Transactions on Energy Conversion*, no. 3 (1999): 402–412.

[Chapple − 03] Chapple, P. J. *Chapple, Principles of Hydraulic Systems Design*. Oxford: Coxmoor Publ. Comp., 2003.

[Chrisanov − 02] Chrisanov, V., and R. Brzesinski. "Proceedings of the EPE-PEMC." *Intelligent soft starters for induction motors on the base of fuzzy logic control*. Dubrovnik, 2002. 1–9.

[Deleroi − 89] Deleroi, W., B. J. Woudstra, and A. A. Fahim. "W. Deleroi, B. J. Woudstra and A. A. Fahim, “Analysis and application of three-phase induction motor voltage controller with improved transient performance." *IEEE Transactions on Industry Applications*, no. 2 (1989): 280–286.

[Dewinter − 89] Dewinter, A. F., and B. J. Kedrosky. "The application of a 3500-hp variable frequency drive for pipeline pump control." *IEEE Transaction on Industry Applications*, no. 6 (1989): 1019–1024.

[Flaviis − 08] Flaviis, F. "Mechanical and electrical analysis of a microelectromechanical switch for RF applications." *Department of Electrical Engineering & Computer Science. The University of California, he Henry Samueli School of Engineering.* 2008. http://www.ece.uci.edu/ rfmems/publications/ papers/mems/C021-EUMTT99.pdf.

[Forenc − 02] Forenc, J. "International Conference on Parallel Computing in Electrical Engineering (PARELEC'02)." *The speculative method of transient state analysis with a variable integration step*. Berlin, 2002. 101–106.

[Geldhof − 06] Geldhof, K., and T. Vyncke. "6th International Conference on Computational Electromagnetics." *Embedded Runge-Kutta methods for the numerical solution of an integrated model including converter, nonlinear inductance and current control loop*. Germany, 2006. 156–162.

[Ginart − 05] Ginart, A., R. Esteller, and A. Maduro. "High starting torque for AC SCR controller." *IEEE Transactions on Energy Conversion*, no. 3 (1999): 553–559.

[Girdhar − 05] Girdhar, P., and O. Moniz. *Practical Centrifugal Pumps. Design, Operation and Maintenance*. Oxford: Newnes, 2005.

[Guevara − 90] Guevara, Y., and R. Carmona. "Unsteady and steady flow control on pumping systems." *IEEE Transaction on Industry Applications*, no. 5 (1990): 954–960.

[Hamed − 90] Hamed, S. A., and B. J. Chalmers. "Analysis of variable-voltage thyristor controlled induction motors." *IEE Proceedings*, no. 3 (1990): 184–193.

[Hamzaoui − 04] Hamzaoui, A., A. Melikhov, V. Tsukanov, and Yu. Kolokolov. "The experience of MATLAB 6.0 usage during of simulation of the pulse-phase control system of the thyristor voltage regulator with the active-inductive load." *International Scientific Journal of Computing* 3, no. 3 (2004): 76–81.

[High-grade − 08] *High-grade steel absolute multi-turn shaft encoder, Baumer electric.* http://www.baumerelectric.com/ downloads/ Produkte/ PDF/ Datenblatt/ Winkel_und_Positionsmesssysteme / en_E-3.38_BEMV.pdf.

[Hoffman − 01] Hoffman, D. *Numerical Methods for Engineers and Scientists.* New York: Marcal Dekker. Inc., 2001.

[Irwin − 08] Irwin, G., and A. Woodford. "Precision simulation of PWM controllers." *Manitoba HVDC Research Centre performs innovative research and development in HVDC and power electronic technologies, instrumentation, and simulation.* 2008. http://www.hvdc.ca/pdf_misc/IPST1231.pdf.

[Kallesøe − 06] Kallesøe, C. S., V. Cocquempot, and R. Izadi-Zamanabadi. "Model based fault detection in a centrifugal pump application." *IEEE Transaction on Control Systems Technology*, no. 2 (2006): 204–215.

[Kallesøe − 07] Kolokolov, Y., A. Melikhov, A. Hamzaoui, N. Essounbouli, and J. Zaytoon. "3rd International IEEE Scientific Conference on Physics and Control (PhysCon 2007)." *Stability analysis of a thyristor voltage controller – induction machine model.* Potsdam, 2007. 344.

[Kolokolov − 07] Kolokolov, Y., A. Melikhov, V. Tsukanov, and A. Hamzaoui. "3rd IFAC Workshop Periodic Control Systems (PSYCO 2007)." *Parametric stability of two induction motor models with unsymmetrical connection to the supply-line.* St. Peresburg, 2007.

[Kolokolov − 08] Kolokolov, Y., A. Monovskaya, and A. Melikhov. "The novel hybrid algorithm on the simulation of the dynamic of high-order pulse energy conversion system. Parh 1 – Design of the hybrid algorithm." *Mechatronics, Automation, Control*, no. 1 (2008): 27–34.

[Kolokolov − 07] Kolokolov, Yu. V., and A. Yu. Melikhov. "Simulation of starting transients of a source pump station." *OrelSTU. Fundamental and applied problems of technique and technology: informational system and technologies*, no. 4/268(535) (2007): 18–23.

[Kolokolov − 06] Kolokolov, Yu., A. Melikhov, and V. Tsukanov. "International Scientific Conf. Informational Technologies in Science, Education and Manufacturing." *Model of induction machine under unsymmetrical condition to the supply line.* Orel, 2006. 106-110.

[Kolokolov − 04] Kolokolov, Yu., A. Melikhov, and V. Tsukanov. "International Scientific Conf. Informational Technologies in Science, Education and Manufacturing." *Application of information technologies to technical system modeling by usage MATLAB 6.0.* Orel, 2004. 70-74.

[Kolokolov − 08] Kolokolov, Yu., A. Monovskaya, and A. Melikhov. "The novel hybrid algorithm on the simulation of the dynamic of high-order pulse energy conversion

system. Path 2 – An optimization of the hybrid algorithm by the time computational reduction." *Mechatronics, Automation, Control*, no. 5 (2008): 18–22.

[Larock – 00] Larock, B. E., R. W. Jeppson, and G. Z. Watters. *Hydraulics of Pipeline Systems*. Boca Raton: CRC Press LLC, 2000.

[Lee – 03] Lee, S., and T. G. Habetler. "An online stator winding resistance estimation technique for temperature monitoring of line-connected induction machines." *IEEE Transactions on Industry Applications*, 2003: 685–694.

[LEM Holding SA – 08] "LEM Holding SA." 2008. http://www.lem.com.

[Lihachev – 02] Lihachev, V. L. *Induction machines*. Moscow: SOLON-P, 2002.

[Lipo – 71] Lipo, T. A. «The analysis of induction motors with voltage control by symmetrically triggered thyristors.» *IEEE Transaction on Power Apparatus and Systems*, № 2 (1971): 515–525.

[Martin – 98] Martin, J. *The J & P Transformer Book*. Oxford: Newnes, 1998.

[McElveen – 01] McElveen, R. F., and M. K. Toney. "Starting high-inertia loads." *IEEE Transactions on Industry Applications*, 2001: 137–144.

[Melikhov – 06] Melikhov, A. "International Scientific Conf. Informational Technologies in Science, Education and Manufacturing." *Electromechanical energy conversion using Maxwell 10.0*. Orel, 2006. 126–130.

[Melikhov and Hamzaoui – 05] Melikhov, A., and A. Hamzaoui. "International Conf. High Technology of Energy Saving." *An analysis of the asynchronous machine transient processes under start mode with sinusoidal power source*. Voronezh, 2005. 60-62.

[Melikhov and Loskutov – 05] Melikhov, A., and I. Loskutov. "International Workshop High-Technologies of Energy-Saving." *Analysis of identification methods of induction machine parameters*. Voronezh, 2005. 55–57.

[Melikhov and Tsukanov – 04] Melikhov, A., and V. Tsukanov. "10th International Student Olympiad on Automatic Control (Baltic Olympiad – BOAC'2004)." *The realization of the algorithms of programmed control in systems of soft start with induction motor*. Saint-Peresburg, 2004. 57-60.

[Melikhov and Tsukanov – 04] Melikhov, A., and V. Tsukanov. "3rd Int. Workshop Computer Simulation of Electromagnetic Processes in Physical, Chemical and Technical Systems." *Three-phase induction machine modeling using MATLAB 6.0*. Voronezh, 2004. 224-227.

[Melikhov and Tsukanov – 04] Melikhov, A., and V. Tsukanov. "All-Russian Conf.

New Technologies in Scientific Researches, Designing, Control and Manufacturing." *Control algorithm of three-phase thyristor voltage regulator with active-reactive load and current synchronization*. Voronezh, 2004. 124-127.

[Melikhov, et al. – 05] Melikhov, A., V. Tsukanov, and Yu. Kolokolov. "All-Russian Scientific Conf. Control and Information Technologies (CIT-2005)." *Stability analysis of a squirrel cage induction machine model*. St. Petersburg, 2005. 250–256.

[Melikhov, et al. – 04] Melikhov, A., V. Tsukanov, and Yu. Kolokolov. "All-Russian Scientific Conf. Methods of Applied Mathematics and Computer Data Processing in Technology, Economics and Ecology." *Stability analysis of a three-phase induction machine model with periodic coefficients*. Orel, 2004. 127-130.

[Mellor, et al. – 91] Mellor, P. H., D. Roberts, and D. R. Turner. "Lumped parameter thermal model for electrical machines of TEFC design." *IEE Proceedings-B*, no. 5 (1991): 205–218.

[Mellor – 04] Menon, E. S. *Liquid Pipeline Hydraulics*. New York: Marcel Dekker, Inc., 2004.

[Mezani, et al. – 05] Mezani, S., N. Takorabet, and B. Laporte. "A combined electromagnetic and thermal analysis of induction motors." *IEEE Transactions on Magnetics*, 2005: 1572–1575.

[Novotny and Lipo – 03] Novotny, D. W., and T. A. Lipo. *Vector Control and Dynamics of AC Drives*. Oxford: Clarendon press, 2003.

[Petrov and Petrov – 02] Petrov, Y., and L. Petrov. *Unexpected in Mathematics and its Relation with Accidents and Catastrophes of Last Years*. St. Petersburg: NIIH SPbGU, 2002.

[Pozdeev and Erezeev – 06] Pozdeev, D. A., and A. N. Erezeev. "Automation soft-start system for high-voltage pumping motors of oil-trunk pipeline “Drujba"." *Elektrotehnika*, no. 6 (2006): 2-10.

[Quarteroni, et al. – 00] Quarteroni, A., S. Riccardo, and F. Saleri. *Numerical Mathematics*. New York: Spriger-Verlag, 2000.

[Sanks – 98] Sanks, R. L. *Pumping Station Design*. Boston: Butterworth-Heinemann, 1998.

[Sannino – 00] Sannino, A. "Improving power quality in industrial plants with induction motor load by using a static transfer switch." *IEEE Industry Applications Magazin*, no. 5 (2003): 50–57.

[Sastry, et al. – 97] Sastry, V. V., M. R. Prasad, and T. V. Sivakumar. "Optimal soft

starting of voltage-controller-fed IM drive based on voltage across thyristor." *IEEE Transactions on Power Electronics*, no. 6 (1997): 1041–1051.

[Seleznov and Aleshin – 07] Seleznov, V E., and V. V. Aleshin. *Novel Computer Simulators in Hydraulic Hookups. Mathematical Simulation Methods and Practical Application*. Moscow: MAKS Press, 2007.

[Solveson, et al. – 06] Solveson, M. G., B. Mirafzal, and N. A. Demerdash. "Soft-started induction motor modeling and heating issues for different starting profiles using a flux linkage ABC frame of reference." *IEEE Transactions on Industry Applications*, no. 4 (2006): 973–982.

[Toyoshima, et al. – 04] Toyoshima, R., T. Funaki, and T. Hikihara. "35th Annual IEEE Power Electronics Specialists Conference." *Anomalous phenomenon of conduction angle in TCR-SVC and Its control*. Aachen, 2004. 3403–3408.

[Tsukanov and Melikhov – 06] Tsukanov, V., and A. Melikhov. "11th International Student Olympiad on Automatic Control (Baltic Olympiad – BOAC'2006)." *Evolution of a non-deterministic self-oscillation mode in a pulse-phase control system with induction motor*. Saint-Petersburg, 2006. 100-104.

[Verner – 92] Verner, J. *A Classification Scheme for Studying Explicit Runge-Kutta Pairs*. Canada: Queen's University at Kingston, 1992.

[Verner – 05] *A Contrast of a New RK56 Pair with DP56*. Canada: Department of Mathematics. PIMS. Simon Fraser University, 2005.

[Volk – 05] Volk, M. *Pump Characteristics and Applications*. Boca Raton.: CRC Press, 2005.

[Wang and Tan – 06] Wang, L., and K. Tan. *Modern Industrial Automation Software Design*. New Jersey: IEEE Press, 2006.

[Zenginobuz and Çadirci – 04] Zenginobuz, G., and I. Çadirci. "Performance optimization of induction motors during voltage-controlled soft starting." *IEEE Transactions on Energy Conversion*, no. 2 (2004): 278–288.

[Zenginobuz and Çadirci – 01] Zenginobuz, G., and I. Çadirci. "Soft starting of large induction motors at constant current with minimized starting torque pulsations." *IEEE Transactions on Industry Applications*, no. 5 (2001): 1334–1347.